2

Damping Theory

Randall D. Peters
Mercer University

Summary

This introductory chapter synthesizes the many, though largely disjointed attributes of friction as they relate to damping (also see Chapter 1). Among other means, events selected from the history of physics are used to show that damping models have suffered from the inability of physicists to describe friction from first principles. To support fundamental arguments on which the chapter is based, evidence is provided for a claim that important nonlinear properties have been mostly missing from classical damping models. The chapter illustrates how the mechanisms of internal friction responsible for hysteretic damping in solids can lead to serious errors of interpretation. Such is the case even though hysteretic damping often masquerades as a linear phenomenon. One attempt to correct common model deficiencies is the author's work toward a "universal damping model," that is described in Section 2.17. Section 2.17 is developed in a "canonical" damping form. It shows the value of a direct, as opposed to an indirect, involvement of energy in model development. To keep a better perspective on how the treatment of damping is likely to evolve in the future, the last section of the chapter addresses some of the remarkable complexities of damping that are only beginning to be discovered. The manner in which technology has played a role in some of these discoveries is addressed in Chapter 3.

2.1 Preface

The sheer volume of published material on the subject is a testament to the difficulty of selecting topics for inclusion in a chapter on damping. Viscoelasticity alone is the basis for several voluminous engineering handbooks. The present chapter is purposely different from similarly titled chapters of other reference books. There is little repetition of well-known and proven classical methods, for which the reader is referred to excellent other sources, such as de Silva (2006) and Chapter 1 of the present handbook. They provide solution techniques for many of the routine problems of engineering. The goal of the present chapter is to provide assistance with problems that are not routine, problems that are being encountered more frequently as technology advances. It is thought that this goal is best served by revisiting fundamental issues of the physics responsible for damping.

Once a multibody system has come to steady state, its damping treatment can be far less formidable than its description during approach to steady state. When dealing with limit cycles involving aeroelasticity and joints in helicopters, nonlinearity has a profound influence on the transient behavior. Attempts to model it have been largely unsuccessful, forcing the empirical selection of elastomers to reduce the vibration. (In the old days hydraulic dampers were used; Hodges, 2003). At a much lower level

of sophistication, our understanding is quite limited on some common phenomena, such as the negative damping character of sound generated by a violin or a clarinet. Historically, when technology "hit the wall" because of too much theoretical handwaving, it became apparent that fundamental assumptions needed to be examined. In physics, a complete alteration of conventional wisdom was sometimes necessary, one of the best examples being the events that gave birth to quantum mechanics. Hopefully, from the multitude of seemingly disparate (but assumed by the author to be connected) observations which follow, the purpose for the architecture of this chapter can be partially realized. The enormous complexity of damping in general makes it unrealistic to hope for complete success.

Physics played a prominent role in developing the classical foundations of damping, starting in the 19th century. Subsequently, engineers uncovered many features of the subject that physicists never even thought about. In recent years, however, physics has been circumstantially forced to reconsider damping fundamentals. With the advent of personal computing, and an increased awareness of the importance of nonlinearity, new discoveries point to serious limitations of the classical foundation. The field of mechanics was severely limited until it began tackling problems of nonlinearity (not of damping type), and became concerned with previously ignored features giving unique system properties. Just as these unique properties could only be solved by techniques more sophisticated than the equations of linear type, there is mounting evidence that nonlinear damping may be the key to understanding some bewildering engineering cases.

It is important to try to identify the major mechanisms responsible for energy dissipation. This is easier said than done, since a host of different friction processes are usually at work. Moreover, the description of friction from first principles remains a daunting task. Thus we are forced to work with phenomenological models. There are also conflicts of nomenclature, with a given word meaning two different things from one profession to another. Thus, much of this chapter will attempt to define carefully terms while focusing on the physics, the treatment of which follows naturally along the lines of historical developments.

Engineers tend to be interested in higher frequencies and higher amplitudes of vibration than are scientists. A perfect damping model would be unconcerned with such differences of application; however, such a model is far from being realized. Because small-amplitude, long-period (low and slow) oscillations provide a valuable means for studying many processes of damping in general, much of this chapter focuses in that direction.

From the multitude of choices available to writers on the subject of damping, this author has selected a single (hopefully) unifying theme — nonlinear damping, especially as found in low and slow oscillations. Because it is a field still in its infancy, many of the ideas that follow are more speculative than one would prefer; however, they deserve discussion because of their perceived importance. To this author's knowledge, damping has not been previously treated in the manner of this chapter. Concerning the earliest relevant paper (Peters, 2001a, 2001b), the following was indicated by oft-cited Prof. A.V. Granato: "I don't know of anyone thinking about internal friction along the lines you have mentioned."

There are two important elements to the unifying theme of nonlinear dissipation: (i) the influence of nonlinear damping on multibody systems in their approach to steady state, and (ii) the close connection between damping and mechanical noise. When vibration decay is not exponential because of nonlinearity, there are significant ramifications and they are only beginning to be appreciated.

The novel features of this chapter are possible because of dramatic improvements in both sensing and data collection/analysis in the last decade. Demonstrating that a decay is not purely exponential requires both (i) a good linear sensor and (ii) the means to study readily long-time records when the damping is small (high Q). The first prerequisite has been met through the use of this author's patented fully differential capacitive sensor. The second has been realized with the availability of good, inexpensive analog-to-digital (A/D) converters having user-friendly, yet powerful Windows-based software. In addition to the "preview" software that comes with Dataq's A/D converter, a proven means for identifying nonexponential decay has been the analysis of records imported to Microsoft Excel. Details of these novel methods will be provided in the various sections that follow.

There are many examples in the engineering literature of nonlinear damping; even Coulomb damping is nonlinear because the friction force involves the algebraic sign of the velocity rather than the velocity itself, as in linear viscous damping. What has been realized for the first time in the course of writing this chapter is the following. As will be shown in the subsequent material, a decay process is not usually a pure exponential. Whatever the reason for a pure exponential, whether fundamentally linear (viscous) or nonlinear (hysteretic present model), the quality factor Q for such a pure exponential decay is constant. When there is a second mechanism, such as amplitude-dependent damping (even if it is the only mechanism), the Q now becomes time dependent. This is significant to mode coupling for the following reason. When a pair of modes couple because of elastic nonlinearity (a process that is impossible assuming linear dynamics), the strength of the coupling is proportional to the product of the individual amplitudes of the pair.

Consequently, variability in Q can influence the evolution to steady state. It is a factor in determining which modes ultimately survive and/or dominate. Moreover, the distribution of the modes which remain depends on initial conditions, including the intensity of excitation.

Long ago, musicians learned to deal with nonlinearity, due in part to properties of the ear that are responsible for aural harmonics. A pair of purely harmonic signals can beat in the ear to produce a "sound" that does not exist when sensed with a linear detector. For example, consider a strong and undistorted 500 Hz signal sounded simultaneously with a pure 1003-Hz sound. The ear will hear a 3-Hz beat due to the superposition of the ear's aural second harmonic of the first with the fundamental of the second. However, there's more to this story. Conductors call for *fortissimo* and *pianissimo* sounds, not only because of the ear's nonlinearity, but also because of nonlinearities inherent to musical instruments. For example, it is easy with a good microphone and LabView (see de Silva, 2006) to demonstrate that the timbre of stringed instruments is intensity dependent. Not only is the mix of harmonics, as displayed in a fast Fourier transform (FFT) power spectrum, different according to volume, but their distribution also changes with time.

Noise is not typically treated in an engineering discussion of damping; however, mechanical noise is an important part of the technical material included in this chapter. Believing that there is a great deal of connectivity among vibration, damping, and noise, evidence will be provided in support of a premise — that the most important and least understood form of internal mechanical damping (material = hysteretic = "universal") is closely allied with the most important and least understood form of noise ($1/f$ = flicker = pink). If this premise is true, then the foundations of damping physics need reconstruction on several counts. Evidence in support of the premise will be provided through tidbits of experimental discoveries from a host of independent investigations. It is hoped that the unusual and lengthy introduction that follows will be beneficial in this regard. Historical elements serve to synthesize the many parts and are offered without apology. Following the introduction, some practical and novel equations of damping will eventually be provided. Even if readers find little identification with the philosophies that birthed them, it is hoped they will at least carefully examine the equations that are presented here in Section 2.17 for the first time.

2.2 Introduction

2.2.1 General Considerations of Damping

The etymology of the word "damping" is difficult to determine. It is obviously allied with the word damper, commonly defined as a "device that decreases the amplitude of electronic, mechanical, aerodynamic or acoustical oscillations," used for centuries, for example, to describe the sound attenuator pedal on the piano. Perhaps the German word *dampfen* (to choke) has had an influence in the evolution of the word. One can only wonder if water, as a moistening agent, played any role. Certainly, liquid water is important to some cases of energy dissipation in oscillators. Moreover, friction determined by the viscosity of a fluid (gas or liquid) is an important type of damping. A curious piece of history, in the

celebrated work of Stokes, is why his expression "index of friction" did not take precedence over our modern word, viscosity. Peculiar terminology is also encountered to describe damping, such as the engineering device known as a dashpot, which is a mechanical damper. The vibrating part is attached to a piston that moves in a liquid-filled chamber.

We will see that the number of adjectives used to describe various types of damping is extensive. This multiplicity of terms to describe the loss of oscillatory energy to heat is no doubt an indicator of the complexity of damping phenomena in general. We will attempt (i) to identify similarities and differences among various types of damping, while (ii) explaining some of the physics responsible for the characteristics observed. Conceptual ideas and techniques of both theory and experiment will be provided, targeting the lowest level of sophistication for which semimeaningful results can be obtained. The reader should be aware that a "grand-unified" theory of damping does not exist, nor is it likely that one will ever be created.

Damping causes a portion of the energy of an oscillator, otherwise periodically exchanged between potential and kinetic forms, to be irreversibly converted to heat, sometimes by way of acoustical noise. Whether by suitable choice of materials during design of passive equipment, or by using feedback in active control of a sophisticated system, control of damping is important since mechanical vibrations can be detrimental or even catastrophic. An oft-quoted example of catastrophe is the Tacoma Narrows bridge, which collapsed in high winds on November 7, 1940. Like the vibration of a clarinet reed, this disaster is probably best described by the term negative damping, which can drive parametric oscillations.

The optimal amount of damping for a given system might fall anywhere in a wide range from great to extremely small, depending on system needs. The engineering world frequently wants oscillations to be as close to critically damped as possible. Physics experiments, such as those searching for the elusive gravitational wave (centered at the Laser Interferometer Gravitational Observatories, or Laser Interferometer Gravitational Wave Observatories [LIGO], in the United States; GEO600 in Germany [involving the British]; VIRGO in Italy [with the French], and TAMA in Japan), want damping in some of their components to be as small as possible. Frequency standards the world over require very small damping to insure high precision for timekeeping.

For the specific components of a system, a successful design frequently requires identification of the specific mechanisms primarily responsible for the dissipation of energy. Even after identifying the dominant sources, the theoretical difficulty of their treatment can also range from great to small, depending on the type of damping. For dashpot fluid damping, adequate models have existed for decades. For material damping, on the other hand, theories of internal friction are numerous and largely lacking in self-consistency.

The fundamental mechanisms responsible for damping are in most cases nonlinear; however, the oscillator's motion can itself be approximated in many cases by a linear second-order differential equation. If the potential energy is quadratic in the displacement, then the undamped linear equation of motion is that of the simple harmonic oscillator, because its solution is a combination of the sine and cosine (harmonic) functions. This undamped equation comprises the sum of two terms, one being a displacement and the other term an acceleration. The constant parameter multiplying each term of the pair depends on the nature of the system. For example, in the case of a mass–spring oscillator, the acceleration is multiplied by the mass, and the displacement by the spring constant. Thus, the equation corresponds to Newton's Second Law applied to a Hooke's Law (idealized) spring. In an electronic L–C oscillator, the "displacement" corresponds to the charge on the capacitor (divided by C) and the "acceleration" corresponds to the second time derivative of the capacitor's charge (multiplied by inductance L).

The usual means to describe damping, which is always present with oscillation, is to add a velocity term to the aforementioned displacement and acceleration. Although the damping could derive from several causes, there is usually a single dominant process. For example, the damping of current in a series-connected resistor, inductor, capacitor (RLC) circuit may depend mostly on Joule heating in the resistor R, in spite of the fact that there must also be energy loss in the form of radiation. Thus, the equation of motion includes a first-time derivative of the capacitor's charge (current) multiplied by R, in accord with Ohm's law.

Whether radiation is important for damping of the RLC circuit depends on the amount of coupling to the environment. If the circuit communicates with a final amplifier connected to an antenna, then radiation may become more important than Joule losses. The frequency of oscillation is a key parameter in this case, and also for damping problems in general. Unfortunately for some common systems, theoretical efforts to account properly for the effects of frequency have proven largely unsuccessful — except for models of phenomenological type developed by empiricism.

2.2.2 Specific Considerations

The mass–spring oscillator is the textbook example of harmonic motion, for which one of the most sophisticated mechanical oscillators ever built is the LaCoste version of vertical seismometer. Significant portions of the experimental data presented in this chapter were generated with an instrument designed around the LaCoste zero-length spring (LaCoste, 1934). The instrument used for this data collection was part of the World Wide Standardized Seismograph Network (WWSSN) during the 1960s. The spring of this seismometer is responsible for hysteretic damping of the instrument, rather than viscous damping as commonly assumed. Contrary to popular belief, air damping is not important for this seismograph at its nominal operating period, which is typically greater than 15 sec. Since every long-period pendulum apparently exhibits similar behavior, we thus find strong synergetic evidence in support of an old (mostly unheeded) claim that hysteretic damping (friction force independent of frequency) is universal (Kimball and Lovell, 1927). Their claim in 1927 to have discovered a universal form of internal friction (damping) is strengthened since the same behavior is seen in three distinctly different systems: (i) a mass–spring oscillator (as demonstrated by Gunar Streckeisen, details given later); (ii) a pendulum whose restoration depends on the Earth's gravitational field (demonstrated by several independent groups); and (iii) a rotating rod strained by a transverse deflection (1927 experiments of Kimball and Lovell).

The assumption of universality for hysteretic damping is a key point of this chapter. It will be shown that the damping of even a vibrating gas column (Ruchhardt's experiment to measure the ratio of heat capacities) is likely also hysteretic. The models that are described represent a departure from common theories of damping. Interestingly, the author's model has similarities to ordinary sliding friction, as given to us by Charles Augustin Coulomb. It effectively modifies the Coulomb coefficient of kinetic friction to yield an effective energy-dependent internal friction coefficient. The energy dependence is necessary to obtain exponential decay, as opposed to the linear decay of Coulomb damping. Just as with conventional Coulomb damping, its form is nonlinear, involving the algebraic sign of the velocity. We will see that the damping capacity predicted by the model permits an equivalent viscous form. Yet the underlying physics is related to creep of secondary type as opposed to the primary creep of viscoelasticity.

It is this author's opinion that much of the existing theory of damping is not the best means for modeling dissipation. The difficulties arise from approximating oscillator decay with linear mathematics. Although most individuals recognize the oft-stated caveat that viscous damping is an approximation to the actual physics of dissipation, they do not recognize some of the many serious limitations of the approximation. The situation is similar to the place in which we found ourselves at the beginning of the era labeled "deterministic chaos." The "butterfly effect" (Lorenz, 1972) has radically altered the thinking of many, but only in relationship to large-amplitude motions of a pendulum, where the instrument is no longer isochronous because of nonlinearity. As an archetype of chaos, the pendulum must be rigid and capable of "winding" (displacement greater than π) before chaos is possible. Nonlinearity is a prerequisite for the chaos, but it is not sufficient, since there are many examples of highly nonlinear but nonchaotic motions. For example, amplitude jumps of nonlinear oscillators, during a frequency sweep of an external drive, have been known for many years. They were observed before chaos was recognized, in systems like the Duffing and Van der Pol oscillators. Yet chaos, with its sensitive dependence on initial conditions (responsible for the butterfly effect), was not contemplated at the time. As with most significant advances, Lorenz's discovery was by accident, as he modeled convection in the atmosphere. The author's confrontation with complexity that derives from mesoscale structures in metals was likewise unexpected. "Strange phenomena" (as Richard Feynman would probably have labeled them)

were encountered while using his patented fully differential capacitive sensor to study various mechanical systems, mainly oscillators.

As with chaos, the pendulum may ultimately serve as an archetype of complexity. When operated at low energy, especially through a combination of long period and small amplitude, the free decay of the physical pendulum departs radically from the predictions based on linear equations of motion. Such complexity can be easily demonstrated when the pendulum is fabricated from soft alloy metals. For example, Figure 2.1 illustrates the decay of a rod pendulum constructed with ordinary (heavy-gauge lead–tin) solder of the type used for joining electrical conductors (Peters, 2002a, 2002b, 2002c).

The "jerkiness" (discontinuities) in the record of Figure 2.1 is in no way related to amplitude jumps of the type previously mentioned; rather, these are jumps of the Portevin–Le Chatelier (PLC) type (Portevin and Le Chatelier, 1923). They are a fundamental, yet "dirty" phenomenon that physics has chosen for decades to try and ignore (even though materials science and engineering took early note of the PLC effect). The most obvious and profound thing that can be said about Figure 2.1 is the following: the presence of PLC jerkiness means that the concept of a potential energy function is not really valid, since the requirement for its definition is that a closed integral of the force with respect to displacement must vanish.

No matter the form of hysteresis, which is the cause for damping, it disallows the curl of the force to be zero, so that potential energy is never formally meaningful for a macroscopic oscillator (since there is always damping). In those cases where the damping is essentially continuous (not true for the example of Figure 2.1), the assumption of a potential energy function retains some computational meaning. For oscillators influenced by the PLC effect, this is no longer true. The resulting properties are important to a variety of technology issues, such as sensor performance, since noise is no longer the simple thermal form predicted by the fluctuation–dissipation theorem (used to characterize white, i.e., Johnson, noise).

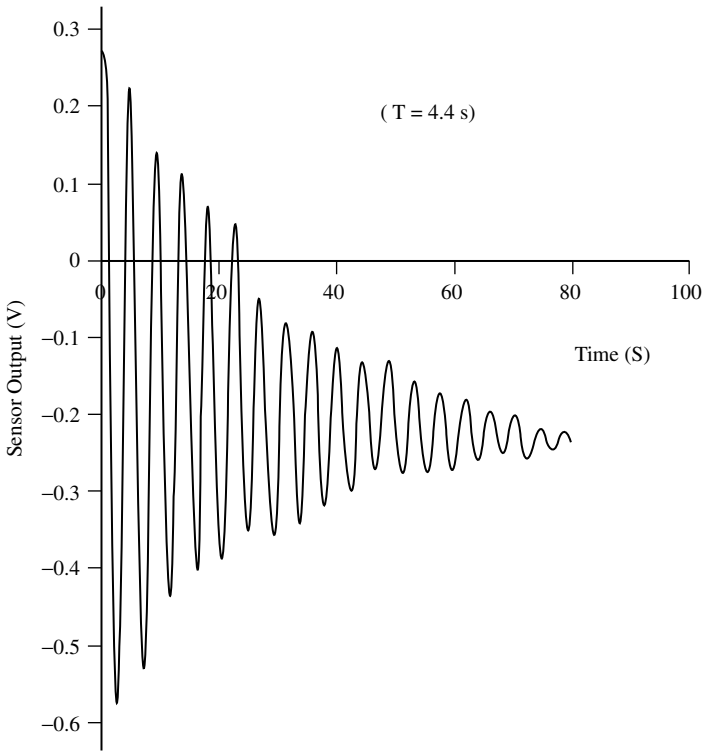

FIGURE 2.1 Free-decay of a rod pendulum fabricated from solder.

Practical means for dealing with systems influenced by "stiction" have been known by engineers for decades. Because of metastabilities in the assumed potential function, the system is prone to latching (stuck in a localized potential well). One means for mastering the metastabilities (unstick the part designed to move) is to "dither" the system. The process has become more sophisticated in the last decade, which saw a major growth of interest in stochastic resonance. In the definition by Bulsara and Gammaitoni (1996):

> A stochastic resonance is a phenomenon in which a nonlinear system is subjected to a periodic modulated signal so weak as to be normally undetectable, but it becomes detectable due to resonance between the weak deterministic signal and stochastic noise.

The phenomenon is related to dithering (Gammaitoni, 1995). It is a case where the signal-to-noise ratio (SNR) can be increased by the counterintuitive act of raising the level of noise. Such a gain in SNR is not possible with a harmonic potential.

In recent studies of granular materials, "tapping" has become a popular means to study behavior that violates the fundamental theorem of calculus. Years ago, this author used tapping as a means to accelerate creep in wires under tension. Evidently, hammering the table on which the extensometer rested caused vibrational excitations of the wire that stimulated length changes of discontinuous PLC type. Because of the broad spectral character of an impulse, various eigenmodes of the wire (de Silva, 2006) could be thus readily excited. After "hammering-down" under load, a silver wire could by this same means be stimulated, after partial load removal, to exhibit length contractions. Since the total number of atoms is fixed, the process must involve exchange of atoms between the surface of the sample and its volume.

Extensometer studies of wires at elevated temperature have also displayed strange behavior. A polycrystalline silver wire of diameter 0.1 mm and approximate length 30 cm was found to exhibit large fluctuations when heated in air to within 100 K of its melting point, using a vertical furnace (Peters, 1993a, 1993b). The large fluctuation in length at these temperatures (reminiscent of critical phenomena and visible to the naked eye) may be associated with oxide states of the metal, since the experiments were not performed in vacuum. When cycled in temperature, fluctuations in the length of a gold wire were found to exhibit dramatic hysteresis. With influence from Prof. Tom Erber of Illinois Tech University, it was postulated in (Peters, 1993a) that there may be some mesoscale quantization of fundamental type responsible for the thermal hysteresis (hysteron).

Mechanical hysteresis resulting from mesoanelastic defect structures is evidently ubiquitous. Piezotranslators, which are used as actuators in atomic force microscopes and other nanotechnology applications, are afflicted with high levels of hysteresis when operating open loop. This behavior is consistent with the anomalously large damping that was observed with a pendulum (reported elsewhere in this document) in which there was a steel/PZT interface for the knife-edge.

Even the common strain gauge exhibits complex hysteresis behavior. The normally large hysteresis that is observed in preliminary cycling of a gauge is typically reduced by significant amounts after repeated cycling, a type of work hardening (if strained well below failure limits). It should be noted that the hysteresis of all the discussions in this chapter is not to be confused with backlash (as in a gear train).

All of these experiments are in keeping with the premise that *mesoanelastic complexity* determines the nature of hysteretic damping. It is seen that there are a plethora of examples where strain (and thus damping) of a sample is not simple, is not smooth, but more like the complex behavior of granular materials. In the case of polycrystalline metals, the same grains that are made visible by methods of acid etching decoration are evidently responsible for mesoscale (nonsmooth) internal friction damping. To assume that damping is quantal at the atomic scale, rather than the mesoscale, is without experimental justification. Nevertheless, this is a popular assumption with which estimates of the noise floor of an instrument such as a seismometer is estimated, to calculate SNR.

2.2.3 The Pendulum as an Instrument for the Study of Material Damping

Because of its early contributions to physics, which in those days was called natural philosophy, one might be tempted to believe that the pendulum is only important to (i) the history of science or (ii) teaching of fundamental principles. A single observation should be sufficient to resist this temptation — (as already noted) the pendulum has in the last 30 years become the primary archetype for the new science of chaos. Additionally, many of the data sets of this document, which show significant and previously unpublished results, were generated with a pendulum.

To a student of elementary physics, the choice of a pendulum may seem unsophisticated. Yet, to the author, who has spent 15 intense years trying to understand harmonic oscillators, the pendulum is the most versatile instrument with which to understand damping. It has been central to the development of science in general. It was studied by Galileo, Huygens, Newton, Hooke, and all the best-known scientists of the Renaissance period. It served to establish collision laws, conservation laws, the nature of Earth's gravitational field and, most of all, it was the basis for Newton's two-body central force theory. This theory was foundational to the development of classical mechanics, which is central to all of physics and engineering. Historian Richard Westfall has remarked: "Without the pendulum, there would be no Principia" (Westfall, 1990).

In 1850, Sir George Gabriel Stokes published a foundational paper (Stokes, 1850). His treatment of pendulum damping permitted the understanding, decades later, of a number of important phenomena in physics and engineering. For example, his studies were foundational to the Navier–Stokes equations of fluid mechanics. Moreover, viscous flow known as Stokes' Law was the basis for Millikan's famous oil drop experiment that determined the charge of the electron.

Stokes noted in his paper that, "… pendulum observations may justly be ranked among those most distinguished by modern exactness." He also noted

> The present paper contains one or two applications of the theory of internal friction to problems which are of some interest, but which do not relate to pendulums. … the resistance thus determined proves to be proportional, for a given fluid and a given velocity, not to the surface, but to the radius of the sphere. … Since the index of friction of air is known from pendulum experiments, we may easily calculate the terminal velocity of a globule [water] of given size. … The pendulum thus, in addition to its other uses, affords us some interesting information relating to the department of meteorology.

The last statement of this quotation speaks to some of the errors in the "common theory" of his day. In similar manner, some of the common-to-physics damping models of today are erroneously applied. Those who hold the viscous damping linear model in unwarranted regard, fail to recognize the limitations under which it is valid. There are frequent misapplications for reason of experimental deficiencies. We can all profit by taking seriously the following well-known words of Kelvin:

> When you can measure what you are speaking about, and express it in numbers, you know something about it. But when you cannot measure it, when you cannot express it in numbers, your knowledge is of a meager and unsatisfactory kind. It may be the beginning of knowledge but you have scarcely in your thoughts advanced to the state of science. William Thomson, Lord Kelvin (1824 to 1907)

Simple (viscous) flow of the Stokes' Law type is possible only according to the restrictive conditions that Stokes spelled out in his paper. We now specify those conditions for viscous flow according to the nondimensional parameter given us late in the 19th century by Osborne Reynolds. Specifically, Stokes' Law is valid only for $\mathrm{Re} = \rho v L/\eta < 60$ (approximately, for spheres); where ρ is the density of the retarding fluid, v is the speed of the object relative to the fluid, L is a characteristic dimension of the object, and η is the viscosity of the fluid. The requirement is not generally met for oscillators, and recent experiments have shown that contributions to the damping from air drag proportional to the square of

the velocity cannot generally be ignored (Nelson and Olssen, 1986). This is just one example of how two or more damping types must sometimes be folded into an adequate model of dissipation. A novel method for combining all the common forms of damping in one mathematical expression is provided in this document. Additionally, it is shown how to calculate analytically the history of the amplitude of free-decay for such cases.

Considering the importance of Stokes' work, it is surprising that some of his requests for further experiments were apparently never seriously considered. On page 75 of his paper, one reads the following: "Moreover, experiments on the decrement of the arc of vibration are almost wholly wanting." Having noted this, Stokes appealed to experimentalists to generate such data. In the 19th century, collecting the data he requested would have been labor-intensive and therefore the experiments were probably never attempted. Sensors and data processing of the modern age now make them straightforward, but the pendulum has by now been viewed by too many as a relic rather than the important instrument described by Stokes. Much of the author's efforts have been directed at showing that the pendulum is still an important research instrument. For example, one physical pendulum of simple design was the basis for the generalized model of damping (modified Coulomb) that is here presented. Another has been used to illustrate surprisingly rich complexities of the motion that results from the ubiquitous defects of its structure (Peters 2002a, 2002b, 2002c). Thus studying the complex motions of "low and slow" physical pendula could yield significant new insight into the defect properties of materials — a field where relatively little first-principles progress has been made.

2.2.4 "Plenty of Room at the Bottom"

Richard Feynman gave a now-famous talk in 1959 titled, "There's plenty of room at the bottom" (presented at the American Physical Society's annual meeting at CalTech). Drawing on observations from biology, he spoke of a solid-state physics world involving "… strange phenomena that occur in complex situations." In the 44 years since Feynman's prophetic comments, there have been spectacular achievements in very large-scale integrated (VLSI) electronics, microelectromechanical systems (MEMS), and even nanotechnology. Progress in the mechanical (including sensor) realm has been much slower than in electronics; consequently, our present processing power far exceeds our acquisition (and actuator) capabilities.

One of the major obstacles to miniaturization involves dramatic change to physical properties that can occur as the size of a system shrinks below the mesoscale toward the atomic. For example, VLSI electronics is already beginning to be impacted by quantum properties of the atom, as component size continues to decrease in accord with Moore's law (Moore, 1965). Among other things, Feynman predicted that lubrication would no longer be "classical" at such a scale. On a related note, a paper by Nobel Laureate Edward M. Purcell (Purcell, 1977) draws a striking contrast between our macroscopic world and that of micro-organisms. At low Reynolds number, inertia becomes unimportant, and mechanics is dominated by viscous effects. The adoption of a new paradigm will be necessary for engineers to deal with these differences.

In the article "Plenty of room indeed" (Roukes, 2001), it is noted that there is an anticipated "dark side" of efforts to build truly useful micro- and nano-sized devices. Gaseous atoms and molecules constantly adsorb and desorb from device surfaces. This process is known to exchange momentum with the surface, even permitting scientific study of the gas–solid interface (Peters, 1990). The smaller the device, the less stable it will be because of adsorption/desorption. As Roukes has noted, this instability may pose a real disadvantage in various futuristic electromechanical signal-processing applications (Cleland and Roukes, 2002).

There is direct evidence, provided in the present chapter, that we need to be more concerned with noise: (i) the evacuated pendulum where it is speculated that outgassing influenced its free-decay, and (ii) the seismometer free-decay that showed both amplitude and phase noise and evidence for nonlinear damping. Concerning (i), when the vacuum chamber pressure is reduced, the preexisting steady state (normal rate balance between adsorption and desorption) becomes disturbed, so that there is a complex

emission of gases from the surface of the pendulum. The emission is not likely to be spatially uniform, but more like the jets seen on Halley's comet when photographed by the Giotto spacecraft in 1986. In case (ii), the noise is seen to derive from mesoanelastic complexity of the structure of the pendulum itself rather than involving gases.

Miniaturized devices have the potential to serve as on-chip clocks, and the importance of phase noise to clocks is well documented. There is another, more subtle issue that points out the importance of phase noise. One of the best means for improving SNR is the technique of phase-sensitive detection, first employed by Robert Dicke at Princeton to improve solar experiments. The performance of miniaturized electromechanical sensors using "lock-in" amplifier methods may be influenced significantly by mechanical phase noise.

Phase noise of miniaturized devices is still mostly speculative. In addition to the mechanism just mentioned (adsorption/desorption), there is the matter that constitutes the theme of this chapter, defect organization. It is not possible to grow materials without dislocations and/or other disturbances to crystalline order, such as vacancies, interstitials, or substitutional impurities. Thus, "when mother nature fills the vacuum she abhors, she rarely does so with perfection."

Long before defects organize to the point of incipient failure (at much larger strains), they still influence vibration. They may even be a primary source of $1/f$ noise. Electronic noise of $1/f$ type is known to involve defects by means of trapping states, and these states derive from crystalline defects sometimes involving the surface. The interaction of the surface and the volume of a solid are important. For example, consider pure copper single crystals of the type used by the author in his doctoral work. A practical joke suggested by Vic Pare (that we never conducted because of the cost of these samples) would be to have a 98-lb weakling bend one by hand, then ask an NFL linebacker to straighten it back out! The striking irreversibility is the result of work hardening as dislocations develop at the surface and propagate into the bulk where they entangle.

In the case of polycrystalline materials, the memory features of hysteresis may be important according to the method of their fabrication. Wires are typically produced by pulling through successively smaller dies. This "swaging" may be conducive to the exchange of monolayer groups of atoms between the volume and the surface during fluctuation length changes. The fluctuation–dissipation theorem does not hold or, if it does, only in terms of larger entities than the atom. Thus, there are many yet-to-be-quantified elements of noise in the vibration of miniaturized devices. Feynman was right when he spoke of strange phenomena of the solid state.

Technology of the future is expected to be confronted increasingly with damping problems that must address issues of scaling — to deal with some factors discussed in this chapter, which, to the author's knowledge, have not been previously published. Until small (MEMS) oscillators become more common to the engineering world, we must study the mechanisms responsible for their damping by other than traditional means. One approach is similar to experimental techniques for the verification of the kinetic theory of gases. As noted by Present in his textbook (Present, 1958), there are two ways that Brownian motion can be studied: either (i) with small objects and an unsophisticated detector, or (ii) with larger objects and a very sensitive detector. It is the latter that provided some of our present knowledge of damping at the mesoscale. The fully differential capacitive transducer, whose patent label is "symmetric differential capacitive" (SDC), is a robust new technology that is sensitive, linear, and user-friendly (Peters, 1993a, 1993b). As with other sensitive detectors that have been used to predict the properties of small objects by studying larger ones, small-energy studies of various macroscopic pendula are demonstrating some of the "strange phenomena" of complex type predicted by Feynman.

From the author's perspective, we of the physics community have been guilty of two significant errors: (i) oversimplification of many problems by assuming a linear equation of motion based on viscous damping, and (ii) losing sight of fundamental issues by working with inappropriate, overly complicated damping models. The goal of this chapter is to assist progress toward a healthier balance between these extremes. It is hoped that readers will be thus better equipped to identify, and then dismantle, some of the impediments to the development of future technologies.

2.3 Background

2.3.1 Terminology

The large number of mechanisms capable of energy dissipation has resulted in a host of adjectives to describe damping phenomena in mechanical systems. They include (nonexhaustive list): viscous, eddy current, Coulomb, sliding, friction, structural, fluid, thermoelastic, internal friction, viscoelastic, material, solid, phonon–phonon, phonon–electron, and hysteretic. For present purposes, damping types will be grouped according to one of the following three categories: (i) fluid (including viscous), (ii) Coulomb, and (iii) hysteretic. Although hysteretic damping has come to be associated in engineering circles with a particular form of material damping in solids, it should be noted that all forms of damping involve hysteresis (for which the Greek meaning of the word is "to come late"). In a plot of periodic stress vs. strain, which is a straight line for displacements of a nondissipative, idealized substance, hysteresis causes the line to open into a loop. The size of the loop — more specifically the area inside this hysteresis loop — is a measure of the amount of nonrecoverable work done per cycle because of the damping. An actual force of friction is not readily recognizable in those cases that are labeled "internal friction." The word friction is used in a generic sense, meaning any process responsible for conversion of the oscillator's coherent motion into incoherent thermal activity.

With each of viscous, eddy current, and Coulomb damping, a force external to the oscillator is responsible for the dissipation of energy. The external force is associated respectively with (i) laminar fluid flow, (ii) induced currents, and (iii) surface friction. The surface friction case is not necessarily the trivial textbook presentation involving a coefficient of kinetic friction and a normal force. The cases just mentioned, along with thermoelastic damping; which is of internal rather than external origin, are much easier to treat theoretically than other cases. Viscous damping and eddy current damping (over the full range of the motion) are adequately described by a velocity term, which yields a linear equation of motion. Coulomb damping, however, is not proportional to velocity, but rather depends only on the algebraic sign of the velocity. The equation of motion is consequently nonlinear. Additionally, and unlike most other forms, Coulomb damping is not exponential. The turning points lie along a straight line when the motion is plotted vs. time. Similarly, if eddy current damping exists only over a small part of the motion, the decay is linear rather than exponential (Singh et al., 2002).

2.3.2 General Technical Features

Historically, viscous damping has been the model of choice because the resulting equation of motion is mathematically attractive and, for the RLC circuit, the form is appropriate. For mechanical oscillators, it is not generally appropriate, since viscous damping amounts to some part of the system moving in an external Newtonian fluid that removes energy because of a friction force that is proportional to velocity.

The defects responsible for material damping, such as dislocations, are also responsible for creep, so that high strength and high damping tend to be incompatible attributes. Magnesium alloys tend to be better than many other metals in this regard. Hardness of a material is neither a prerequisite for toughness nor for small damping, as recognized by those familiar with the mechanical properties of cast iron.

On a different scale, defects determine "how things break"; concerning which Marder and Fineberg have stated the following:

> the strength of solids calculated from an excessively idealized starting point comes out completely wrong; it is not determined by performance under ideal conditions, but instead by the survival of the most vulnerable spot under the most adverse of conditions. (Marder and Fineberg, 1996)

Three famous scientists are primarily responsible for the highly popular viscous damping model of the simple harmonic oscillator; they are Lord Kelvin (Thomson and Tait, 1873), G.G. Stokes and

H.A. Lorentz. Stokes is best known for his equations of fluid dynamics that also include the name Navier. Stokes' Law, which describes the terminal velocity of a raindrop, was developed through his treatment of the damping of a pendulum. Not only does his law provide a basis for the simplest approximation for damping of a macroscopic oscillator, it was used by Robert Millikan to determine the charge of the electron. It should be noted that harmonic oscillation in a fluid (even at low Reynolds number) is much more complicated than steady-flow viscous friction. This topic is treated in Chapter 3, Section 3.9.

The first individual to use the term "simple harmonic oscillator" was probably Lord Kelvin. Such an oscillator is a key tool of experimental physics and also the foundation for much of theoretical physics. It is the basis for communication via electromagnetic waves and even esoteric theories of superfluids and superconductors.

Much of the underpinnings of theory involving harmonic oscillation derive from the work of Hendrik Anton Lorentz (1853–1928). Lorentz is well known for a variety of classical physics contributions, such as (i) the transformation of special relativity associated with Einstein and (ii) the force law for the acceleration of charged particles, both of which bear his name. Before the existence of electrons was proved, Lorentz proposed that light waves were due to oscillations of an electric charge in the atom. For his development of a mathematical theory of the electron, he received the Nobel Prize in 1902. The importance of his contributions is further realized by noting that it is common practice to describe the lineshape of atomic spectra by the term Lorentzian. The Lorentzian is equivalent to the resonance response of the driven viscous-damped simple harmonic oscillator.

It is easy to show how resistance in an electric network is responsible for damping; however, it is a challenge to understand anelastic processes of mechanical damping in terms of viscosity. From comments of his Ph.D. dissertation, it has been said that even Lorentz was never apparently satisfied with the velocity damping term in his equation — not knowing just how to relate it to the underlying physics. It is also clear from Stokes' paper that he recognized the need for caution in the use of his law of viscous friction. It appears that both Lorentz and Stokes were very careful compared with the carelessness with which the viscous model has been employed by many individuals in recent years.

The failure of solids influenced by "hysteretic" damping to be adequately described by the methods of viscoelasticity is not widely appreciated. It is unfortunate that too few people have expanded their view of damping to include other important types, such as derive from the anelasticity of solids. It is important in this work to recognize some subtle differences, for example, inelastic (not elastic) is not to be equated with anelastic (other than elastic).

2.3.3 Active vs. Passive Damping

With improvements in cost/performance of electronics, active damping is increasingly popular. Using force-feedback with integration/differentiation circuitry (opamps), a mechanical oscillator can sometimes be tailored for a specific purpose. A sophisticated example of this technology is the broadband seismometer that began to replace earlier version (passive) instruments roughly 35 years ago. The Sprengnether–LaCoste spring instrument that was used for some of the experiments reported in this document has been superceded by force-feedback units such as the Streckeisen STS-1 and STS-2.

In lieu of feedback, another way actively to influence the damping of a mechanical oscillator is to connect the sensor to an amplifier having a negative input resistance. The seismometers marketed by Lennartz Electronics in Germany use this in a patented technique to improve the performance of ordinary, off-the-shelf electrodynamic geophones.

Active damping depends on the nature of the transfer function of the composite system (electronics plus mechanical). The characteristics of the transfer function are determined by the location of its poles and zeros in the complex plane. Seismometers operate nominally near 0.707 of critical damping. This is done for two reasons: (i) the instrument is easier to adjust and (ii) the interpretation of earthquake records is simpler. Of course, to increase damping is to decrease sensitivity because of the fluctuation–dissipation theorem.

The force-feedback technique is not practical for some situations, regardless of cost. Additionally, it must be recognized that the method is not the answer to all problems, since electronics cannot compensate for a poor mechanical design. The description of commercial products is in some cases highly exaggerated, giving the impression that almost any sensor can perform flawlessly in this manner. Some accelerometers have employed dithering to offset the effects of "stiction" in bearings. The dithering was necessary because the potential energy function is not truly harmonic, being afflicted with the consequences of nonlinear damping. Even with sensing schemes that do not use a bearing, the effects of nonlinearity persist. In "Seismic Sensors and their Calibration" (Bormann and Bergmann, 2002), Erhard Wielandt, in talking about transient disturbances in the spring of a seismometer, says the following:

> Most new seismometers produce spontaneous transient disturbances, quasi-miniature earthquakes caused by stress in the mechanical components.

In other words, internal friction from defects at the mesoscale cause behavior that is in some ways similar to ordinary sliding friction, where the static coefficient is greater than the kinetic coefficient. The postulate of Bantel and Newman is consistent with this idea (Bantel and Newman, 2000) when they refer to their observations as being consistent with a "stick–slip" model of internal friction.

It is seen then that one must use a detector that responds faithfully to the signal around which the servo-network functions. The linearity and sensitivity of that sensor are of paramount importance, since the basis for force-feedback design is linear system theory. For some less-challenging cases, the design approach is straightforward, since software packages like MATLAB® (see de Silva, 2006) have built in functions to describe behavior.

2.3.4 Magnetorheological Damping

A recent approach to damping control, that is quite different from the servo-networks mentioned above, is one that uses an magnetorheological (MR) fluid. It takes advantage of the large variation in viscosity of certain compound fluids according to the size of an applied magnetic field. J. David Carlson (Carlson, 2002) describes how an MR sponge damper is activated during the spin cycle of a washing machine to keep it from "walking out of the room." The peak in the Lorentzian (resonance response) of the machine is shown in his article to be substantially lowered by supplying current to the electromagnet of the damper.

2.3.5 Portevin–LeChatelier Effect

Physics, engineering, geoscience, and mathematics have all contributed greatly to a better understanding of damping phenomena; however, there has been little cross-discipline exchange of ideas and lessons learned. Some of the impediments to strong interdisciplinary programs derive from (i) the complexity of damping problems in general and (ii) the tendency for physics and mathematics research to be, on the one hand, less pragmatic and, on the other hand, highly specialized — focused on specific energy dissipation mechanisms. A good example of (i) involves the PLC effect, discovered in 1923. Why physics mostly ignored this early example of "dirty science" by two of their own number is not easily understood, although the birthing of quantum mechanics around this time may have been a factor. Had history turned in a different direction, perhaps we would already be able to explain from first principles the most important, but still barely understood, form of noise known as $1/f$, or flicker, or pink noise. Even though R.B. Johnson (well known for his discovery of white electronics noise in a resistor) was one of the first to see this form of noise, it still is not explained from first principles — although recent discoveries suggest an intimate connection with fractal geometry involving self-similarity. Such geometry is associated with the mesoscale of materials where the grain, rather than the atom, is the basic element of statistical mechanics.

For alloys, the PLC effect appears to be, in some ways, what the Barkhausen effect is to magnetic systems. In the case of ferrous materials, the noise which derives from the mesoscale has long been recognized; however, similar noise of mechanical type has not been seriously studied. This oversight is even more puzzling when one considers the admonition by G. Venkataraman, as recorded in the

proceedings of a Fermi conference, for scientists to get involved in what he felt should become an important new field (Venkataraman, 1982).

2.3.6 Noise

Noise is purposely discussed in this chapter (also see the chapters in Section IX of this handbook) because it has been a, largely, missing component of efforts to understand the physics of damping. A feel for the importance of noise to damping research is to be gleaned from a comment by Kip Thorne in his foreword to the English translation of a book by V.B. Braginsky et al. (1985). Mainly because of instrumental needs of the Laser Interferometer Gravitational Wave Observatories (LIGO), Thorne writes,

> The central problem of such experiments is to construct an oscillator that is as perfectly simple harmonic as possible, and the largest obstacle to such construction is the oscillator's dissipation. If dissipation were perfectly smooth, it would not be much of an obstacle, but the fluctuation–dissipation theorem of statistical mechanics guarantees that any dissipation is accompanied by fluctuating forces. The stronger the dissipation, the larger the fluctuating forces, and the more seriously they mask the signals that the experimenter seeks to detect.

This comment by Thorne suggests a frequently important impediment to dialogue between engineering and physics — concern for different issues. LIGO is trying to minimize damping, whereas many engineering problems are concerned with just the opposite — making the damping as large as possible without compromising strength. More detailed discussions of noise are provided later.

2.3.7 Viscoelasticity

Within the world of polymers, damping is frequently described by the expression "viscoelasticity." This word, around which handbooks have been written (e.g., Lakes, 1998), is a combination of the two words, viscous and elastic. We like to think of ideal fluids as being viscous in the manner described by Newton. Likewise, ideal solids that obey Hooke's Law (stress proportional to strain) are described as elastic. Unfortunately, nature contains neither ideal solids nor ideal fluids. Real springs do not obey Hooke's Law, but rather are influenced by "anelasticity" (other than elastic) which gives rise to hysteresis in the stress–strain relationship. Real fluids usually have some (if not near total) degree of non-Newtonian character. Thus an envisioned "mixing" of fluid-like and solid-like character has dominated the thinking of those who, through the decades, attempted to develop theoretical models of damping.

It should be noted that the springs and dashpots used in models of viscoelasticity do not actually exist. They serve as a phenomenological means for (hopefully) understanding the elementary processes which their arrangement is designed to mimic. Consider, for example, high polymers, in which the interwoven structure of the long-chain molecules is one of extensive mechanical interference. (One popular visualization is that of an entanglement of a huge number of long, writhing snakes.) An increase of temperature is met with overall length reduction (negative temperature coefficient of expansion for the so-called entropy spring), which stands in stark contrast with metals. Such behavior is clearly important to damping since, as noted by Gross years ago, "…thermal movement interferes with the orientation and disorientation of the molecules and ultimately causes delay in the expansion and contraction of the specimen" (Gross, 1952).

2.3.8 Memory Effects

In this same article, Gross is one of the first to mention "memory" properties of creep. He describes a by-then old demonstration in which a "firmly suspended metal or plastic wire is twisted first in one direction for a long time and then in the other direction for a short time. Immediately after release,

the deflection will be in the direction of the last twisting, but it decreases rapidly. Presently, a reversal occurs, and the wire begins to turn in the other direction, corresponding to the first twisting — the memory of the recent short-term handling has been obliterated by that of the more remote but longer lasting and therefore more impressive one!" Perhaps this old demonstration (sometimes today called the anelastic after-effect) is not so startling to those familiar with more modern shape-memory-alloys, which are expected by many to play increasingly important roles in the applied science of damping.

2.3.9 Early History of Viscoelasticity

Those who provided seminal influence in the development of the theories of viscoelasticity during the 19th century were some of the most famous names in physics, like Maxwell and Kelvin. Maxwell is best known for the electromagnetic equations associated with his name. He is far less known for two other significant contributions: (i) kinetic theory of gases and (ii) viscoelasticity — both of which are important to theories of oscillator damping. Maxwell's interest in the problem of viscoelasticity is first documented in a paper during his teen years, titled "The Equilibrium of Elastic Solids." Through his development with Boltzmann of the kinetic theory of gases, Maxwell showed a counterintuitive property of the viscosity of a gas. The viscosity does not decrease significantly as the pressure is reduced, until the mean free path between collisions of the molecules begins to approach dimensions of the chamber holding the gas. Important even to modern innovations such as MEMS oscillators, his surprising prediction was quickly verified by experiment. Maxwell's model of viscoelasticity combines a purely elastic spring with a purely viscous dashpot (fluid damper in which the friction force is proportional to the velocity).

Kelvin, probably the first to include a viscous damping term in the equation of motion of the simple harmonic oscillator, developed a similar model of viscoelasticity. Each of the two models is usually represented in literature (without original references) as containing a single spring and a single dashpot. They differ in that one connects the pair in series (Maxwell), while the other connects them in parallel (Kelvin–Voigt).

Both the Maxwell model and the Kelvin–Voigt model have been found by engineers to be less useful than the standard linear model (SLM) of anelasticity, largely advanced in the 20th century by Clarence Zener (Zener, 1948). In the three-component Zener model, a spring is connected in series with a parallel combination of spring and dashpot. Curiously, Zener is widely associated with electronics because of the common diode named after him, but fewer people know of his work in anelasticity. No doubt, his understanding of anelasticity helped him to better understand the complex processes at work in his diode.

2.3.10 Creep

The prevailing models of anelasticity appear frequently in the literature, but mostly in relationship to primary creep. Some of the papers exceptional to this rule are those by Berdichevsky (Berdichevsky et al., 1997). Recent work of a more heuristic type has shown that the equations of viscoelasticity are also able to accommodate secondary creep, in which the decay of strain rate with time has disappeared (Peters, 2001a, 2001b).

The importance of creep (and relaxation) physics to damping warrants some discussion. When a sample is subjected to a constant stress, the strain evolves through three phases of creep: (i) primary, (ii) secondary, and (iii) tertiary. An example of the first two of these phases is shown in Figure 2.2.

In the primary stage, the sample is deformed by anelastic processes involving defects of the crystalline structure. Influence of the disordering mechanisms is progressively reduced as the sample undergoes work hardening (such as pinning of dislocations). Work hardening would result in a purely exponential creep, in the absence of thermal effects which strive to undo the hardening (via diffusion processes). (At zero Kelvin, the creep would eventually cease, if described by a single time constant.) In the secondary stage, a balance between work hardening and thermal softening is attained, in which the strain vs. time has converted from exponential to linear. This balance cannot continue forever, if the stress is larger than

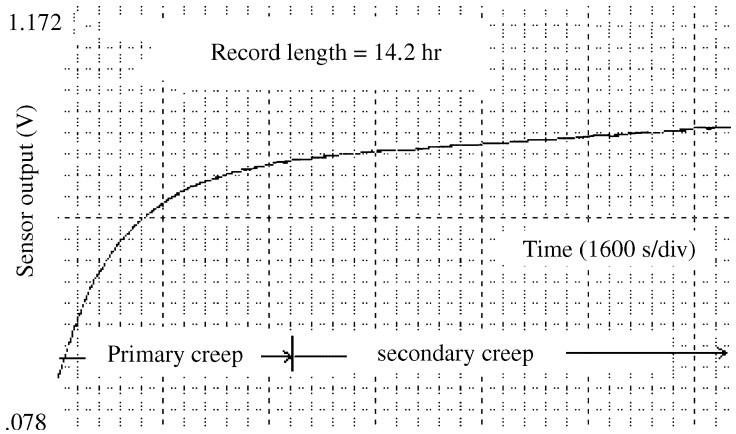

FIGURE 2.2 Example of creep in the spring of a vertical seismometer.

a threshold associated with failure (the elastic limit), and thus a final complex fracture of the sample finally occurs as the sample passes through the tertiary stage. Although one might want to divorce the issues of tertiary creep from considerations of damping, there is clearly a link between damping and failure, involving defects. We will return to this point later.

In Figure 2.2, creep resulted from the instrument having been severely disturbed (relocated accidentally by plumbers working in the building). As with any long-period mechanical oscillator, it is necessary for this instrument to stabilize after a major rebalancing. Primary creep is seen to have endured for about 5 h and what is labeled secondary creep in the figure does not continue indefinitely with the implied constant rate. Thus, the instrument will typically stabilize after one or several days, when the period of oscillation is of the order of 20 sec.

The total amount of creep in Figure 2.2 deserves mention. In the indicated 14.2 h, the mass of the seismometer moved a vertical distance of only 0.25 mm, which can be ascertained from the ordinate axis using the sensor calibration constant of 2000 V/m.

2.3.11 Stretched Exponentials

Systems typically demonstrate a more complex behavior than can be simply described by the SLM of viscoelasticity. In 1847, Kohlrausch (1847) discovered that the decay of the residual charge on a glass Leyden jar followed a *stretched exponential* law. The functional form that he discovered is often associated with a broad distribution of relaxation times, and has been found to describe a remarkably wide range of physical processes. To describe damping that is of the stretched exponential type, Kelvin chains or Maxwell elements in parallel have been used. Although an improved fit to the data can be realized by this means, the technique results in a high number of material parameters which have to be identified.

2.3.12 Fractional Calculus

A promising alternative to multiexponential decay models is to replace classical rheological dashpots by "fractional" elements. It is claimed that with only a few parameters, material behavior of many viscoelastic media can be described over large ranges of time and/or frequency (Hilfer, 2000). It may also be possible with fractional derivatives to treat the discontinuities that are sometimes present in decay (Asa, 1996). The disadvantages of fractional calculus are (i) the increasing computational/storage requirements and (ii) the esoteric mathematics, which is alien to the training of most.

2.3.13 Modified Coulomb Damping Model

Published here formally for the first time, with details described later, the heuristic "modified Coulomb" model is an alternative to all of the aforementioned damping models. It is thought to be closely related to secondary creep (Peters, 2001a, 2001b) and (like fractional calculus) accomplishes good fits with a small number of parameters. Developed from energy considerations, its equations are expressed in canonical form involving the quality factor Q.

2.3.14 Relaxation

Formally, relaxation is defined by the behavior of a sample subjected to a constant strain. Because of the mechanisms just discussed in relationship to creep, the stress relaxes exponentially toward zero (in the simplest approximation). In practice, the definition just given can be misleading since the word relaxation is used to describe a host of processes in which some quantity decays exponentially in time — for example, the relaxation of strain at constant stress in the Kelvin–Voigt model of viscoelasticity.

Some of the viscoelastic models using dashpots and springs have been quite successful in the limited regime of their applicability. For example, the Zener (Debye) model, which will be discussed again later, has been used for years to describe a particular form of damping in solids, which derives from relaxations associated with dislocations. Seminal experimental work of this type was conducted by Berry and Nowick in the 1950s (Berry and Norwich, 1958). A well-known theoretical model to describe dislocation damping was developed by Granato and Lucke (Granato and Lucke, 1956). The Granato model is that of a vibrating string (bowed Frank–Read source), where the end points of the "string" are points on the dislocation line that have been pinned. Recent theory shows that the Granato model is not always adequate; that "dislocation interactions may alter substantially the dislocation component of the spectrum observed during internal friction experiments." (Greaney et al., 2002) (excellent introductory material on this subject is to be found online at http://mid-ohio.mse.berkeley.edu/alex/rachel/rachel/rachel.html).

Bordoni (1954) performed experiments that led to his observation of relaxation-type internal friction processes where the acoustic attenuation is seen to peak at certain temperatures. The so-called Bordoni peaks occur at low temperatures or at ultrasonic frequencies. These losses, which are maximum when dislocation relaxations can take place in step with the driving frequency, were first observed in the FCC metals: lead, copper, aluminum, and silver.

Dislocation damping as just described is characterized by a temperature-dependent relaxation that exhibits Arrhenius behavior. By plotting the internal friction vs. reciprocal temperature, one may estimate the activation energy of the process responsible for the damping. The following quotation from the introduction of the Berry paper assists in defining some of the many expressions used historically to describe damping:

> Internal friction is often loosely described as the ability of a solid to damp out vibrations. More strictly, it is a measure of the vibrational energy dissipated by the operation of specific mechanisms within the solid. Internal friction arises even at the smallest stress levels if Hooke's Law does not properly describe the static stress–strain curve of the material. The nonelastic behavior which Zener has called anelasticity arises when the strain in the material is dependent on variables other than stress.

In a recent private communication, Prof. Granato has indicated the following:

> Dislocations do follow the Zener (or Debye) form fairly well for the damping, but not for the elastic modulus. This is because the response to a stress is given as a Fourier series. The higher order terms in the series have little effect on the damping, but a strong effect on the modulus at high frequencies. This makes the modulus fall off more slowly than with the reciprocal frequency.

2.4 Hysteresis — More Details

Hysteresis and creep are common to many systems, such as electromechanical actuators, especially when used at high drive levels. Their transfer function is influenced by "rate-independent memory effects." The state of the actuator depends not only on the present value of the input signal but also on the nature of their past amplitudes, especially the extremum values, but not on rates of the past (Visintin, 1996). This statement is in support of the author's secondary creep model of hysteretic damping, where the amplitude of the previous turning point determines the magnitude of the internal friction force for the half-cycle that follows. One of the most dramatic examples of a memory effect is the demonstration mentioned above, by Gross in the 1950s, concerning a twisted wire.

Damping complexities derive from the defect structures that are found in real materials and which give rise to hysteresis, which in the Greek language means to "come late." Although, almost everybody seems to appreciate magnetic hysteresis at some level, too few individuals (at least in physics) have been trained in the mechanisms of mechanical hysteresis responsible for damping. Dislocations, for example, are usually an add-on chapter to a solid-state physics text — even though they are known to be indispensable with regard to actual, as opposed to idealized, properties of materials.

In the case of ferrous materials, the magnetization of a specimen lags behind the field generated by an electric current, to which the specimen responds. In the case of real springs that do not obey Hooke's Law $F = -kx$, the displacement x lags behind the spring's restoring force F. It is convenient to express the resulting hysteresis in terms of "intrinsic" variables instead of x and F. Thus, the strain ε (fractional change in the spring's length if it were a wire in tension) lags the stress σ (force per unit area). Usually in engineering practice, the stress is reckoned with respect to the external force (negative of the spring F), so that the equivalent to Hooke's Law is $\sigma = E\varepsilon$, where E is an elastic modulus descriptive of the material from which the spring is fabricated. In the case of a straight wire, E would be Young's modulus but, for coil springs, E is determined primarily by the shear modulus. Some of the ways in which hysteresis can be represented for a freely decaying oscillator are shown in Figure 2.3. The generalized coordinate q would be spring elongation for the force case shown, or it would be strain when the ordinate quantity is stress. The graph of velocity vs. displacement is referred to as a phase-space plot. It is commonly used in describing chaotic systems and, if "strobed" at the frequency of the oscillator, becomes the Poincaré section. Notice that the circulation is of opposite sign when using external force as opposed to spring force, in addition to the curves occupying different quadrants. It is important to recognize this difference, particularly when discussing negative damping where the oscillation amplitude builds in time, as illustrated in the right hand part of the figure.

Although not very common in mechanical oscillators, it is possible to realize negative damping. One example is that of an optically driven pendulum, because of the LiF crystals that were placed in its support structure (containing a high density of color centers produced by radiation) (Coy and Molnar, 1997). An interesting feature of this pendulum was its unwillingness to entrain to the driving laser.

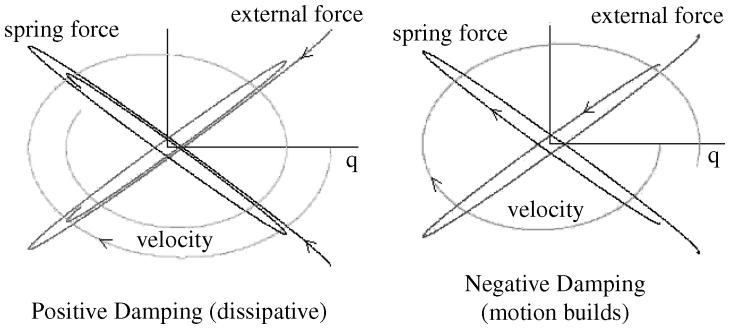

FIGURE 2.3 Three different ways to represent hysteresis damping for an oscillator in free-decay. Cases of both positive and negative damping are illustrated.

There are also examples of negative damping from aerodynamics, such as flutter. Since buildings and bridges can experience negative damping in catastrophic manner (Tacoma Narrows bridge as an example), it is not a subject to be ignored.

Another example of hysteresis that is very much like negative damping (though not usually labeled as such) is to be found in a heat engine (Peters, 2001a, 2001b). The motion is not simple harmonic; rather, the speed with which the hysteresis curve is traversed (in pressure vs. volume) increases as the size of the hysteresis loop increases. A larger loop (greater work done by the gas) results in higher revolutions per minute (r/min) of the engine as opposed to a larger amplitude of the motion at constant period. The gas pressure provides a force similar to the Hooke's Law force of the spring in a mass/spring oscillator.

It is usually assumed that hysteresis loops are "smooth," which is not necessarily true. For example, in the case of magnetic hysteresis, the "jerky" parts known as the Barkhausen effect (Barkhausen, 1919) are well known. The equivalent jerky behavior in metallic alloys is known as the Portevin–LeChatelier effect (Portevin and LeChatelier, 1923). Although we have historically avoided these cases that appear to be intractable in a mathematics sense (not obeying the fundamental theorem of calculus), their presence is undeniable testimony of the complex nature of hysteresis.

2.5 Damping Models

2.5.1 Viscous Damped Harmonic Oscillator

As first seen by students in a textbook, the equation of motion for a damped, driven harmonic oscillator is likely as follows:

$$m\ddot{x} + c\dot{x} + kx = F(t) \tag{2.1}$$

where m is mass, k is spring constant, c is a "constant" of viscous damping, and $F(t)$ is the external force driving the oscillator. It is convenient to work with a coefficient of performance, or quality factor Q, and rewrite Equation 2.1 in canonical form as

$$\ddot{x} + \frac{\omega_0}{Q}\dot{x} + \omega_0^2 x = \omega_0^2 \frac{F(t)}{k}, \text{ with } \omega_0^2 = \frac{k}{m} \tag{2.2}$$

For $F(t) = 0$ and an assumed solution, $x = A\exp(p\theta)$ with $\theta = \omega_0 t$, the differential equation becomes algebraic (quadratic) in $x(\theta)$, with the roots given by

$$p = -\frac{1}{2Q} \pm \sqrt{\frac{1}{4Q^2} - 1} \tag{2.3}$$

Depending on the value of Q, the motion is either overdamped (nonoscillatory), critically damped, or underdamped. Here, we restrict our attention to the last case corresponding to $Q > 1/2$, in which the square root term of Equation 2.3 is imaginary. Moreover, we are mostly concerned with systems in which $Q >> 1$.

2.5.2 Definition of Q

The quality factor Q is in general defined as 2π times the ratio of the energy of the oscillator to the energy lost to friction per cycle. For viscous damping (and hysteretic damping, later discussed), the Q is independent of the amplitude of oscillation. For other types of damping, we will see that the Q is not constant. In the case of the viscous damped oscillator, $Q = \omega_0/2\beta$ where β appears in the solution as an amplitude decay "constant." The parameter β is not really constant, as discussed in Chapter 3, Section 3.9.

$$x = A\, e^{-\beta t} e^{\pm j\omega_0 t\sqrt{1-1/4Q^2}} \tag{2.4}$$

Since x is real, we use the real part of Equation 2.4 and employ Euler's identity to obtain

$$x(t) = A\,\mathrm{e}^{-\beta t}\cos(\omega_1 t - \phi),\ \text{with}\ \omega_1 = \sqrt{\omega_0^2 - \beta^2} \tag{2.5}$$

where ϕ is a constant determined by the initial conditions.

2.5.3 Damping "Redshift"

It is seen that the frequency of oscillation depends on the damping constant, β; however, the fractional change $\Delta\omega/\omega_0$ is almost always negligibly small. For example, the reduction in frequency is only 1.4% for $Q = 3$, which is close to critical damping of $Q = 0.5$. At these small values of Q, the lifetime of a freely decaying oscillator is so short that the frequency is ill-defined because of the Heisenberg uncertainty principle. At larger Qs, where the frequency is well-defined, the shift is negligible; i.e., at $Q = 100$, the fractional shift is only 1.3×10^{-5}. In the case of internal friction (hysteretic) damping, there is no redshift anyway because the oscillator is isochronous.

2.5.4 Driven System

When $F(t)$ is not zero, but rather corresponds to harmonic drive at angular frequency ω and amplitude A, the response involves the sum of Equation 2.5 (transient) and a particular solution (steady state).

$$x_p(t) = A_p\cos(\omega t - \delta),\ \text{with}\ \delta = \tan^{-1}\left(\frac{2\omega\beta}{\omega_0^2 - \omega^2}\right). \tag{2.6}$$

The system resonates (amplitude a maximum) at $\omega \rightarrow \omega_R = \sqrt{\omega_0^2 - 2\beta^2}$, and the variation of the amplitude with ω at steady state at any drive frequency ω is given by

$$A_p = \frac{A\omega^2}{\sqrt{(\omega_0^2 - \omega^2)^2 + 4\omega^2\beta^2}} \tag{2.7}$$

The resonance response curve described by Equation 2.7 is called the Lorentzian. More frequently in physics, the term is used to describe pressure-broadened line widths (Milonni and Eberly, 1988). As noted previously, Lorentz was never apparently content with the damping term, $2\beta\,\mathrm{d}x/\mathrm{d}t$. In his Ph.D. dissertation concerned with the damping of electron oscillators through electromagnetic radiation, he was not able to satisfactorily describe the damping from first principles. Although we might be tempted to say that this failure derived from his classical (prequantum mechanics) description of the problem, such a viewpoint is an oversimplification.

2.5.5 Damping Capacity

2.5.5.1 Viscous Damping

The loss per cycle, called the damping capacity, is computed for the viscous damping case as follows (per unit mass):

$$d_v = 2\beta\oint \dot{x}\,\mathrm{d}x = 2\beta\omega A^2\int_0^{2\pi}\sin^2\theta\,\mathrm{d}\theta = 2\pi\beta\omega A^2 \tag{2.8}$$

where A is the amplitude of the oscillation. Because the total energy per unit mass is $\omega^2A^2/2$, we see that $Q = \omega/(2\beta)$.

2.5.5.2 Hysteretic Damping, Linear Approximation

The equation of motion in this case is given by $m\ddot{x} + h/\omega\dot{x} + kx = 0$ where h is a constant. The energy loss in one cycle is given by

$$-\Delta E = md_h = \frac{h}{\omega}\int_0^T \dot{x}^2\,\mathrm{d}t = \frac{h}{\omega}\omega A^2\int_0^{2\pi}\cos^2\theta\,\mathrm{d}\theta = \pi hA^2 \rightarrow d_h = \frac{\pi}{m}hA^2 \tag{2.9}$$

so that $Q = m\omega^2/h$.

2.5.5.3 Hysteretic Damping, Modified Coulomb Model

The nonlinear equation of motion introduced in this chapter to describe hysteretic damping is as follows:

$$\ddot{x} + c\sqrt{\frac{2E}{k}}\,\mathrm{sgn}(\dot{x}) + \omega^2 x = 0 = \ddot{x} + \frac{\pi\omega}{4Q_h}\sqrt{\omega^2x^2 + \dot{x}^2}\,\mathrm{sgn}(\dot{x}) + \omega^2 x = \ddot{x} + cA_{\mathrm{prev}}\,\mathrm{sgn}(\dot{x}) + \omega^2 x \tag{2.10}$$

where, in the last expression, the subscript "prev" implies amplitude at the last (previous) turning point of the motion. This particular form for the damping term (Peters, 2002a, 2002b, 2002c), thought to result from secondary as opposed to primary creep (Peters, 2001a, 2001b), is not as computationally useful as the middle expression involving the Q. The damping capacity is given by

$$-\Delta E = md_h = 4cmA\int_0^{\pi/2} A\cos\theta\,\mathrm{d}\theta \rightarrow d_h = 4cA^2 \tag{2.11}$$

yielding $Q = \pi\omega^2/(4c)$, so that the constant in the nonlinear model is related to the linear approximation constant through

$$c = \pi h/(4m)$$

2.5.6 Coulomb Damping

One of the simplest friction models is that in which a Hooke's Law spring is connected on one end to a mass that slides on a level table. The other end of the spring is connected to a stationary wall. The friction force of the mass against the table is of the type first described quantitatively by Charles Augustin Coulomb (1736–1806), although Leonardo da Vinci is probably the first to consider it scientifically. The equation of motion and its solution, for the free-decay of an oscillator damped by Coulomb friction, is given by

$$\begin{aligned} &m\ddot{x} + f\ \mathrm{sgn}(\dot{x}) + kx = 0 \\ &\text{Solution} \\ &x(t) = [x_0 - (2n+1)\Delta_x]\cos\omega t + (-1)^n\Delta_x \end{aligned} \tag{2.12}$$

The equation is nonlinear because of the sign of the velocity term, but it is easily integrated numerically; additionally, it is one of the few nonlinear equations for which an analytic solution is known and is given above (for more details, the reader is referred to Peters and Pritchett, 1997). The integer, n, specifies the number of half-cycle turning points from $t = 0$, and Δ_x is the decrement (linear, not logarithmic, having units of m) per half-cycle. There are occasions to use Equation 2.12; for example, problems in civil engineering where relative motion of members (slipping) occurs at a structural joint. The work against friction in one cycle can be obtained from energy considerations and is given by

$$f(4x_0 - 8\Delta_x) = \frac{1}{2}kx_0^2 - \frac{1}{2}k(x_0 - 4\Delta_x)^2 \tag{2.13}$$

which, for small decrement, yields

$$\Delta_x = \frac{f}{k} = \frac{f}{m\omega^2} \tag{2.14}$$

Damping characteristics for the models presently treated are summarized in Box 2.1.

Box 2.1
Damping Characteristics

Type	Equation of Motion	Damping Capacity	Q
Viscous	$\ddot{x} + 2\beta\dot{x} + \omega_0^2 x = 0$	$2\pi\beta\omega A^2 m$	$\frac{\omega}{2\beta}$
Hysteretic (linear approximation)	$\ddot{x} + \frac{h}{m\omega}\dot{x} + \omega^2 x = 0$	$\pi h A^2$	$\frac{m\omega^2}{h}$
Hysteretic (modified Coulomb)	$\ddot{x} + c_h A\ \mathrm{sgn}(\dot{x}) + \omega^2 x = 0$	$4c_h A^2 m$	$\frac{\pi\omega^2}{4c_h}$
Coulomb	$\ddot{x} + \frac{f}{m}\mathrm{sgn}(\dot{x}) + \omega^2 x = 0$	$4fA$	$\frac{\pi m\omega^2 A}{4f}$
Amplitude dependent	$\ddot{x} + c_f A^2\ \mathrm{sgn}(\dot{x}) + \omega^2 x = 0$	$4c_f A^3 m$	$\frac{\pi\omega^2}{4c_f A}$

2.5.7 Thermoelastic Damping

A microphone with Labview was used to analyze vibratory data of an aluminum rod. A rod of 1 m length can be excited to ear-piercing intensities by holding it at its center between thumb and finger of one hand, and stroking along the length with the other hand that is coated with violin-bow rosin. The decay of this "singing rod", which is a common part of physics demonstration equipment, was found to be in agreement with the following theoretical expression for thermoeleastic damping (Landau and Lifshitz, 1965):

$$\frac{1}{Q_{\mathrm{Th.d}}} = \frac{\kappa T\alpha^2\rho\omega}{9C^2} \tag{2.15}$$

where ω is the vibrational angular frequency, T is the temperature, ρ is the density of the bar, C is the heat capacity per unit volume, α is its thermal expansion coefficient, and κ is the thermal conductivity. The expression assumes adiabatic vibrations and there is no thermoelastic dissipation in pure shear oscillations (e.g., torsional oscillations of a bar) because the volume does not change and hence there is no local oscillation of the temperature. Notice, in particular, that the Q is inversely proportional to frequency, unlike viscous damping that is proportional to the frequency, or hysteretic damping that is proportional to the square of the frequency. Thermoelastic damping is important for high-frequency compressional oscillations in materials with significant thermal coefficients, and especially for metals because of their large thermal conductivity.

The demonstration of comparable behavior in polymers (entropy spring, but opposite sign compared with metals) is quite easy. Stretch a rubber band between the hands and immediately touch it to the forehead. The increase in temperature is easily sensed. Conversely, releasing the tension in the band cools it enough to be sensed by placing the band to a part of the face that is sensitive to temperature change. Equation 2.15 does not apply to polymers.

2.6 Measurements of Damping

2.6.1 Sensor Considerations

The challenge to any measurement is to accomplish the task without significantly altering the system under study (see de Silva, 2006). For measurements on mechanical oscillators of the type described in

this document, two types of sensor are generally superior to every other kind: (i) optical and (ii) capacitive. Optical sensors are probably the least perturbative but they do not readily yield themselves to large dynamic range with good linearity (and small quantization errors for digital type). Inductive sensors, such as the linear variable differential transformer (LVDT), are known from seismology to be inherently more noisy (up to 100 times) because of ferromagnetic granularity. Additionally, transformers are not amenable to miniaturization, and the components are inherently less stable. It is therefore a mystery why the widespread use of the fully differential inductive sensor (LVDT) continues when we have available the superior fully differential capacitive sensor, which is electrically equivalent (apart from its reactance type) and capable of miniaturization to the MEMS level. The challenge with really small capacitive sensors is the increase in output reactance of the device as they approach femtoFarad levels of individual capacitors.

All measurements reported in this document were taken with the fully differential unit whose patent name is "symmetric differential capacitive" (see Peters, 1993a, 1993b). It is especially useful for studying mechanical oscillators of macroscopic size and, morphed to various forms, it recently has found application in MEMS. It is capable of great sensitivity when configured in the form of an array, as shown in Figure 2.4.

Various lines in Figure 2.4 correspond to narrow insulator strips, such as the single vertical line in the set that connects to the amplifier. In the cross-connected static set, the plates labeled "1" are electrically distinct from the others labeled "2". The total-plate arrangement constitutes a symmetric AC bridge, and the central position of the moving set ($x = 0$ as shown in the figure) corresponds to bridge balance with $V_0 = 0$. Displacement away from balance gives a voltage output that is linear between $-w/4$ and $w/4$, as illustrated in the graph at the bottom of Figure 2.4.

The oscillator frequency is typically tens of kHz, and the amplifier is of instrumentation type (Horowitz and Hill, 1989). Unlike a bridge null detector, the linear response through $x = 0$ is realized

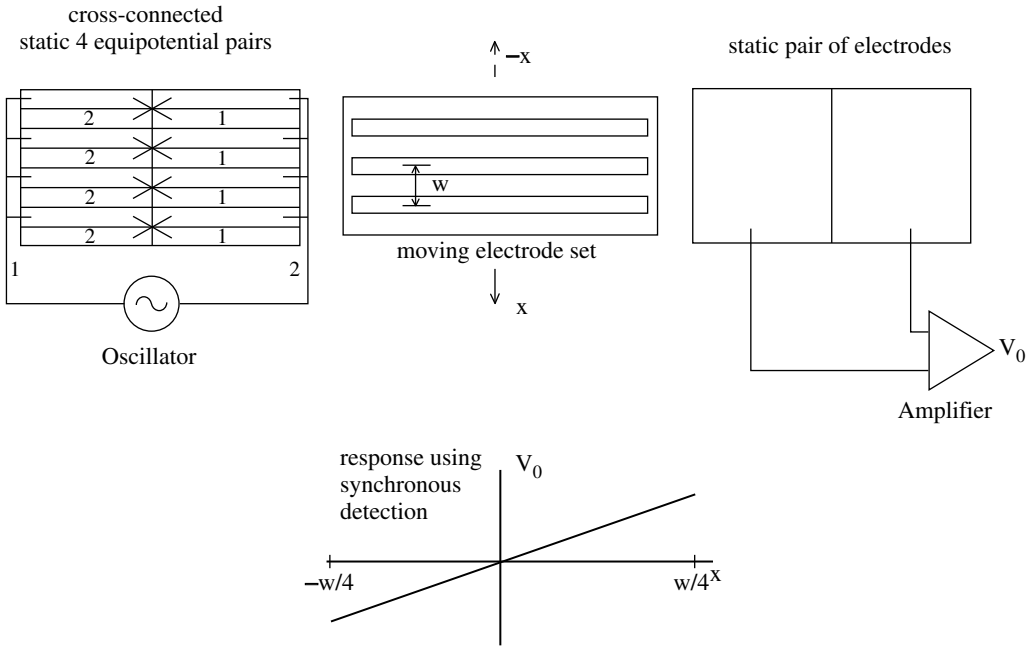

FIGURE 2.4 Illustration of a fully differential capacitive transducer array. For clarity, the three electrode-sets are shown separated from their operating positions (parallel with a small separation gap, with the moving electrodes in the middle).

when synchronous detection is employed. This can be accomplished with a lock-in amplifier, but the most recent Cavendish balance to employ the sensor uses diodes (Tel-Atomic Inc., online at http://www.telatomic.com/sdct1.html).

A tutorial ("detailed explanation") of the SDC sensor using diodes can also be found at this website.

In Figure 2.4, four individual SDC units have been shown connected in parallel. The total number, N, of individual units in an array depends on the characteristic width, w, for which the total range of detectable motion is $w/2$. If the requirement on range is small, then N can in principle be made very large, which is desirable for the following reason. The sensitivity of this position sensor is inversely proportional to w if output capacitance of the device is not a factor. As w is reduced, however, the degrading influence of increased output reactance (capacitive) is more significant than the improved sensitivity that would result if the sensor could be connected to an amplifier with infinite input impedance. Since the instrumentation amplifier's input capacitance is not negligible, shrinking w is beneficial only if the output reactance can by some means be kept low. This is accomplished with the array of individual units. In principle, the output capacitance could be held reasonably constant as N approaches 100, by using photolithographic techniques and small spacing between the parallel electrodes. The concept has been deemed feasible because of existing technologies as well as the following: although not in the form of an array, Auburn University has fabricated a mesoscale accelerometer around the SDC sensor. The prototype was built on printed wire board (PWB) under U.S. Army contract (Dean, 2002).

No doubt the popular silicon-based MEMS accelerometers marketed by Analog Devices utilize the impedance advantages of an array, employing a large number of "fingers" in a force-feedback arrangement. Although employed mostly otherwise, the first case of a fully differential capacitive transducer using force-feedback was one based on simultaneous action of actuator and sensor functions in a single unit of nonlinear type (Peters et al., 1991).

2.6.2 Common-Mode Rejection

In attempts to measure damping, one can be confronted with difficulties of mode mixing. For example, the historical Cavendish experiment, using optical detection, has been traditionally difficult unless the instrument is placed in a very quiet location to avoid pendulous swinging of the boom. The high-frequency pendulous motion (of the order of 1 Hz) as a "noise" becomes superposed on the low-frequency torsional signal. The computerized Cavendish balance sold by Tel-Atomic overcomes this problem by means of a mechanical common-mode rejection feature. An SDC sensor placed near one boom end is connected in electrical phase opposition to a second SDC sensor placed near the other end of the boom. The boom itself serves as the moving electrode for both sensors. Neither sensor has a first-order response to boom motion parallel to its long axis. Pendulous motion perpendicular to the boom orientation is largely canceled.

2.6.3 Example of Viscous Damping

The aforementioned Sprengnether–LaCoste spring seismometer is well-suited to the demonstration of viscous damping, when damping is imposed in the following manner: the instrument was built with a Faraday Law (velocity) detector; i.e., a coil that moves with the mass of the instrument, in the field of a stationary magnet. As originally employed, the coil was connected to the amplifier of a recorder. In the present configuration, however, the velocity detector is not employed, since its sensitivity is severely limited at low frequencies. Instead, an SDC array of the type shown in Figure 2.4 is used to measure the position of the mass (a pair of lead weights, total mass 11 kg). If the instrument is operated with the coil open-circuit, there is no induced current. By connecting a resistor across the coil (through very fine copper wires that go to terminals on the case), mass motion induces a current. The induced current opposes the motion through Lenz's Law, resulting in damping. The damping depends on the size of the

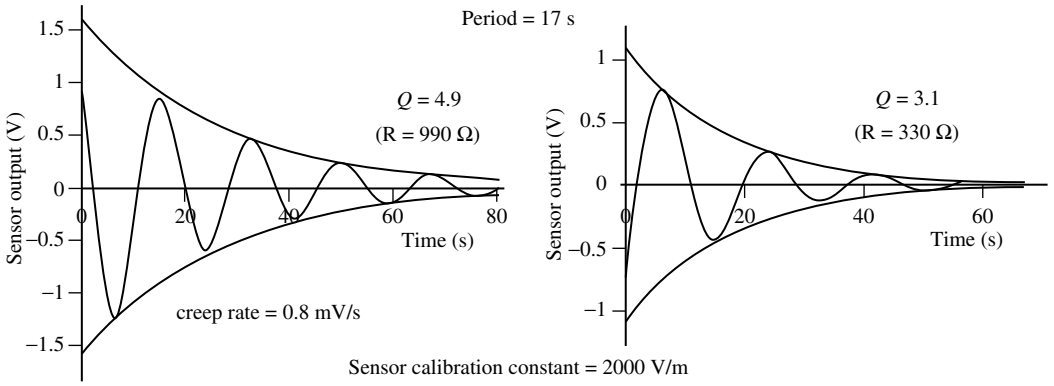

FIGURE 2.5 Examples of induced current damping of a vertical seismometer using two different resistors.

current and is thus an inverse function of the resistor's magnitude through Ohm's Law. The phenomenon is illustrated in Figure 2.5.

As compared with the "undamped" instrument, whose Q is approximately 80 at a period of 17 sec, it is seen that the addition of a 990-ohm resistor lowered the Q by more than an order of magnitude to 4.9. A 330-ohm resistor reduced it even further to 3.1. The amount of damping is also governed by the resistance of the coil winding, which is 480 ohm.

The envelopes that have been fitted to the decay curves were the basis for estimating the Q. The decay data were imported to Excel by first outputting the Dataq DI-154RS A/D generated record as a *.dat (CSV) file. The fits were produced by trial and error using the drag and autofill functions. Notice that the 990-ohm resistor (first) case is not as pure an exponential decay as the other case because of creep. The rate of creep is greater at large initial amplitudes of the motion.

2.6.4 Another Way to Measure Damping

Curve fitting (full nonlinear, in general) is the best way to estimate damping parameters, especially if the decay is not exponential. For more routine cases, simpler methods can be used. Among the host of ways that have been defined to specify the damping of an oscillator, one of the most common uses the logarithmic decrement. The solution to Equation 2.1 with zero right-hand side is given by

$$x(t) = x_0 \, \mathrm{e}^{-\beta t} \cos(\omega t + \phi). \tag{2.16}$$

The full-cycle turning points, $x_N = x_0 \, \mathrm{e}^{-\beta NT}$, with $N = 0, 1, 2, \ldots$ can be used to compute the logarithmic decrement through

$$\beta T = \frac{1}{N} \ln \frac{x_0}{x_N} \tag{2.17}$$

Unfortunately, an estimate based on Equation 2.17 can be difficult due to the presence of either or both of two problems: (i) mean position offset in the decay record or (ii) asymmetry of the decay, where the turning points on one side of equilibrium decay at a different rate than those on the other side. Case (ii) occurs more often than one might expect; it is frequently a consequence of material complexity and not the result of nonlinearity in the electronics of the detector. It is important, however, to be sure that the detector is either linear or that corrections for the nonlinearity be utilized before estimating the damping.

A method to provide partial compensation uses half-cycle turning points $n = 2N$, and works with a minimum of three such points.

$$\beta T = -2 \ln[1 - (x_{n-1} - x_{n+1})/(x_{n-1} - x_n)] \tag{2.18}$$

Advantage is taken of random error reduction by using Equation 2.18 on a set of turning points (optimal number sometimes being about a dozen). The calculations are straightforward in a spreadsheet such as Excel by means of the autofill function.

2.7 Hysteretic Damping

2.7.1 Equivalent Viscous (Linear) Model

The few mechanical oscillators governed by Equation 2.1 tend to be those in which there is an external control, such as eddy current damping. For oscillators in which the damping derives from internal friction of its members, the following linear approximate form of the hysteretic damping model has been used:

$$m\ddot{x} + \frac{h}{\omega}\dot{x} + kx = F \tag{2.19}$$

It should be noted that hysteresis is the cause for all damping; however, engineers have come to use the term "hysteretic damping" for systems described by Equation 2.19. This equation differs in two important ways from Equation 2.1. For the viscous damped oscillator, Q is proportional to the frequency, but for the hysteretic damped oscillator, Q is proportional to the square of the frequency. Also, viscous damping changes the frequency of the oscillator, since $\omega_1 < \omega_0$ and, for resonance, the frequency is even lower. However, the hysteretic oscillator is isochronous, requiring only a single frequency $\omega = \sqrt{k/m} \rightarrow \omega_r$ to describe all features of the motion. For example, it is easy to show that the oscillator resonates at this frequency. Off resonance, the response is not the standard Lorentzian. To show this, assume steady state and use the phasor method given to us by Steinmetz, 1893 (complex exponential form for the variables); i.e., $F = F_0\, e^{j\omega t}$ and $x = x_0\, e^{j\omega t}$ to get the frequency transfer function

$$\frac{kx}{F} = \frac{1}{1 - \omega^2 \dfrac{m}{k} + j\dfrac{h}{k}} = \frac{1}{1 - r^2 + j\alpha} = Z, \text{ with } r = \frac{\omega}{\omega_r} \text{ and } \alpha = \frac{h}{k} = \frac{1}{Q} \tag{2.20}$$

for which the real and imaginary parts are given by

$$\text{Re } Z = \frac{1 - r^2}{(1 - r^2)^2 + \alpha^2}, \qquad \text{Im } Z = \frac{-\alpha}{(1 - r^2)^2 + \alpha^2} \tag{2.21}$$

which is expressible in polar form as

$$Z = |Z|\, e^{j\delta}, \text{ where } |Z| = \frac{1}{\sqrt{(1 - r^2)^2 + \alpha^2}} \text{ and } \delta = -\tan^{-1}\frac{\alpha}{1 - r^2} \tag{2.22}$$

It is interesting to compare the steady-state response of the driven, hysteretic damped oscillator with that of the driven, viscous damped oscillator; i.e., Equation 2.22 compared with normalized Equation 2.7. A Bode plot comparison (log–log, for the amplitude case) is provided in Figure 2.6. At small values of the damping parameter α (large Q), there is insignificant difference between the two cases. At large values, however, the difference is significant.

2.7.2 Examples from Experiment of Hysteretic Damping

The vertical seismometer that was used for several of the present studies is known to decay according to hysteretic damping. In Section 2.16.4 titled "Failure of Viscoelasticity", details are provided of the work by Gunar Streckeisen (1974) that showed this to be true. Decay curves of the instrument are

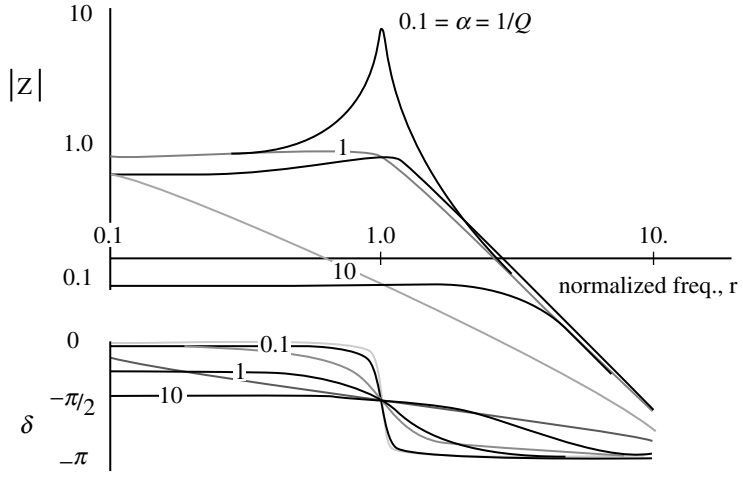

FIGURE 2.6 Bode plot comparison of steady-state driven system with (i) hysteretic damping (dark curves) and (ii) viscous damping (light curves).

frequently a near-perfect exponential, once corrected for secular drift of the record. Sometimes, this drift is the result of creep in the spring of the instrument, but it may also be the result of other factors, such as (i) temperature change, or (ii) barometric pressure variation, or even (iii) tidal influence. The temperature sensitivity is due to the difference of thermal coefficients of the materials from which the instrument is constructed, and the pressure variation is a buoyancy effect. Tidal influence is the smallest of the three, which causes minute accelerations of the crust of the Earth with a period of about 12 h.

In the discussions which follow, two different decay records are provided. In both cases, the initial amplitude of oscillation is quite large, being a significant fraction of 1 mm, and the period for the two cases is different — the first case being 17 sec and the second one 21 sec. The first case time record, shown in Figure 2.7, contains 9800 points. Once a 12 μV/s (upward) drift was removed, the decay (left curve) is seen to be "nearly textbook" exponential.

The adjective "nearly" is appropriate because there is a 12% difference in the decay constants defining the upper and lower turning points (0.0022 top, 0.0025 bottom), which were determined by trial and error "eyeball" exponential fits using Excel. In this author's experience, such is the norm for virtually all mechanical oscillations; perfectly symmetric exponential decays have rarely been seen in the hundreds of cases studied.

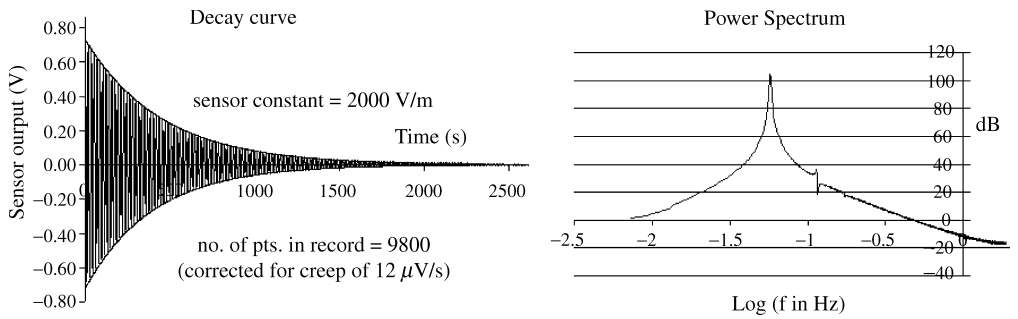

FIGURE 2.7 Free-decay of a vertical seismometer due to hysteretic damping. The period of oscillation is 17 sec.

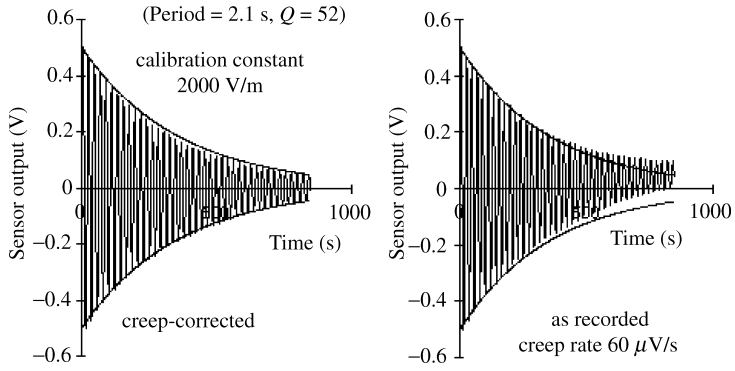

FIGURE 2.8 Free-decay of a seismometer due to hysteretic damping.

Because there are roughly 150 oscillations in the time record of Figure 2.7, it is not possible to resolve individual turning points of the motion, but the oscillations are very nearly that of a pure damped sinusoid, as noted from the right-side graph of the figure. This spectrum was generated with a 4096-point FFT, comprising the first 1090 sec of the time record. The second harmonic is the only distortion observed, and it is about 65 dB below the fundamental. For the case presented in Figure 2.7, $Q = 80$.

Another example of free-decay hysteretic damping is provided in Figure 2.8. As usual, the record was afflicted by drift, possibly from creep in the spring, in this case a constant rate of 60 μV/s, as observed in the graph on the right. All of these graphs were produced with Excel, as noted earlier in the discussion of induced current damping. As with the decay curve of Figure 2.7, the creep-corrected graph on the left was generated by adding a secular term to the raw data. Once corrected, the decay is a near-perfect exponential of hysteretic type. We will see other examples (from pendulum studies) in which two damping mechanisms are simultaneously active in a decay.

The Q values corresponding to Figure 2.7 and Figure 2.8 are consistent with hysteretic damping; i.e., 80 for the 17-sec oscillation and 52 for the 21-sec oscillation. As noted elsewhere in this document, $Q\alpha\omega^2$ for hysteretic damping as opposed to an exponent of 1 for viscous damping. Of course, one must collect data over a very much larger range of frequencies to verify this, as was done by Streckeisen (1974).

2.8 Failure of the Common Theory

Many mechanical oscillator studies in decades past, mainly by engineers, have shown that the so-called decay constant β is proportional to ω^{-1} instead of being constant (e.g., Bert, 1973). The damping for these cases came to be called "material", "structural", or "hysteretic." A common way to obtain the correct frequency dependence was to divide the velocity by frequency and call the result an "equivalent viscous" form of damping. The adjective "equivalent" draws attention to the fact that internal friction in a solid cannot really result from fluid effects. Moreover, elsewhere in this document, there is plenty of support for the position that the linear equations of viscous damping type cannot produce truly meaningful (predictive) models when doing modal analysis on multibody systems.

An important early work by Kimball and Lovell (1927) is evidently the first experiment to show that internal friction ("force") of many solids is virtually independent of frequency. In other words, their elegant technique, in which a rotating rod is deflected by a transverse force, was the first to demonstrate the "universality" of hysteretic damping. Although both researchers were physicists at General Electric in the time of Steinmetz, few physicists of the 21st century know of this important work. As with the important contributions of Portevin and LeChatelier, their study of systems influenced by "dirty physics" was evidently ignored in favor of the "clean" new quantum mechanics of that era.

It is interesting that a bell made of lead does not tinkle at room temperature, but it can be made to do so at 77 K, by immersion in liquid nitrogen. This demonstration, which is often employed in physics "circuses," shows clearly that the internal friction of lead at audio frequencies can be reduced substantially by lowering the temperature. An important lesson to be learned from these observations is that damping, in general, is a complex function of temperature, frequency, conductivity, …(who knows where to terminate this list). Not only is a multitude of state variables necessary for a complete description of dissipation, but the previous history of stress–strain cycling may also be critical. Such is the nature of defect structures responsible for damping.

2.9 Air Influence

Even when operating an oscillator in high vacuum, there is a significant remanent damping that derives from internal friction. This fact is illustrated in Figure 2.9, which provides data for two different "simple" pendula. They are simple in the sense that the bob mass is concentrated near the bottom of the pendulum structure. In the figure, decay time (reciprocal of the decay constant, β) has been plotted against the natural log of the pressure in mtorr. Pressure reduction was done with a high-quality roughing pump, and the pressure was measured with (i) a mechanical gauge in the range 8 torr $< P <$ 760 torr and (ii) a thermocouple vacuum gauge for $0 < P <$ 100 mtorr. In the range from 100 mtorr to 8 torr, the pressure could not be accurately measured with either of these gauges. Similarly, pressures below 1 mtorr could not be presently measured, but in similar other experiments with this pump, and using an ion gauge, it was easy to pump below 0.01 mtorr.

The period of each pendulum was very close to 1 sec, and the starting amplitude of the motion for every case was about 25 mrad. The heavier pendulum used a pair of pointed steel supports resting on single-crystalline silicon wafers to provide the axis of rotation. At the bottom of the pendulum was attached a solid lead ball whose mass was approximately 1 kg. The lighter pendulum was supported by a steel knife-edge resting on hard ceramic flats, and a large (10.3 cm dia.) lightweight (143 g) hollow metal sphere was attached at the bottom to provide as much air drag as possible. The motion was measured with an SDC sensor feeding the computer through a Dataq DI-154RS A/D converter.

Although air damping is evident in Figure 2.9, it is not as influential as one might expect, at least for the heavy pendulum. Moreover, at atmospheric pressure, it was easy to demonstrate the importance of nonlinear drag. As also noted in Nelson and Olssen (1986), this form of fluid friction caused a significant amplitude-dependent damping.

The remanent damping, once air influence is eliminated (pressure below 1 mtorr), is substantial relative to atmospheric damping, for both pendula. Removing the air increased the Q from 7500 to

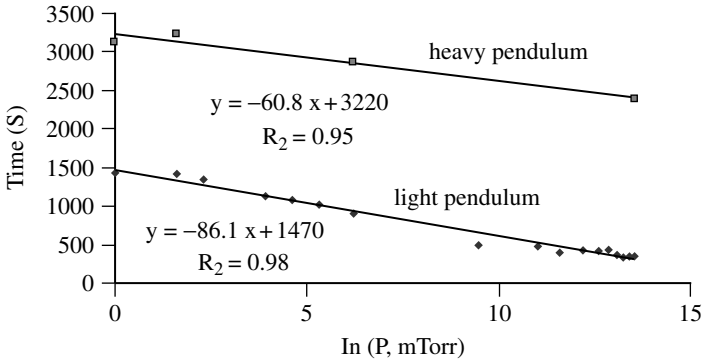

FIGURE 2.9 Pendulum damping as a function of pressure in a vacuum chamber.

10,100 for the heavy pendulum and, for the light pendulum, the increase was from 1000 to 4600. We thus see that even a pendulum designed to be heavily influenced by air drag also has significant damping that depends on the material from which the pendulum is fabricated or on the material upon which it rests.

The difference in internal friction damping between the heavy and light instruments was not expected to be so great. Although this might be due to the difference in axis-type (points for the heavy instrument and knife-edge for the light), no systematic effort was made to determine the primary source of the damping difference. In addition to different axis designs, the means for holding the instruments together was different. The light pendulum used a large-diameter solid brass wire between the axis and the lower mass, and the heavy pendulum used an aluminum tube.

Both of the pendula used to generate Figure 2.9 were relatively high-frequency instruments (period of 1 sec). The pivot was located, in each case, near the top end of the instrument. As such, they stand in stark contrast with the instruments that motivated this paper, where long-period pendula were used. A simple instrument to demonstrate some of the complexities of long-period instruments is a rod-pendulum of adjustable period (refer to Figure 2.1 above). The closer the axis to the center, the longer the period and the greater the influence of internal friction. It is easy to show that the sensitivity of a pendulum to external forces is proportional to the square of the period. Similarly, the ability to detect influence of internal configurational change is quadratic in the period.

2.10 Noise and Damping

2.10.1 General Considerations

Damping is inseparable from noise issues having nothing to do with undesirable sounds that might be produced by oscillation. In the simplest cases, the noise associated with damping can be described by the fluctuation–dissipation theorem. The viscous damped, thermally driven oscillator is a classic example of thermodynamic equilibrium, for which this theorem is applicable. The classic electronics analogous case is the Johnson noise of a resistor, described by the Nyquist (white) noise formula.

The largest obstacle to constructing a perfectly simple harmonic oscillator is the oscillator's dissipation. If damping were perfectly smooth, this would not be so great a challenge. However, the fluctuation–dissipation theorem of statistical mechanics guarantees that damping is accompanied by fluctuating forces. The larger the damping, the larger the fluctuating forces, i.e., the larger the noise. It is a standard problem in statistical mechanics to show that the magnitude of relative fluctuation is inversely proportional to the square root of the number of particles involved. In the case of internal friction noise, defects associated with mesoscale structures cause the effective number of particles responsible for the noise to be much smaller than the total number of atoms in a sample. Unfortunately, the fluctuation–dissipation theorem probably does not apply. It has been long known that it does not apply to the Barkhausen effect (Barkhausen, 1919). It has been recently demonstrated that it does not apply to structural glass (Grigera and Israeloff, 1999). The close relationship postulated by the author between the PLC effect and the Barkhausen effect implies that the fluctuation–dissipation theorem should also not generally apply to internal friction damping.

Internal friction noise is not white but rather more like $1/f$ (or flicker = pink) noise, a ubiquitous form that has not yet been explained from first principles. A frequently cited paper on self-organized criticality states the following:

> We shall see that the dynamics of a critical state has a specific temporal fingerprint, namely "flicker noise," in which the power spectrum $S(f)$ scales as $1/f$ at low frequencies. Flicker noise is characterized by correlations extended over a wide range of timescales, a clear indication of some sort of cooperative effect. Flicker noise has been observed, for example, in the light from quasars, the intensity of sunspots, the current through resistors, the sand flow in an hourglass, the flow of rivers such as the Nile, and even stock exchange price indices. Despite the ubiquity of flicker noise, its origin is not well understood. Indeed, one may say

> that because of its ubiquity, no proposed mechanism to date can lay claim as the single general underlying root of 1/*f* noise. We shall argue that flicker noise is in fact not noise but reflects the intrinsic dynamics of self-organized critical systems. Another signature of criticality is spatial self-similarity. It has been pointed out that nature is full of self-similar "fractal" structures, though the physical reason for this is not understood. (Bak, 1988)

It should be noted that controversy exists concerning this self-organized criticality paper, summarized in the following excerpt from Bak's book on 1/*f* noise called *How Nature Works: The Science of Self-Organized Criticality* (page 95):

> In an earlier work (CFJ), performed while an undergraduate student in Aarhus, Denmark, (Kim Christensen) showed that our analysis of 1/*f* noise in the original sandpile article was not fully correct. Fortunately, we have since been able to recover from that fiasco in a joint project by showing that for a large class of models, 1/*f* noise does indeed emerge in the SOC state.

In the last few years, mathematicians have been drawn to "… an analogy, in which three areas of mathematics and physics, usually regarded as separate, are intimately connected. The analogy is tentative and tantalizing, but nevertheless fruitful. The three areas are eigenvalue asymptotics in wave physics, dynamical chaos, and prime number theory" (Berry and Keating, 1999). Some mathematicians speculate that a dynamical system (perhaps some form of a mesoanelastic pendulum, in the thinking of this author) could become a "machine" to generate prime numbers.

2.10.2 Example of Mechanical 1/*f* Noise

Shown in Figure 2.10 is an example of mechanical flicker noise made worse by creep that originates in the spring (LaCoste type) of a Sprengnether vertical seismometer. The data are from two separate time records, the first run preceding the second run by about a half-hour. Just before collecting the data of the first run, a clamping pin was removed from the seismometer. Used to constrain the mass from moving, this pin had been left in place overnight to determine the amount of electronics noise, including drift. The measured electronics noise (white $= 1/f^0$) was more than an order of magnitude smaller than the smallest (high frequency) noise components of mechanical (seismometer) type. The peak-to-peak amplitude of the oscillation in both cases was 0.5 mm (calibration constant for the sensor being 2000 V/m). The peak-to-peak amplitude for SNR = 1 for this system is of the order of 1 μm.

Although the spring force was not unloaded with the pin in place overnight, nevertheless, its removal caused a significant change to defect structures in the spring, as noted by the residuals between the data and their harmonic fits (magnified by a factor of ten).

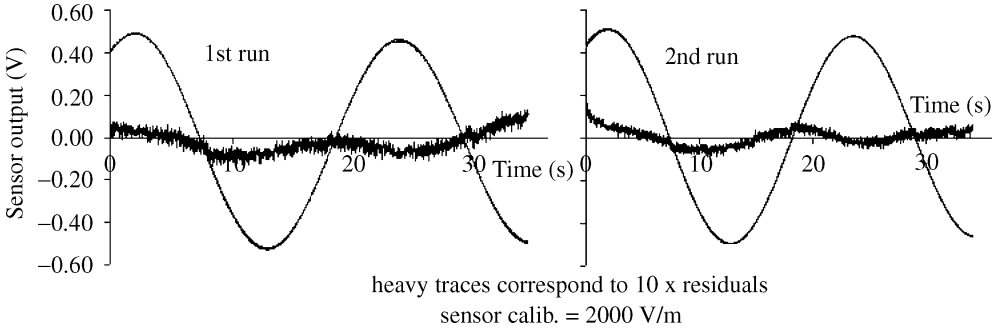

FIGURE 2.10 Evidence in support of 1/*f* mechanical noise in a seismometer.

The flicker character of the noise was demonstrated by computing power spectra of the residuals (not shown). The log–log plot, generated with the FFT (Cooley–Tukey FFT), showed $1/f$ frequency dependence for the second run. The larger noise of the first run was concentrated in the upper frequencies. The relaxation toward $1/f$ character suggests that flicker noise is a remanent of "work hardening." To demonstrate that the flicker noise was not due to the electronics, sensor output was recorded with the mass of the instrument locked. The electronics noise proved to be more than an order of magnitude smaller and "white" in character, probably mainly the result of A/D quantization (see Chapter 16).

Because the spring was not in equilibrium at the time the pin was removed (perhaps because of temperature change while the system was clamped), a great deal of initial molecular rearrangement occurred, involving atoms at grain boundaries. It is seen that the amount of fluctuations has noticeably decreased during the half-hour separating the two runs. Although the creep-noise would be undoubtedly much greater if the spring were relaxed altogether, it is not easy in such a case to quickly rebalance the seismometer to oscillate with a period in excess of 20 sec. These observations are in keeping with known properties of sensitive seismometers, as noted by Erhardt Wieland in "Instrumental self noise — transient disturbances" (ed. Borman and Bergmann, 2002):

> Most new seismometers produce spontaneous transient disturbances, quasi miniature earthquakes caused by stresses in the mechanical components. Although they do not necessarily originate in the spring, their waveform at the output seems to indicate a sudden and permanent (step-like) change in the spring force. Long-period seismic records are sometimes severely degraded by such disturbances. The transients often die out within some months or years; if not, and especially when their frequency increases, corrosion must be suspected. Manufacturers try to mitigate the problem with a low-stress design and by aging the components or the finished seismometer (by extended storage, vibrations, or alternate heating and cooling cycles). It is sometimes possible to relieve internal stresses by hitting the pier around the seismometer with a hammer, a procedure that is recommended in each new installation. (Wielandt, 2001)

Material damping noise appears to have features that are similar to Barkhausen noise — a magnetic phenomenon involving a system far-from-equilibrium. Such noise is associated with the granular nature of ferromagnetic domains and has consequence in the design of electronic instruments using iron alloys. For example, it is known (though not widely) that the popular LVDT is inherently less sensitive than a capacitive sensor of equivalent electrical type, because of its ferrous component (the rod-component that moves). As noted by Wielandt (2001), the capacitive sensor "…can be a hundred times better than that of the inductive type." Fully differential capacitive sensors, being electrically equivalent to the LVDT have still greater advantages borne of the higher symmetry. Additionally, by configuring the capacitive device as an array, it is possible for the sensitivity to also be greater.

Barkhausen noise and hysteretic damping noise may be much more similar than has been realized — involving granularity at the mesoscale, intermediate between micro- and macrophenomena. For such systems, first principle methods are very difficult to employ due to complexities that originate from a host of nonlinear interactions. For example, in the case of internal friction of solids, damping derives from stress–strain hysteresis determined by defect structures in the solid. Involving roughly 10^{12} atoms per "grain" in metal specimens, flicker noise evidently derives from self-similar structures of fractal geometry with a higher degree of spatial correlation than is true of white noise. The ubiquitousness of $1/f$ noise is consistent with the labeling of hysteretic damping as "universal," as first suggested by Kimball and Lovell (1927).

2.10.3 Phase Noise

The previous example was concerned with amplitude noise. It is also possible to see phase noise of mechanical type, as illustrated in Figure 2.11.

For the sensor calibration constant of 2000 V/m, it is seen that the initial amplitude of oscillation is 1.3 mrad, which is much too large to observe the discontinuities of mechanical Barkhausen type.

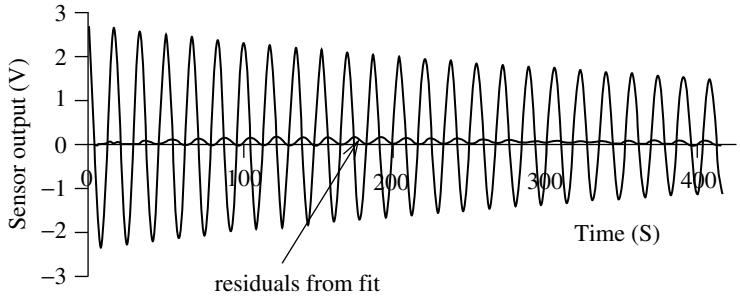

FIGURE 2.11 Illustration of phase noise in the free-decay of a vertical seismometer.

The phase noise is made obvious by comparing the decay to a "reference," i.e., by looking at the residuals from an Excel-generated fit to the data. By adjusting in a computer-generated damped sinusoid, (i) the initial values of amplitude and phase, (ii) the decay parameter, and (iii) the frequency, one can visually by trial and error come close to an optimum fit to the data. Having done so with Figure 2.11, the striking feature of the residuals (difference between data and fit) is the structure that looks something like "beats" but is not. The phase noise responsible for this behavior is thought to be consistent with $1/f$ mechanical noise. To visualize the noise, it is convenient to think in terms of a small randomizing (noise) vector whose tail is positioned at the head of the phasor used to generate the record. The component of the noise vector that is in the direction of the phasor generates amplitude noise as in Figure 2.10, whereas the perpendicular component is responsible for the phase noise of Figure 2.11.

Vibration phase noise imposes a serious limit on the performance of precision quartz crystal oscillators, since they are sensitive to acceleration. The phase noise in these oscillators can be observed by beating against a reference oscillator of known character; i.e., the reference serves the same purpose as the computer "fit" of Figure 2.11. To reduce the phase noise, crystals are isolated with low natural frequency vibration isolators (as described in the marketing literature of Wenzel Assoc., Austin, X).

2.11 Transform Methods

2.11.1 General Considerations

For linear systems, the Laplace and Fourier transforms (Laplace being more general) have been pre-eminent tools with which to study equations of motion (see Appendix 2A and Chapter 10). The author's transform experience (like most physicists) is mainly with Fourier transforms (FT). The discrete FT can be understood in terms of phasors (Peters, 1992). For linear differential equations, transforms are the means to convert differential forms to an equivalent algebraic form. Unfortunately, they cannot be directly employed on nonlinear equations due to the failure of superposition. Nevertheless, the linear approximations continue to be very valuable, so a chapter on damping deserves to mention some of their properties.

Ideas concerning the FFT were evidently originally treated by Gauss in the early 1800s, but the digital signal processing (DSP) "explosion" of the 1960s was largely due to the work of Cooley and Tukey (1965). For an interesting historical account about an "accident" in the publication of their paper, the reader is referred to Cipra (1993), who says the following about the FFT:

> The Fourier transform stands at the center of signal processing, which encompasses everything from satellite communications to medical imaging, from acoustics to spectroscopy. Fourier analysis, in the guise of x-ray crystallography, was essential to Watson and Crick's discovery of the double helix, and it continues to be important for the study of protein and viral structures. The Fourier transform is a fundamental tool, both theoretically and

computationally, in the solution of partial differential equations. As such, it is at the heart of mathematical physics, from Fourier's analytic theory of heat to the most modern treatments of quantum mechanics. Any kind of wave phenomenon — be it seismic, tidal, or electromagnetic — is a candidate for Fourier analysis. Many statistical processes, such as the removal of "noise" from data and computing correlations, are also based on working with Fourier transforms.

Concerning the last statement about noise, this author has used autocorrelation as a powerful means for identifying short-lived, low-frequency periodic signals in time records that do not readily show up in power spectra (FFTs). For example, they are the means for studying free-earth oscillations — eigenmodes excited by rapid relaxations of the Earth under tidal stressing (12 h periodic) (Peters, 2000). The FFT is used to generate the autocorrelation by means of the Wiener–Khintchine theorem (Press et al., 1986).

The great advantage of the FFT compared with the DFT has to do with degeneracy. The DFT proceeds to calculate the components of every "vector" in the reciprocal space (frequency reciprocal to time, units of "second", or wave number (spatial frequency) reciprocal to displacement, units of "meter") with disregard for the fact that many components have the same value, apart from a change of sign.

2.11.2 Bit Reversal

The key to the power of the FFT (central processor unit [CPU] time proportional to $n \log n$) compared with the discrete Fourier transform (DFT) (CPU time proportional to n^2) is the bit reversal scheme of the Cooley–Tukey algorithm. It is illustrated very simply by the following. Instead of a practically sized number of samples in the record to be transformed (minimum of $n = 1024$, typically), consider (for pedagogy) $n = 8$, distributed on the unit circle as shown in Figure 2.12.

Observe that the roots of unity in the complex plane, which have been numbered 0 to 7, divide the "pie" into eight equal pieces. (The algorithm requires that n be expressible as a power of 2). The usual decimal counting scheme for the eight "vectors" is as indicated, traversing the phasor diagram (circle on left) sequentially. In the Cooley–Tukey algorithm, a choice is made to reverse the bits of the binary representation of the vector. Usually, the least significant bit is on the right and the most significant bit on the left, so that decimal counting is as shown on the right in the table, from 0 to 7. With bit reversal, "lsb" becomes the leftmost binary digit and the "msb" is the rightmost digit. Thus, for example, binary 110 (usually 6) becomes 3.

Using bit reversal, the phasor diagram is not traversed in the usual phasor (circulatory) sense, but rather in a "flip-flop" back and forth across the circle. By this means, there is no needless repetition in the calculation of "vector" components (real and imaginary values of a given term in the transform). For example, 5 is the simple negative of 1. It is much faster to reverse the sign on 1 to get 5 than to

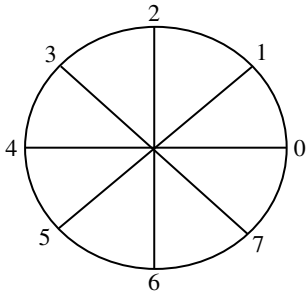

decimal (bit-reversed)	binary number	decimal (usual)
0	000	0
4	001	1
2	010	2
6	011	3
1	100	4
5	101	5
3	110	6
7	111	7

FIGURE 2.12 Graphical illustration of why the Cooley–Tukey FFT algorithm is significantly faster than the original DFT.

needlessly calculate values for sine and cosine terms a second time. The saving in time is substantial as n gets large, since there are then a great number of circulations of the phasor circle. For a 1K record, the FFT computes the transform 102.4 times faster than does the DFT. Additional details are provided in Peters (2003a, 2003b, 2003c).

2.11.3 Wavelet Transform

Recent work suggests that the wavelet transform (WT) may in the future replace the FT in some applications. It uses the Haar function, which is orthogonal on $[0,1]$, as opposed to the orthogonality of the harmonic functions (sine and cosine) corresponding to $[0,2\pi]$ (Strang, 1993). It is claimed that the WT is better able to address features of the Heisenberg uncertainty principle than the FFT.

2.11.4 Heisenberg's Famous Principle

The heart and soul of quantum mechanics is the Heisenberg uncertainty principle. As noted elsewhere in this chapter, it has things to say about damping models. According to well-known physicist Hans Bethe (1992), the principle has received "bad press":

> Many people believe that the uncertainty principle has made everything uncertain. It is quite the opposite. Without the uncertainty principle there could not exist any atoms, there could not be any certainty in the behavior of matter. So it is in fact a certainty principle.

Curiously, a failure figured in Heisenberg's discovery of the principle. During his thesis defense, in front of great theoretical physicist Arnold Sommerfeld (his director) and the famous experimentalist Wilhelm Wien, he proved unable to derive the magnifying power of a simple microscope. The scandal culminated with Professor Wien asking him to explain how a battery works, and he could not answer that question either. Knowing his extraordinary theoretical giftings, Sommerfeld gave him the highest possible grade to compensate for Wien's choice of an F. Thus, Heisenberg was awarded his doctorate.

Later, in an ironic turn of events, Heisenberg chose a microscope to illustrate features of the matrix quantum mechanics that he originated, and which corrected problems with the Bohr wave mechanics theory. His greatest source of embarrassment served to make Heisenberg famous!

2.12 Hysteretic Damping

2.12.1 Physical Basis

The model of simple harmonic oscillation with viscous damping assumes dissipation from an externally acting force. It is not suited to a conceptual understanding of hysteretic damping. To accommodate internal friction requires more than a single mass connected to the elastic component responsible for restoration. Two systems are pedagogically useful in this regard, one being a long-period physical pendulum (mechanical), and the other being the oscillator used by Ruchhardt to measure the ratio of heat capacities of a gas (mainly thermodynamic). Because of widespread confusion concerning the difference between viscous and hysteretic damping, both cases are presented here. The treatments are provided as evidence for the premise that hysteretic damping is the more important case for applied physics and engineering.

It is common knowledge that the damping of a mechanical oscillator results from the conversion of mechanical energy into thermal energy. One might expect, then, that a direct consideration of thermodynamics could yield conceptual understanding of the underlying physics. Although an ideal gas is rarely considered in this context, there is a classic experiment which speaks to its relevance. It is the ingenious technique used first in 1929 by Ruchhardt to measure γ, the ratio of heat capacity at constant pressure to that at constant volume (Zemansky, 1957).

2.12.2 Ruchhardt's Experiment

Consider a piston of mass m moving in a cylinder of cross-sectional area A, alternately compressing and expanding a volume of ideal gas V_0 about the residual pressure P_0. Assume that there is no sliding friction between the piston and the cylinder. A small displacement x of the mass results in volume change $\Delta V = V - V_0 = Ax$. There is a restoring force $F = A\Delta P$, where the pressure difference ΔP relates to ΔV through an assumed adiabatic process; i.e., the period of the motion is assumed too short for appreciable heat transfer into and out of the gas. Using $PV^{\gamma} =$ constant, one obtains

$$\gamma P_0 V_0^{\gamma-1}\Delta V + V_0^{\gamma}\Delta P = 0 \tag{2.23}$$

from which one obtains

$$m\ddot{x} + \frac{\gamma P_0 A^2}{V_0}x = 0 \tag{2.24}$$

This is the equation of motion of a simple harmonic oscillator. There is no damping because of the assumed adiabatic process. By measuring the period $T = 2\pi/\omega = 2\pi\sqrt{V_0 m/\gamma P_0 A^2}$, one can estimate γ.

Historically, it appears that such measurements slightly underestimate γ, which can be understood as follows.

The ideal gas equation of state $PV = NkT$ yields, through differentiation

$$P_0 xA + V_0\frac{F}{A} = Nk\Delta T$$

$$m\ddot{x} + \frac{P_0 A^2}{V_0}x = \frac{NkA}{V_0}\Delta T(t) = F_{\mathrm{d}}(t) \tag{2.25}$$

Notice the difference between Equation 2.24 and Equation 2.25. In Equation 2.25, damping is possible (a type of "negative drive" term) from temperature variations associated with heat transfer during traversal of the cycle. If it were possible for the oscillation to be isothermal ($\Delta T = 0$ at very low frequency, essentially quasistatic), then the frequency would be lower than that of the adiabatic case, since $\gamma > 1$ is missing from Equation 2.25. In the isothermal case, there would also be no damping, since the heat into the gas during compression would be balanced by that which leaves during expansion. The only way to get damping is for the paths of compression and expansion in a plot of pressure vs. volume to separate, i.e., for there to be hysteresis. Reality must correspond to something between the two extremes of adiabatic and isothermal, with experiment obviously favoring adiabatic. The process must depart somewhat from adiabatic, however, since there is damping, which Equation 2.25 shows to derive from temperature variations yielding hysteresis. It is interesting to look at the temperature variations relative to a "driving force," $F'_{\mathrm{d}}(t)$. In the Ruchhardt experiment, there must be small variations $\Delta T'(t)$ that lag behind $x(t)$. (These are not the reversible temperature variations of the adiabat, onto which the $\Delta T'(t)$ are superposed.) By comparing with Equation 2.25, the right-hand zero of Equation 2.24 may be replaced with a damping force that can be written in terms of the velocity as

$$F'\mathrm{d}(t) \propto \Delta T'(t) \rightarrow -\frac{c}{\omega}\dot{x} \tag{2.26}$$

where $c =$ constant. Notice that the multiplier on the velocity is not simply a constant, but rather a constant divided by the angular frequency. The use of velocity is mathematically convenient, but the magnitude of the velocity (speed) is not expected to be a first order influence on the temperature changes of hysteresis type. The derivative of x with respect to time not only shifts the phase by 90°, which accommodates the lag with which heat is transferred, but it also introduces a frequency multiplier through the chain rule. Thus, to make damping proportional to the velocity would cause increased dissipative heat flow and thus increased damping as the frequency is increased. Since this does not happen, and lest we introduce a nonphysical term into the equation, it is necessary to divide by the frequency. Replacing the right-hand-side zero of Equation 2.24 with Equation 2.26, we obtain the

modified equation of motion, with damping

$$m\ddot{x} + \frac{c}{\omega}\dot{x} + \frac{\gamma P_0 A^2}{V_0}x = 0 \tag{2.27}$$

Additional justification for the form of the damping term in Equation 2.27 can be realized by looking at cases where there is negative damping, i.e., $c < 0$. Such is true when the gas is caused to cycle as an engine. An illustrative case study was that of a low temperature Stirling engine (Peters, 2002a, 2002b, 2002c), in which reasonable agreement between theory and experiment was realized through the use of an equation based on the same arguments used to derive Equation 2.27.

It is seen that a straightforward modeling of Ruchhardt's experiment to include damping yields an equation of motion that is in the form of hysteretic damping. It appears that, for many systems in which the dissipation is dominated by internal friction, hysteretic damping is a near universal form.

2.12.3 Physical Pendulum

In the paper by Speake et al. (1999), one finds the following statement:

> the logarithmic decrement (Q^{-1}) varied as the inverse of the square of the frequency. We interpreted this as evidence that, in Cu–Be over this frequency range, the imaginary component of Young's modulus was independent of frequency, contrary to that which was predicted by the Maxwell model.

To fit their theory with experiment, they used a "modified" Maxwell model with a distribution of time constants that ranged from 30 sec to more than 4000 sec. Motivation for their continued modeling efforts derived partly from the observation by Kuroda (1995) that anelasticity was cause for some of the huge errors that have been present in estimates of the Newtonian gravitational constant, G, by the time-of-swing method.

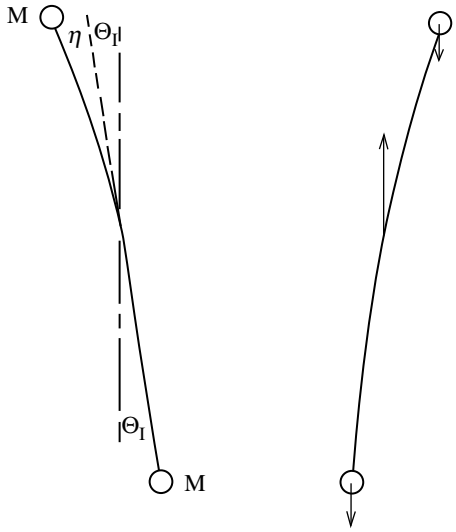

FIGURE 2.13 Idealized physical pendulum used to develop the modified Coulomb damping model.

Although it gives agreement with their particular experiment, the model of Speake et al. (1999) does not have the blessing of Occam's razor. Moreover, their claim that damping derived primarily from their flex pivot of Cu–Be may not be true. Other studies suggest that the material defining the axis of a long-period pendulum is for many cases no more important (and sometimes much less important) to the damping than the material from which the pendulum proper is constructed. A model which also agrees with experiment of the type they conducted, but which is simpler, is now presented.

Illustrated in Figure 2.13 is an idealized long-period mechanical oscillator which could be labeled a "physical pendulum." The top and bottom masses are the same, M, assumed to be much greater than the mass of the connecting structure, which is represented by the curved line.

A primary mechanism for internal friction damping can be understood by looking at the external forces acting on the pendulum, which are pictured in the "negative displacement" (b) case. The upward "normal" force that acts through the pivot (usually a knife-edge) is opposed by the pair of bob-weights situated left and right, respectively, of the axis of rotation. As the pendulum swings alternately between positive and negative displacements, the structure undergoes periodic flexure. It should be pointed out that internal friction could still be operative throughout the structure even without net bending; i.e., there

could be complementary pieces of the structure undergoing compression and tension. Even if the oscillator were in the weightlessness of space, a drive torque would result in dynamic reactionary forces that give rise to damping by this means.

Assume that the masses are separated a distance $2L$ and the axis of rotation is ΔL above the geometric center. Applying Newton's Second Law, with the lower mass causing a restoring torque and the upper mass a "destoring" torque, yields

$$\ddot{\theta}_1 + \frac{g}{2L}\left(1 + \frac{\Delta L}{L}\right)\theta_1 - \frac{g}{2L}\left(1 - \frac{\Delta L}{L}\right)\theta_2 = 0, \quad \theta_2 = \theta_1 + \eta \tag{2.28}$$

(*Note:* Equation 2.28 can be rewritten to accommodate larger displacements, where elastic nonlinearity gives rise to unusual behavior. The amplitude trend of the period is opposite to that of the gravitational nonlinearity, thus providing for improved isochronism. For details refer to Peters, 2003a, 2003b, 2003c).

The difference in displacement of the masses involves an elastic term proportional to θ_1 and a dissipative term that depends on its time rate of change, i.e.

$$\eta = c\left(\theta_1 \cos\delta - \frac{\dot{\theta}_1}{\omega}\sin\delta\right), \quad \omega = \sqrt{g\frac{\Delta L}{L^2}} \tag{2.29}$$

where c is a dimensionless constant. This result can be obtained by the complex exponential Steinmetz (phasor) method. The equation is consistent with the common assumption that stress and strain are related through a complex constant. The angle δ is the phase angle with which η strain) lags behind θ_1 (stress). To describe the motion of the lower mass, we can ignore the elastic part of η, since it does not contribute to the damping (or if the rod does not bend, assuming there still is damping as noted previously). We thus remove the subscript, and after some algebra obtain the result

$$\ddot{\theta} + \frac{\alpha}{\omega}\dot{\theta} + \omega^2\theta = 0, \quad \alpha = \frac{gc}{2L}\sin\ \delta, \ \text{ for } \Delta L \ll L \tag{2.30}$$

which can also, in terms of $Q = 2\pi E/(-\Delta E)$, be expressed as

$$\ddot{\theta} + \frac{\omega}{Q}\dot{\theta} + \omega^2\theta = 0, \quad Q = \frac{2L}{gc\delta}\omega^2, \ \ \delta \ll 1 \tag{2.31}$$

If, as a material property, δ is independent of frequency, then Q is quadratic in the frequency; i.e., the damping of the pendulum due to internal friction is inversely proportional to the square of the frequency — even though the internal friction (determined by δ) is itself frequency-independent. It is important to note that the frequency dependence of internal friction is not to be equated with the frequency dependence of the Q of the oscillator, even though internal friction is frequently stated as simply $1/Q$. This will be discussed in greater detail in Section 2.13.2.

2.12.3.1 Test of *Q* Dependencies

The dependence of Q on frequency and length in Equation 2.31 was tested experimentally with a physical pendulum. Two Pb spheres, each of mass approximately 1 kg, were each drilled through a diameter to allow the insertion of the shaft of an aluminum alloy arrow (length approx. 70 cm) of the type commonly used with compound hunting bows. A second hole was drilled perpendicular to the first and tapped for a set screw. The shaft was sawed into two pieces, which were rigidly rejoined around a carbon–steel knife-edge using force fit and epoxy to machined protuberances above and below the knife-edges. The knife-edges extend perpendicularly outward on opposite sides of the arrow at its center.

2.12.3.2 Simple Method to Measure Damping

Although an SDC sensor could have been employed instead, the experiments to be described were performed with a measurement technique that warrants description because of its novel simplicity — yet it is reasonably accurate. To measure both period and damping, a small "flag" was super-glued to the top of the upper shaft. This flag was a small, thin, U-shaped piece of plastic in which the upper legs of the U were about 1 mm wide, with a spacing between centers of about 0.5 cm. An infra-red photogate of the

type used in general education laboratories was mounted so the flag would trip the photogate during pendulum oscillation. Two different timing measurements were then performed, using a Pasco Smart Timer. In every run, the pendulum was displaced initially about 10° by hand and then released. There was no need for precision initialization.

In the pendulum mode of the timer, the period was directly measured. For this case, the photogate was positioned, relative to the U-shaped flag (for which one vertical arm is slightly longer than the other), so as to be interrupted only once by the pendulum per pass. In the time-interval mode, the flag was positioned so that both arms interrupted the photogate beam. The reciprocal of this time of interruption proved to be a reasonable measure of the instantaneous speed of the pendulum at the position of the photogate, which was that of maximum kinetic energy. The time intervals were recorded manually for traversals separated by one period, through five cycles of oscillation. These numbers were then typed into Excel and their reciprocals graphed. A trendline (using the option to print the slope) was applied to the near linearly declining graph. The decrement of this line (fractional decrease per cycle) proved to be a good approximation to the logarithmic decrement of the motion, which could have been estimated with exceptional precision by means of the other techniques mentioned in this chapter.

In the first set of experiments, the sphere on the lower shaft was maintained at a constant distance from the knife-edge, while the mass on the upper shaft was positioned at increasingly greater distances from the knife-edge to lengthen the period. Over the full range of periods considered, the distance between the two masses changed by a small amount around its nominal value of 67 cm. The results of this first study are shown in the left graph of Figure 2.14, where the log-decrement has been plotted vs. the square of the period. The Q of the pendulum (π/Δ) may be calculated for any value of the period using the indicated slope of 0.0004. For example, the Q at a period of 10 sec was 76, this being near the shortest period considered. Near the other extreme of $T = 35$ sec, $Q = 6$. At the shortest possible periods, damping due to air drag would begin to become important.

The reasonable fit of the linear regression vs. period squared is consistent with the prediction by Equation 2.31 that Q should be quadratic in the frequency.

The Equation 2.31 also indicates that the log-decrement should be proportional to the reciprocal of the distance, L, between the masses. To test this prediction, the period of the pendulum was measured as a function of mass separation, also using the smart timer. In generating the data for the right graph of Figure 2.14, the period was maintained constant at 20 sec. For every datum, the top sphere was always only slightly closer to the knife-edge than the lower sphere. At 0.049, the intercept of the trendline differs enough from zero, relative to the size of the error bars, to imply a systematic error. Possible sources of the error include: (i) the masses are of finite size, rather than being points as assumed by the model, and (ii) a nonnegligible mass from parts other than the spheres. Nevertheless, the data show a clear size dependence of the Q.

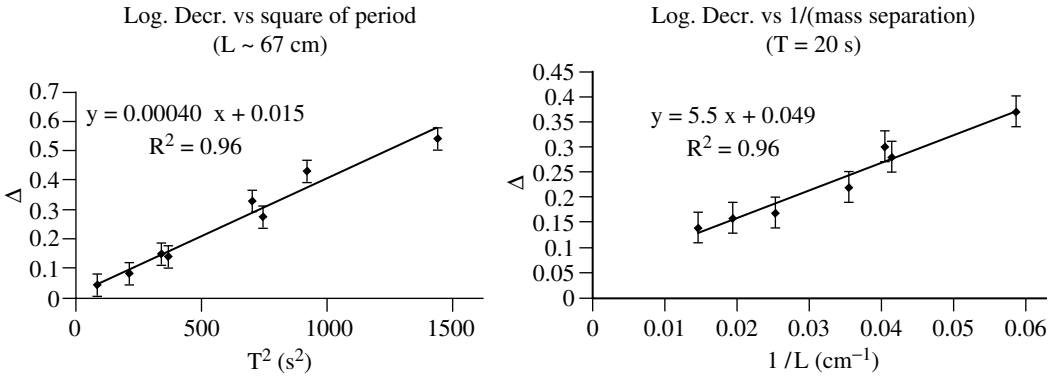

FIGURE 2.14 Results of experiments to test the dependencies of Q on (i) frequency and (ii) length of pendulum.

The experiments just described do not permit one readily to isolate the source of the damping, which, for the cases in Figure 2.14, had the knife-edge resting on silicon wafers (integrated circuit stock material). It is not known to what extent the dissipation was dominated by strain in the knife-edge–silicon interface or by flexure of the aluminum arrow. Although the model that generated equation 2.31 assumed only the latter, there is nevertheless theoretical and experimental basis for model acceptance, regardless of the details of the damping.

2.12.3.3 Highly Dissipative, yet Hard Materials

The same pendulum was used to demonstrate some counterintuitive features of internal friction damping by replacing the Si wafers with various materials. When very soft material, such as lead, was the support for the knife-edges, there was a significant increase of the damping, as expected. It was also found, however, that cast iron increased the log-decrement (10-sec period) by more than 40%. The same was also true of ceramic PZT wafers of the type used to ignite gas grills by striking the wafer impulsively. Both the cast iron and the lead–zirconate–titanate samples are very hard, so the internal friction must derive from large defect densities in which atomic disorder is a sensitive function of stress. Some other hard interfaces, such as steel on glass, or steel on sapphire, did not show a difference from steel on Si, which suggests that the dominant source of damping for the pendulum in all these cases was flexure of the aluminum shaft.

The observation involving cast iron is consistent with its known excellent damping properties at higher frequencies — important, for example, to engine blocks. Some magnesium alloys have also been developed that have excellent damping characteristics without seriously sacrificing strength.

2.13 Internal Friction

2.13.1 Measurement and Specification of Internal Friction

Mechanical spectroscopy is a popular means for measuring internal friction of materials (Fantozzi, 1982). Typically, a torsion pendulum is used to stress harmonically a sample and the lag of the response (strain), relative to the stress, provides the loss tangent and thus the internal friction. In such experiments, it is widespread practice to report internal friction as Q^{-1}. There can be confusion because of this practice, depending on the nature of the measurement technique, i.e., whether one actually measures Q as opposed to measuring something proportional to the stress–strain lag angle. If Q is obtained from an oscillatory free decay, using the logarithmic decrement defined as follows, then there is no problem.

$$\Delta = \ln \frac{x_n}{x_{n+1}} = \beta T = \frac{\pi}{Q} \tag{2.32}$$

Here, x_n and x_{n+1} are adjacent turning point amplitudes separated by one period of the motion, T. In practice, it is very difficult to adjust a mechanical system to oscillate over a wide frequency range. The widest range known to the author, for a mass–spring system, involved the work of Gunar Streckeisen (1974), in which a vertical seismometer using the LaCoste spring was adjusted to have periods in the range between 7 and 140 sec. Because of the difficulties in attaining a wide range of eigenmodes, internal friction is typically determined with a specimen that does not oscillate. We now consider that case.

2.13.2 Nonoscillatory Sample

In the typical torsional pendulum used to measure internal friction, the sample is of very small mass. Such a pendulum was built, for example, around the original version of the fully differential capacitive sensor, to study magnetoelastic wires (Atalay and Squire, 1992). As with many delicate instruments, the Atalay and Squire instrument was of the type labeled "inverted." A silk fiber at the top of the specimen was used to provide minimal tension in the sample. They used one linear rotary differential capacitance

transducer (LRDCT) (Peters, 1989) in the drive mode to provide a known stress to the delicate magnetoelastic sample and a second LRDCT to measure the strain magnitude and the angle by which it lags behind the stress because of an elasticity. As such, they were measuring the lag angle and not Q, as will now be shown.

Without an inertial term, the sample response x to a periodic external force F is governed by

$$F = Kx = (k + \mathrm{j}\zeta)x = F_0 \mathrm{e}^{j\omega t} \tag{2.33}$$

so that the transfer function is given by

$$\frac{x}{F} = k^{-1} - j\frac{\zeta}{k^2} \tag{2.34}$$

from which it is seen that the measurement does not yield Q^{-1} but rather the lag angle ζ/k, where k is constant. Perhaps the measured angle, which is an indicator of the internal friction, has been called Q^{-1} because $k = m\omega_0^2$ for an oscillator of frequency ω_0, and $Q = m\omega_0^2/\zeta$ for the freely decaying oscillator. Bear in mind, however, that this expression for k does not apply to the nonoscillatory measurement just described. There is a frequency square difference between such a measurement and what would be measured if an adjustable oscillator were being considered.

An example of the importance of this issue is found in the article by Lakes and Quakenbush (1996), in which one reads from the abstract the following statement:

> The damping, tan δ, followed a ν^{-n} dependence, with $n \approx 0.2$, over many decades of frequency ν. This dependence corresponds to a stretched exponential relaxation function, and is attributed to a dislocation-point defect mechanism. It is not consistent with a self-organized criticality dislocation model which predicts tan $\delta \propto A^{-2}$. Dislocation damping in metals is relevant to development of high damping metals, the behavior of solders and of support wires in Cavendish balances.

The present arguments suggest that the experiment by Lakes and Quackenbush is (1996) not in strong disagreement with the SOC model; that the magnitude of the exponent difference between theory and experiment is really 0.2 and not 1.8 as they have indicated.

2.13.3 Isochronism of Internal Friction Damping

It is well known that, in the viscous damping free-decay case, the frequency of oscillation is lowered by damping according to

$$\omega_1 = \sqrt{\omega_0^2 - \beta^2} = \omega_0\sqrt{1 - (2Q_v)^{-2}} \tag{2.35}$$

and the resonance frequency of the driven oscillator is lowered even further (Marion and Thornton, 1998). It is not well known how difficult it is to measure this damping "red-shift," which brings in features of the Heisenberg uncertainty principle. Additionally, it is not well known that extensive damping experiments suggest that the frequency may not, for some systems, depend on the damping at all; i.e., the oscillator is isochronous. Isochronism cannot be realized with a linear homogeneous differential equation, but it can be realized with a nonlinear form that is obtained by modifying the damping term as follows:

$$\frac{\omega}{Q}\dot{x} \rightarrow \frac{\pi}{4}\frac{\omega}{Q}\sqrt{\omega^2[x(t)]^2 + [\dot{x}(t)]^2}\,\mathrm{sgn}(\dot{x}) \tag{2.36}$$

where sgn(dx/dt) is the algebraic sign of the velocity — it causes the equation of motion to be nonlinear even if the square root term were not present. For small damping, the square root term can be shown to be equal to the time-dependent amplitude of the motion multiplied by the angular frequency.

Other damping types are possible and are indicated in Peters (2002a, 2002b, 2002c) (…universal…) where evidence is also provided for harmonic distortion in the waveform because of the nonlinearity. It is shown in Peters and Pritchett (1997) that the oscillation is isochronous.

For large values of Q, the lag angle (radian measure) is given by $\delta = 1/Q$. Researchers usually measure δ and specify the magnitude of the internal friction as Q^{-1}. As noted previously, Q is proportional to frequency for the viscous damped oscillator. Thus, for viscous damping, the internal friction is inversely proportional to the frequency.

For hysteretic damping we obtain the result

$$\tan \delta = \alpha = \frac{h}{k} \tag{2.37}$$

where the variables are defined in Equation 2.19. For small damping in which $\tan \delta = \delta = Q^{-1}$, we find that the internal friction for hysteretic damping is inversely proportional to the square of the frequency, since h is constant and $k = m\omega^2$.

2.14 Mathematical Tricks — Linear Damping Approximations

2.14.1 Viscous Damping

In the Hooke's Law expression, $F = -kx$, it is common practice to approximate hysteresis of oscillatory motion by letting k become a complex coefficient. This is also standard practice in a variety of fields, such as the description of lossy electromagnetic media. No doubt the practice has been further popularized by the standard approach of solving electrical engineering ac circuit problems by means of phasors, the technique developed by Steinmetz (1893).

We recognize in the expression $x(t) = x_0\, e^{j\omega t} = x_0 \cos \omega t + jx_0 \sin \omega t$ that harmonic variation is contained in the real part (or alternatively the imaginary part) of the complex exponential form. Using Newton's Second Law, and representing the spring constant by $k\, e^{j\delta}$ with $\delta << 1$ (small damping), we obtain the damped harmonic oscillator equation

$$m\ddot{x} + kx + (jk\delta)x = 0 \tag{2.38}$$

where the approximations $\cos \delta \rightarrow 1$ and $\sin \delta \rightarrow \delta$ have been employed.

However, since $\dot{x} = j\omega x$, and $\dfrac{k}{m} = \omega^2$, Equation 2.38 can be rewritten as

$$\ddot{x} + \omega\delta\dot{x} + \omega^2 x = 0 \tag{2.39}$$

We thus see that the damping constant $\omega\delta = \omega/Q = 2\beta$ permits us to express the logarithmic decrement Δ in terms of the angle δ with which x lags F; i.e., $\Delta = \beta T = \pi\delta$. (Note that we are making no distinction here between the periods with and without damping, since the difference is small and hard to measure.) If β were independent of frequency, then δ would be inversely proportional to the frequency, which is rarely realized in practice.

2.14.2 Hysteretic Damping

Equation 2.39 does not properly represent some of the most important engineering systems. For those labeled "hysteretic," we must use a different form for the complex spring constant. We assume that $F = -(k_{\text{complex}})x = (k + jh)x$ where h is a real constant. Since $dx/dt = j\omega x$, this yields the equation of motion

$$\ddot{x} + \frac{h}{m\omega}\dot{x} + \omega^2 x = 0 \tag{2.40}$$

Since h is assumed to be a true constant (independent of frequency), the lag angle between displacement and force is given by

$$\delta = \frac{h}{k} = \frac{1}{Q} = \frac{h}{m\omega^2} \tag{2.41}$$

which is seen to be inversely proportional to the square of the frequency. (Note that δ here is the same as α in Figure 2.6.) It should be noted that the complex form for the spring constant is not simply obtained using the common theory of viscoelasticity. Such theory requires a multitude of relaxation times (stretched exponentials) (Speake et al., 1999).

2.15 Internal Friction Physics

2.15.1 Basic Concepts

All damping derives from varying degrees of complexity because of the myriad interactions that are present, either internal of nonconservative type or external involving the environment. This is true even for systems that come closest to being governed by the textbook equations. For example, the author has attempted to produce ideal harmonic oscillators using viscous liquids for damping. Even they are complicated and do not strictly obey Stokes' Law of drag force proportional to the velocity. The nonlinear Navier–Stokes equation may be capable of describing them, but not in a simple form except to a first approximation that is not really very good relative to the precision that is possible with modern sensors.

Perhaps the closest to being an ideal viscous damped oscillator is that in which the damping force derives from eddy currents through Faraday's Law. A magnet is attached to the oscillator and, as it moves in proximity to a conductor, the time rate of change of magnetic flux gives rise to a retarding force that is proportional to velocity. Because there really is a force involved, and because of Lenz's Law, the damping term makes sense physically. This case might be completely ideal except for one factor — the magnet is part of a mechanical system that must possess structural integrity if it is to oscillate. Because of loads present in the structure (reactionary normal forces to the various weights), there will always be some creep. The creep is ultimately unavoidable, since there is apparently no stress threshold below which plastic deformation ceases to exist. It is important to realize that forces associated with inertial mass (Newton's Second Law) are just as important as the weights. Systems designed around an elastic member (such as a spring, in contrast to a simple pendulum) will experience damping in the weightlessness and the airlessness of space.

2.15.2 Dislocations and Defects

The extent to which mechanical defects, such as dislocations, have been ignored by large segments of the scientific community is surprising. The surprise is even greater when one considers the importance of defects in another field — that of electronics. Our present information age (world of computing) came into existence only after widespread recognition of the importance of the defects called impurities. The n-type and p-type semiconductor materials necessary to our modern age result from the substitution of silicon atoms with others of pentavalent and trivalent type in surprisingly small concentrations.

The strength of solids is very much less than as predicted by theories of an ideal (perfect) crystal. Dislocations are the primary culprits. Their influence on materials used in engineering has prompted the statement: "when mother nature fills the vacuum she abhors, she rarely does so with perfection." Unfortunately, few students exposed to fundamental science receive training in defect physics. Moreover, it is difficult to provide a self-consistent fundamental description of their properties, so very few scientists have more than a superficial knowledge of their importance.

"Viscoelasticity" is a misleading term. To combine the words viscous and elastic suggests that the state variables vary smoothly in time, i.e., as a fluid in the viscous part. Unfortunately, this is not true of hysteresis associated with either "domains" or with "grains." In the case of magnetic domains, it is quite easy to demonstrate nonsmooth (jerky) behavior that is called Barkhausen noise. Although the phenomenon was demonstrated by Barkhausen in 1919, only recent studies have begun to understand some of its complexities better (Urbach et al., 1995a,b).

A similar phenomenon, that must relate in some manner to the Barkhausen effect, is the PLC effect. Under applied stress, alloys frequently display discontinuous strain increase (jumps). The author has

even demonstrated strain recovery of a similar type, catalyzed by "tapping." The polycrystalline metals that demonstrate these effects are obviously influenced by "granularity." They differ from the "granular materials" that have become a hot topic of recent research. Even pure polycrystalline metals exhibit these features. The German word to describe the deformation of tin under large stresses is *zinngeschrei* (=tin cries). Anyone who has ever bent large-diameter tungsten wire has experienced this phenomenon, since the nonsmooth strain can be both felt and heard.

There is still another type of material, thought to have great engineering potential in the future, that shows "granular" behavior — that of shape memory alloys (SMA). If an SMA specimen is cycled in temperature around the martensitic phase, it generates acoustic emissions (Amengual et al., 1987). For a figure taken from their work and other good pages about hysteresis, refer to the webpages of Prof. Sethna at http://www.lassp.cornell.edu/sethna/hysteresis/ReturnPointMemory.html. These emissions are probably related to the PLC effect and are characterized by surprising reproducibilities in spite of their complex behavior.

Thus, there is abundant experimental evidence against the overly simplistic view that hysteretic damping can be meaningfully described by simple, linear differential equations. The nonlinear terms necessary for a good mathematical treatment go beyond "chaos" to the world of "complexity." Chaos of deterministic type, though bewildering to many, is in many cases tractable (using equations that can be integrated numerically). Damping problems are much more complex than deterministic chaos. The challenges to our understanding derive in part from the long time that it has taken before there were any serious investigations of the mesoscale, the place where defect structures abide. If, as with Zener, we use the word anelasticity to describe systems that are "other than" elastic, then the term *mesoanelastic complexity* is an appropriate label for this poorly understood physics that is important and yet mostly unknown to many fields of both science and engineering.

2.16 Zener Model

2.16.1 Assumptions

The SLM of viscoelasticity provides a sound basis for some damping phenomena, yet it fails badly as an approximation for hysteretic damping. Its prominence in both the worlds of physics and engineering warrants the following detailed discussion so that the failure case may be properly documented.

Following the example of Zener, the following linear differential equation relates the stress, σ, the strain, ε, and their first time derivatives:

$$\sigma(t) + \tau_\varepsilon \dot{\sigma} = E_1(\varepsilon + \tau_\sigma \dot{\varepsilon}) \tag{2.42}$$

The τs are relaxation times (subscript ε meaning at constant strain and subscript σ at constant stress), and E_1 is the relaxed elastic modulus (ratio of stress to strain in a very slow process). Nominally, $\tau_\sigma > \tau_\varepsilon$, consistent with strain lagging stress. For periodic variations

$$\sigma(t) = \sigma_0 \, \mathrm{e}^{\mathrm{j}\omega t}, \quad \varepsilon(t) = \varepsilon_0 \, \mathrm{e}^{\mathrm{j}\omega t} \tag{2.43}$$

which, when substituted into Equation 2.42, yields

$$(1 + \mathrm{j}\omega\tau_\varepsilon)\sigma_0 = E_1(1 + \mathrm{j}\omega\tau_\sigma)\varepsilon_0 \tag{2.44}$$

The complex modulus of elasticity is defined by

$$E_\mathrm{C} = \frac{1 + \mathrm{j}\omega\tau_\sigma}{1 + \mathrm{j}\omega\tau_\varepsilon} E_1 \tag{2.45}$$

and is seen to relate stress and strain according to

$$\sigma(t) = E_\mathrm{C}\varepsilon(t) \tag{2.46}$$

From Equation 2.45, the real and imaginary parts of the modulus are found to be

$$\text{Real } (E_C) = \frac{1 + \omega^2 \tau_\varepsilon \tau_\sigma}{1 + \omega^2 \tau_\varepsilon^2} E_1 \tag{2.47}$$

$$\text{Imag } (E_C) = \frac{\omega(\tau_\sigma - \tau_\varepsilon)}{1 + \omega^2 \tau_\varepsilon^2} E_1 \tag{2.48}$$

The independent variable, or "frequency," for all cases is the convenient dimensionless parameter, $\omega\tau = \omega\sqrt{\tau_\varepsilon \tau_\sigma}$.

It is convenient to use polar form, so that

$$E_C = |E_C| \, e^{j\delta} \tag{2.49}$$

where $|E_C|$ is obtained by computing the square root of the sum of the squares of the real and imaginary parts. In this form, it is apparent that δ is a lag angle which determines the damping loss for the system. Moreover, from Equation 2.47 and Equation 2.48, it is seen to obey

$$\tan \delta = \frac{\omega(\tau_\sigma - \tau_\varepsilon)}{1 + \omega^2 \tau_\sigma \tau_\varepsilon} \tag{2.50}$$

2.16.2 Frequency Dependence of Modulus and Loss

The essential features of the Zener model are illustrated in Figure 2.15, where the "unrelaxed" high-frequency modulus obeys the relation $(E_1 E_2)/(E_1 + E_2) = E_1(\tau_\sigma/\tau_\varepsilon)$.

In viscous damping models, the damping is quantified by the product βT, which is equal to the logarithmic decrement. The logarithmic decrement is directly proportional to the period when the damping "constant" β is truly constant. The graph in Figure 2.16 compares the logarithmic decrement computed by the standard model against a case where $\beta =$ constant. Also shown in the figure is a set of hysteresis curves for $\omega\tau = 10, 1$, and 0.1, respectively. Notice that the damping is large only for $\omega\tau$ near 1, in accord with the bottom plot of Figure 2.15. For that case, points (a) to (f) and back to (a) are shown, labels to illustrate work done by the stress in traversing the hysteresis loop. The algebraic sign of the work changes around the loop and the net work done in one cycle is just the area enclosed by the loop.

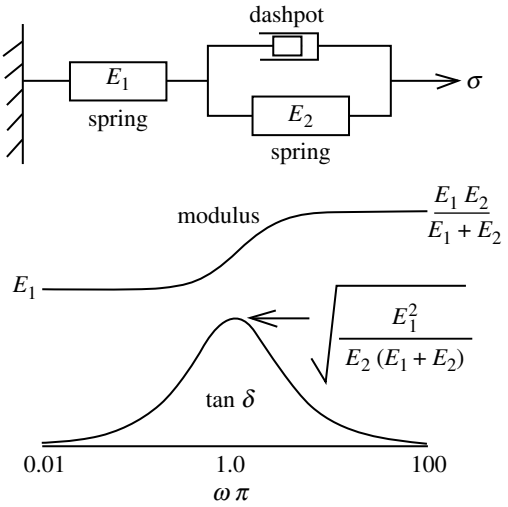

FIGURE 2.15 Zener Model of anelasticity. Bottom curves are "frequency" variation of modulus and loss respectively.

For damping based on the Zener (standard linear) model to agree with the simple viscous approximation, it is necessary that $\omega\tau >> 1$; i.e., the period of the oscillator must be significantly shorter than the smaller of the relaxation times, as illustrated in the bottom graph of Figure 2.16.

2.16.3 Successes — Models of Viscoelasticity

Viscoelasticity, as an approximation for damping, is evidently quite adequate for some materials. The assumption of fluid character as a basis for hysteresis is expected to be closest to correct when

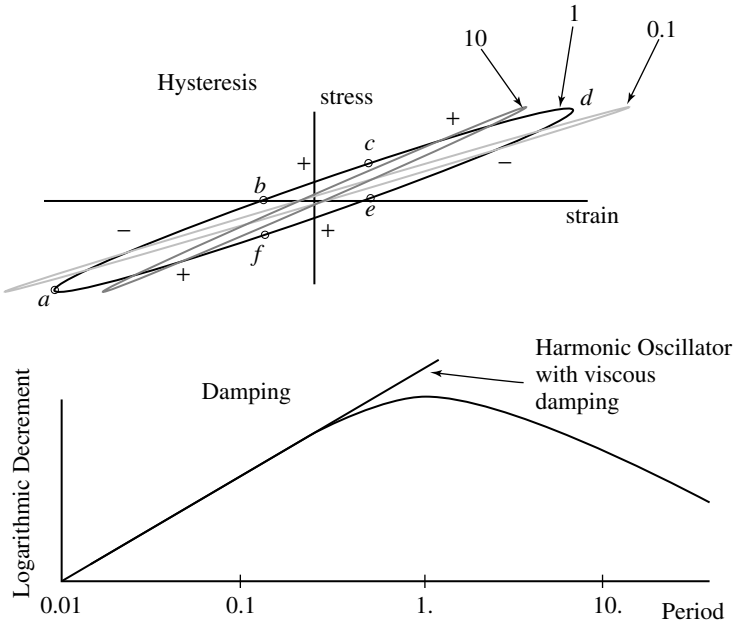

FIGURE 2.16 Characteristics of the Zener model.

applied to those cases in which variations in strain are almost continuous. The materials of rheological type for which this appears to be most true are solids built from long chain polymers, i.e., various plastics. Such materials can yield surprising results, however. Shown in Figure 2.17 are results from a study that used a nylon monofilament sample (8-lb fishing line). The pair of torsional free-decay records corresponds to two different temperatures — 290 K (room temperature) and 390 K (above the glass transition temperature of the nylon). Although a significant increase in the period was observed as the temperature was increased above the glass transition temperature (changing from 18.2 to 27.8 sec), the logarithmic decrement was found to be almost unchanged. This was not in keeping with the expectation that softening of the material at the higher temperature would result in significantly greater damping. The effect is just the opposite of what was mentioned concerning cast iron, which, though very hard, does not have small damping. Here, a softening does not result in significantly increased damping.

Although there was some creep observed for both the decays of Figure 2.17, the creep was more pronounced in the higher temperature case. This is illustrated by the lower curve of the bottom graph, which is a computer fit in which the secular term necessary for best fit was removed to illustrate the creep. In both decay cases, the log decrement was calculated by importing the A/D data (Dataq DI-154RS) to Excel and then using trial and error adjustment of parameters to achieve the best fit.

Although the damping of glasses is normally treated using the theory of viscoelasticity, Granato (2002) has recently modeled these materials via defects. In his paper, Granato states the following: "As dislocations carry the deformation in crystals, interstitials are the basic microscopic elements carrying the deformation in glasses near and above the glass temperature."

2.16.4 Failure of Viscoelasticity

Unfortunately for the elegant theory of the Zener model that has been presented, there are many mechanical systems for which the Q is not proportional to frequency, but rather proportional to the square of the frequency. The logarithmic decrement ($\Delta = \pi/Q$) has been measured for a host of

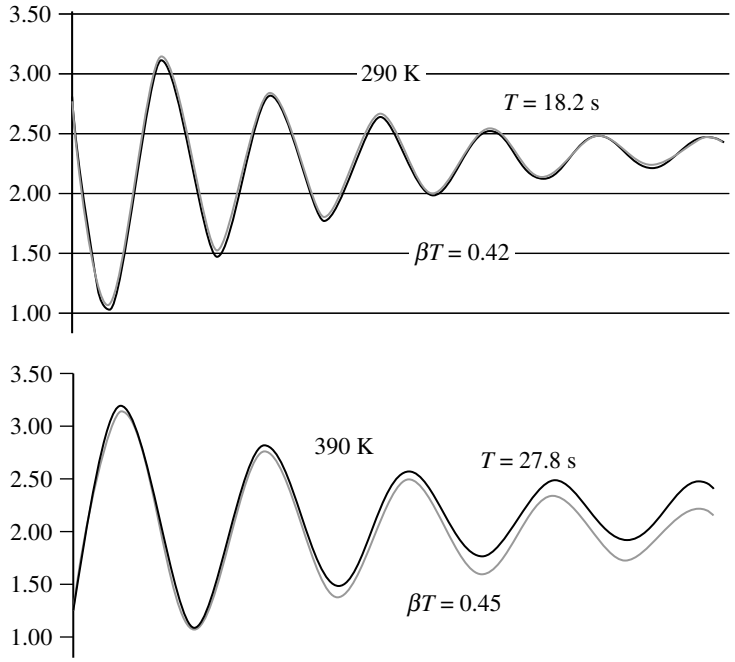

FIGURE 2.17 Torsional free-decay records of monofilament nylon at temperatures first below and then above the glass transition temperature. Although the modulus decreased dramatically at the higher temperature, the damping did not.

long-period mechanical oscillators, configured as some form of a pendulum. In all cases, these systems were described approximately by $\Delta = \beta T \alpha T^2$ rather than by $\beta T \alpha T$. Similar behavior has been noted in mechanical oscillators other than the pendulum — for example, in the geophysics research of Gunar Streckeisen and Erhard Wielandt, who are well known for the development of the widely employed STS-1 seismometer. During his pursuit of the Ph.D., Streckeisen (1974) measured the numerical damping (fraction of critical damping) of a vertical Sprengnether long-period seismometer 5100-V. After removing the magnet of the velocity transducer (to eliminate eddy currents and reduce viscous air damping, he found that the numerical damping was proportional to the square of the period between periods of 7 and 140 sec. He took about 30 measurements over this interval of periods, and showed that the damping increased from about 0.0008 to about 0.3 — a factor of roughly 400, not 20 as one would expect for viscous damping. To quote Wielandt (private communication), "the data are very clear."

2.17 Toward a Universal Model of Damping

2.17.1 Damping Capacity Quadratic in Frequency

The quadratic dependence on frequency of Q (log decrement proportional to period squared) is equivalent to friction force being frequency-independent. In support for the claim of universality, it was noted in the Introduction (Section 2.2.2) that three very different systems showed this characteristic: (i) the vertical seismometer just discussed, (ii) various pendula, and (iii) the rotating rod direct measurement of internal friction first done by Kimball and Lovell (1927), who measured the transverse deflection of the end of a rod when it was rotated about a horizontal axis.

2.17.2 Pendula and Universal Damping

An example of one of the author's experiments that illustrate universal (hysteretic) damping is provided in Figure 2.14. Other works that illustrate hysteretic damping include those by Peter Saulson of Syracuse University, who has been frequently cited in the literature (see Saulson et al., 1994).

The pioneering work of Braginsky (important to LIGO) has already been mentioned in the context of small force measurements and noise. He and his Moscow group members argue that the internal friction in fused silica may be roughly independent of frequency from 0.1 Hz to 10 kHz (Braginsky et al., 1993).

An oft-cited paper speaking to the issues of hysteretic damping is an article by Quinn et al. (1992) concerned with material problems in the construction of long-period pendula. (The type of pendulum on which they based their studies was first described in the scientific literature 2 years earlier (Peters, 1990).) In a follow-on paper, Speake et al. (1999) state the following: "The analogues of anelasticity and its resultant $1/f$ noise are seen in a wide range of other processes (for example, dielectric and magnetic ones) described in terms of frequency-dependent susceptibilities."

The jerkiness (discontinuous change) that is the hallmark of the Barkhausen effect may have been first seen mechanically in the experiments that generated the metastable states paper. From a consideration of the chapter by James Brophy (Brophy, 1965), it was postulated in this 1990 paper that the jerky behavior of a mesodynamic pendulum is a type of mechanical Barkhausen effect.

2.17.3 Modified Coulomb Model — Background

The results that follow grew naturally out of the application of fully differential capacitive sensors to the study of mechanical oscillators. Efforts to model internal friction influence on long-period pendula uncovered something surprising to most — that the foundation for physics laid by Charles Augustin Coulomb may be much broader than had been realized. Most individuals in the physics community do not associate Coulomb's name with contributions other than to the laws of electrostatics. Engineers, however, have long used his name in the context of sliding friction, since, in fact, Coulomb gave us the empirical description which involves static and kinetic coefficients. Because of his interest in the civil engineering of soils (Heyman, 1997), Coulomb also provided something else — a basis for understanding granular flows and even some types of fracture. Concerning the latter, the Mohr criterion, applied to the Coulomb failure envelope, defines a "coefficient of internal friction," which is used to predict brittle failure (Gere and Timoshenko, 1996).

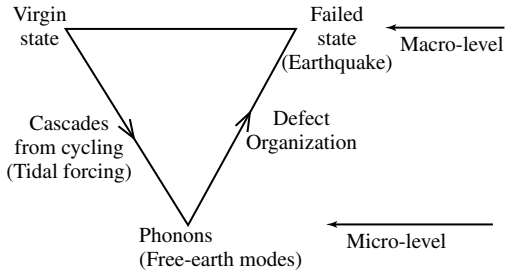

FIGURE 2.18 Heuristic description of how materials fail — processes connected with damping.

Coulomb friction is empirically simple, at least as a first approximation, since it depends only on the normal force between surfaces and the algebraic sign of the velocity when there is relative motion. Like so many problems of multibody type, a complete theory of sliding friction is far from being realized. Simplistic textbook efforts to explain energy loss, by picturing "hills and valleys" of the surface of two solids in contact, are useless. An example of such naivete can be realized by trying to understand the phenomenon of optical contacting. Two orthogonally oriented fused silica cylindrical fibers, allowed to touch, can experience atomic bonding forces that are surprisingly strong, being much greater than the weak attraction of the van der Waals type. Cleanliness of the surfaces is paramount for success in such a demonstration, which speaks to another issue — a connection between internal friction and surface physics.

The conversion of mechanical energy to thermal energy must involve nonlinear (avalanche or cascade) processes. A heuristic description of defect structural interactions that generate heat and eventual failure is the phonon triangle of Tom Erber (Illinois Tech University) shown in Figure 2.18. The author has

extended Erber's triangle to include the larger-scale Earth in an attempt to explain earthquakes. Everybody recognizes that the bending of a wire does not take it from the virgin initial state to the failed state along the macroscopic upper leg.

There must first be a downward path to the microlevel, through cascading. These cascades can cause Barkhausen noise in the case of ferromagnetic samples, and acoustic emission in nonmagnetic metallic alloys (PLC effect). Failure requires the upward path of defect organization, the mechanisms of which are not yet understood. One of the first theories with possible implications to the organization leg is that of self-organized criticality. In the magnetic case, Erber has used a fluxgate magnetometer to improve failure predictions, since magnetic hysteresis is proving to be a sensitive indicator of mesoscale structure changes during cycling toward failure. Inferred from these studies is some yet-to-be discovered connectivity between noise, damping, and failure.

Surface friction is expected somehow to be connected with internal friction, the biggest difference being that the surface has many more defect states with which to redistribute energy. The larger density of states of the surface (reduced order) is probably an important factor in the difference between surface friction and the modified internal friction model which follows.

2.17.4 Modified Coulomb Damping Model — Equations of Motion

In the following damping model for internal friction, Coulomb's law of sliding friction is modified by assuming that the coefficient of friction is not constant, but rather involves the energy of oscillation E in a power law; i.e.

$$m\ddot{x} + cm\left[\frac{2E}{k}\right]^{\lambda} \operatorname{sgn}(\dot{x}) + kx = 0, \qquad E = \frac{1}{2}m\dot{x}^2 + \frac{1}{2}kx^2 \tag{2.51}$$

where c = constant that is different for each λ. For Coulomb (sliding) friction $\lambda = 0$. For amplitude-independent damping of hysteretic type, $\lambda = \frac{1}{2}$. For amplitude-dependent (such as large Reynolds number fluid) damping, $\lambda = 1$. In all cases, if $c << 1$ (small damping), the damping capacity is quadratic in the frequency, so that the internal friction $Q^{-1} \sim \omega^{-2}$. Equation 2.51 is easily implemented, in spite of its nonlinearity, which we will see later to be a cause for harmonics in the decay.

It is convenient to rewrite Equation 2.51 in canonical form so as to involve the Q of the oscillator. For the case of hysteretic damping ($\lambda = \frac{1}{2}$), the equation becomes

$$\ddot{x} + \frac{\pi\omega}{4Q_h}\sqrt{\omega^2x^2 + \dot{x}^2}\ \operatorname{sgn}(\dot{x}) + \omega^2 x = 0 \tag{2.52}$$

Similarly, for amplitude-dependent damping ($\lambda = 1$)

$$\ddot{x} + \frac{\pi}{4y_0Q_{f0}}(\omega^2x^2 + \dot{x}^2)\operatorname{sgn}(\dot{x}) + \omega^2 x = 0 \tag{2.53}$$

where y_0 is the initial value of the amplitude of x (largest maximum of x), and Q_f is found not to be constant, as in the case of hysteretic damping. Rather, in this case, the Q increases as the amplitude decreases. On the other hand, the Q of an oscillator influenced only by Coulomb ($\lambda = 0$, sliding) friction decreases with the amplitude, and the equation of motion in canonical form is given by

$$\ddot{x} + \frac{\pi\omega^2 y_0}{4Q_{c0}}\ \operatorname{sgn}(\dot{x}) + \omega^2 x = 0 \tag{2.54}$$

In Equation 2.53 and Equation 2.54, the subscript 0 is used to identify the initial value of the time varying Q. Equation 2.54 is equivalent to equation 2.12 with $Q_{c0}/y_0 = \pi/(4\Delta_x)$.

As will be illustrated with some examples, it is possible for an oscillator to be influenced simultaneously by all three types of friction. One may treat such a system with the following equation of motion

$$\ddot{x} + \left[\frac{\pi\omega^2 y_0}{4Q_{c0}} + \frac{\pi\omega}{4Q_h}\sqrt{\omega^2 x^2 + \dot{x}^2} + \frac{\pi}{4y_0 Q_{f0}}(\omega^2 x^2 + \dot{x}^2) \right] \mathrm{sgn}(\dot{x}) + \omega^2 x = 0 \tag{2.55}$$

At any instant during the decay, the total (time-dependent Q) is given by

$$\frac{1}{Q(t)} = \frac{1}{Q_c} + \frac{1}{Q_h} + \frac{1}{Q_f} \tag{2.56}$$

in which it is seen that the smallest Q in the set (largest damping term) is dominant in a manner reminiscent of capacitors connected in series.

It is instructive to look at the analytical solution for the time dependence of the amplitude (turning points, $y(t) = |x_{\max}|$), when all the Qs $>> 1$. Such a solution is obtained from energy considerations by noting first that the time rate of change of the energy is zero in the absence of friction, i.e.

$$\dot{E} = \frac{\mathrm{d}}{\mathrm{d}t}\left(\frac{1}{2}m\dot{x}^2 + \frac{1}{2}kx^2\right) = \dot{x}(m\ddot{x} + kx) = 0, \qquad \text{no friction} \tag{2.57}$$

With friction, dE/dt is determined by the rate of doing work against the friction force; i.e., dE/dt is proportional to $\omega y f$, where f is the friction force. In the case of Coulomb friction, f is constant (determined by y_0,) so dE/dt is proportional to $E^{1/2}$. For hysteretic damping, f is proportional to y, so dE/dt is proportional to E. For fluid damping, f is proportional to y^2, so dE/dt is proportional to $E^{3/2}$. Thus, the general case is described by

$$\dot{E} = -\left(c_1 + c_2\sqrt{E} + c_3 E\right)\sqrt{E} \tag{2.58}$$

Because the energy is proportional to y^2, we can write down the equation for the time varying amplitude as

$$\dot{y} = -c - by - ay^2 \tag{2.59}$$

where a, b, and c are constants. The solution to this first-order equation can be found in integral tables, and the result depends on the size of c relative to the product ab. For present purposes, we will restrict ourselves to the case where Coulomb damping is not dominant, in which the solution involves an exponential. (For large c, one may develop the corresponding general case in terms of the tangent or its inverse.) The present result is as follows, using $r = (b^2 - 4ac)^{1/2}$, where $4ac < b^2$

$$\text{with } \alpha = 2ay_0 + b - r, \qquad \beta = 2ay_0 + b + r, \qquad p = \frac{\alpha}{\beta}\mathrm{e}^{-rt}$$

$$y = \frac{b(p-1) + r(p+1)}{2a(1-p)} \tag{2.60}$$

In the case where $c = 0$, Equation 2.60 can be simplified to the following form, which is useful for curve fitting:

$$\frac{1}{y} = \left(\frac{a}{b} + \frac{1}{y_0}\right)\mathrm{e}^{bt} - \frac{a}{b} \tag{2.61}$$

For the case where $a = 0$, the better form for curve fitting is

$$y = \left(y_0 + \frac{c}{b}\right)\mathrm{e}^{-bt} - \frac{c}{b} \qquad (\text{until } y = 0) \tag{2.62}$$

Curve-fits based on the modified Coulomb damping model are summarized in Box 2.2.

Box 2.2
Curve-Fit to the Turning Points

If no damping

$$\dot{E} = \frac{\mathrm{d}}{\mathrm{d}t}\left(\frac{1}{2}m\dot{x}^2 + \frac{1}{2}kx^2\right) = \dot{x}(m\ddot{x} + kx) = 0, \qquad \text{no friction}$$

with damping (E prop. to y^2, $\dot{E}$ prop. to $\omega y \cdot$ friction force)

$$\dot{E} = -\left(c_1 + c_2\sqrt{E} + c_3 E\right)\sqrt{E}$$

equivalent to (c for Coulomb, b for hysteretic, a for fluid)

$$\dot{y} = -c - by - ay^2$$

general solution

$$\text{with } \alpha = 2ay_0 + b - r, \qquad \beta = 2ay_0 + b + r, \qquad p = \frac{\alpha}{\beta}\mathrm{e}^{-rt}$$

$$y = \frac{b(p-1) + r(p+1)}{2a(1-p)}$$

special case, $c = 0$

$$\frac{1}{y} = \left(\frac{a}{b} + \frac{1}{y_0}\right)\mathrm{e}^{bt} - \frac{a}{b}$$

special case, $a = 0$

$$y = \left(y_0 + \frac{c}{b}\right)\mathrm{e}^{-bt} - \frac{c}{b} \qquad (\text{until } y = 0)$$

2.17.5 Model Output

Shown in Figure 2.19 is a case in which the decay is influenced by all three types of friction. Notice how the Q rises initially, peaks at a value less than what would be true for hysteretic damping alone (constant Q case), and then later declines. The initial rise is due to the amplitude-dependent damping term (size determined by coefficient a), and the later decline is due to the Coulomb damping term (determined by coefficient b).

The code in Table 2.1 that was used to generate Figure 2.19 has been reproduced here for two reasons: (i) to show the ease with which the modified Coulomb model may be numerically applied in general to a damping problem, and (ii) to illustrate an integration algorithm that has proven to be intuitive, simple, and powerful — the Cromer–Euler technique, which Alan Cromer first described as the "last point approximation (LPA)" (Cromer, 1981) in contrast to the unstable "first point approximation" given to us by Euler. Over the last 20 years, the author has employed the LPA in a host of applications that span from the generation of satellite ephemerides in the U.S. antisatellite program to both simple and several-body nonlinear problems of deterministic chaos type.

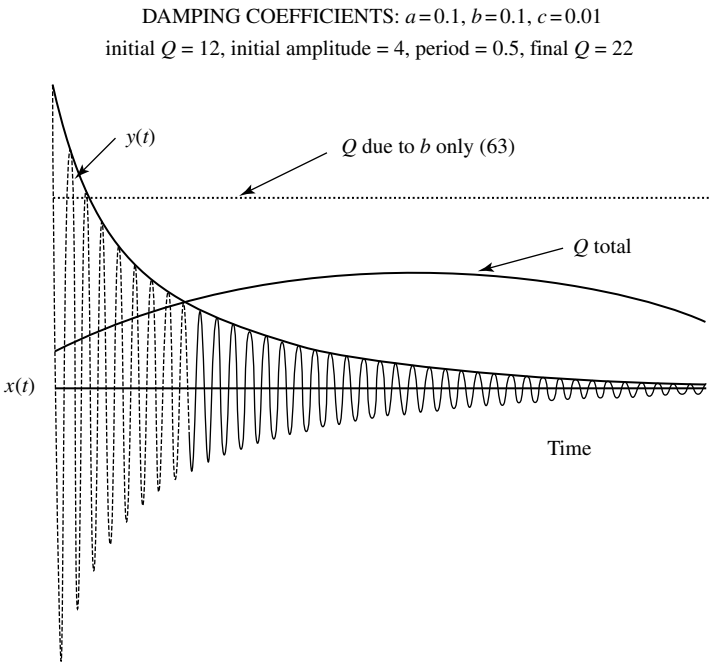

FIGURE 2.19 Model generated results based on Equation 20.55 and Equation 2.60.

2.17.6 Experimental Examples

The code of Table 2.1 is useful in determining the nature of a given experimental case. Too frequently in the past, it has been naively assumed that the entire decay record was exponential. Particularly when longer records are collected, it is found that most damping is nonlinear. In the two experimental examples that follow to backup this claim, one is a near-perfect (nonlinear) particular case of amplitude-dependent (fluid) damping, and the other is a mixture of amplitude-dependent and hysteretic damping, but devoid of any Coulombic influence. Coulomb friction frequently tends to be either "all or nothing," depending on whether there is an unwanted mechanical contact that involves slippage. A notable exception is found in the case where a pendulum is influenced by eddy current damping in a narrow region of its total motion (Singh et al., 2002).

The pendulum that was used to generate the data displayed in Figure 2.14 was also used as follows. A large flat piece of plastic was attached to the bottom of the pendulum, so that its movement (normal vector to the surface in the direction of motion) would disturb a great amount of air in turbulent manner. As expected, there was a dominant initial (large level) amplitude-dependent damping, as shown in Figure 2.20.

The speed (maximum) was measured with a photogate as previously discussed. The expressions shown in the figure are consistent with Equation 2.59 and Equation 2.61. The data, which were collected by hand and typed into Excel, produced the "jagged" curve, and the computerized fit according to Equation 2.61 is the smooth curve of the pair. It is noteworthy that the quadratic drag of the air (determined by $a = 0.036$) is 40% greater than the viscous drag at the start of the decay. By cycle 37, the quadratic part has become much less significant than the constant Q viscous part, having become roughly 60% smaller.

The fluid damping "soup-can" pendulum data of Figure 2.21 was generated with a can of Bush's black-eye peas. The container with enclosed unbroken contents, being a right circular cylinder of length 11 cm × diameter 7.4 cm, was suspended horizontally by a pair of knife edges under opposing end-lips

TABLE 2.1 QuickBasic Code to Calculate Amplitude History $y(t)$ and Integrate Equation of Motion to Obtain $x(t)$; Accommodates Three Common Forms of Friction

```
CLS
  REM: setup display
SCREEN 12: VIEW (0, 0) − (600, 470): WINDOW (− .2, − 5) − (1, 5)
  REM: assign constants and initialize variables
pi = 3.1416: dt = 0.002: t = 0
x0 = 4: x = x0: y0 = x0: xd = 0
Period = .5: omega = 2*pi/period: b = .1: a = .1: c = .01
  REM: print damping coefficients
PRINT "DAMPING COEFFICIENTS: a = "; a; ", b = "; b; ", c = "; c
r = SQR(b^2 − 4*a*c): alpha = 2*a*x0 + b − r
Beta = 2*a*x0 + b + r
  REM: Use a, b and c — set Q's to dampen (quadratic, linear, and constant resp.)
qf = omega/2/a/y0: qh = omega/2/b: qc = y0*omega/2/c
  REM: start integration loop
LOOP0:
t = t + dt
  REM: analytically compute amplitude (y = magnitude of x) at each time point
p = alpha*EXP(−r*t)/beta
y = (b*(p − 1) + r*(p + 1))/2/a/(1 − p)
  REM: integr. the eq. of motion to get x(t), using 3 fric. force/mass terms
  REM: The coeff.'s ff, fh & fc correspond to: quadratic in speed (fluid),
  REM: linear in speed (hysteretic), and independ. of speed (Coulomb) resp.
ff = (pi/4)*(1/y0)*(1/qf)*(omega^2*x^2 + xdot^2)
fh = (pi/4)*(omega/qh)*SQR(omega^2*x^2 + xdot^2)
fc = (pi/4)*omega^2*y0/qc
  REM: check algebraic sign – USE SIGN BUT NOT MAGNITUDE OF VELOCITY
IF xdot > 0 THEN GOTO SKIP
ff = − ff: fh = − fh: fc = − fc
SKIP: xdoubledot = − ff − fh − fc − omega^2*x
xdot = xdot + xdoubledot*dt: x = x + xdot*dt
  REM: calculate the energy and then the amplitude to evaluate Q
  REM: could instead use analytical result q = (pi/4)*omega2*x/abs(ff + fh + fc)
Energy = .5*xdot^2 + .5*omega^2*x^2
Amplitude = SQR(2 * energy)/omega
  REM: calculate loss per period due to friction
loss = ABS(ff + fh + fc)*4*amplitude
q = 2*pi*energy/loss
IF t < 1.2*dt THEN PRINT "initial Q = "; 10*INT(q)/10;
IF t < 20 THEN GOTO SKIP2
PRINT ", initial Amplitude = "; x0; ", Period = "; period;
PRINT ", final Q = "; 10*INT(q)/10
  REM: DO GRAPH
SKIP2: PSET(.04*t, .5*q/omega): PSET (.04*t, .5*qh/omega), 4
PSET (.04*t, 4*x/y0): PSET (.04*t, 0): PSET (.04*t, 48*y/y0)
IF t > 20 OR y < 0 THEN GOTO pause
GOTO LOOP0
Pause: GOTO pause
RETURN: END: STOP
```

(Peters, 2002a, 2002b, 2002c). The motion of the can was measured with an SDC sensor connected to a Dataq A/D converter. Whereas experiments of similar type, with homogeneous fluid contents, have produced viscous decay records, the present case involved only friction of so-called "fluid" type; i.e., quadratic in the "velocity." To generate the figure, the A/D record was exported to the Microsoft software package, Excel. Fits to the data were then obtained by adjusting, through trial and error, the a, b, and c

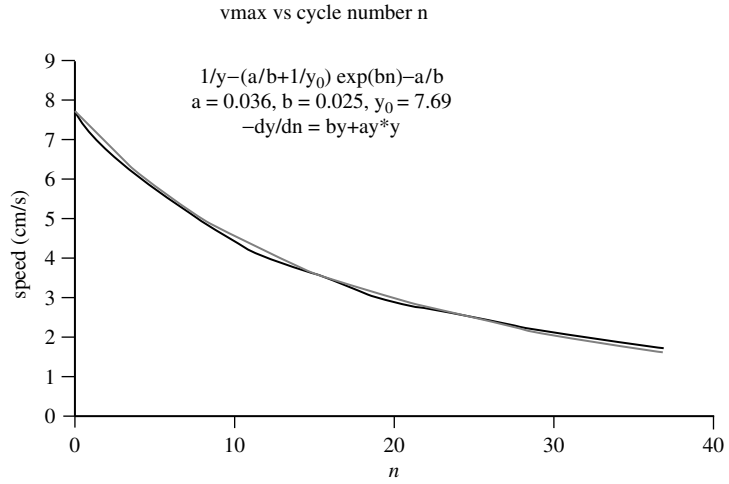

FIGURE 2.20 Decay of an air-damped pendulum as a function of cycle number *n*.

coefficients of a "fit" to the amplitude. For this case, the fit was easily accomplished because both *b* and *c* proved to be essentially zero.

The second case, involving an evacuated pendulum, was not a single pure type of damping, but can be seen in Figure 2.22 to have both hysteretic and amplitude-dependent contributions. Although fluid damping is amplitude-dependent in the same manner, with the damping term being proportional to the square of the amplitude, the word "fluid" is not used to describe this case since the system involved exclusively solid materials.

Not all decay records of this pendulum in vacuum yielded a mix of friction types as displayed in the figure. The effect was observed to be transient, and it is speculated that outgassing of components may have been a factor.

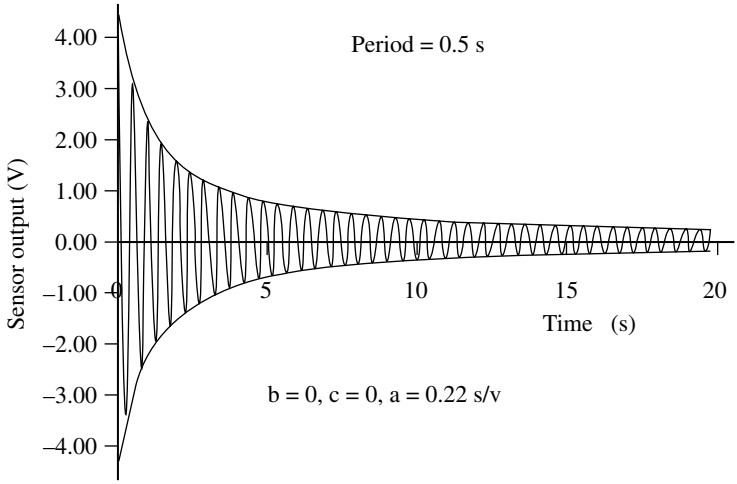

FIGURE 2.21 Example of fluid damping of a "soup-can" pendulum. The granular contents (black-eye peas and water) result in a friction force that is quadratic in the velocity.

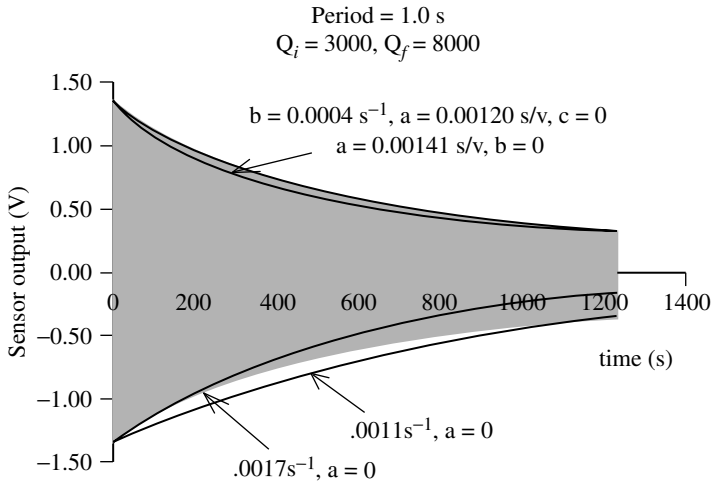

FIGURE 2.22 Example of a mix of two damping types, hysteretic and amplitude-dependent.

2.17.6.1 Numerical Integration

Instead of integrating the second-order equation of motion twice — first the acceleration, followed by the resulting velocity — more accurate results are obtained by integrating the equivalent pair of first-order equations.

For example, the equation of the simple harmonic oscillator with viscous damping is expressible as

$$\dot{p} = -q - kp \qquad \dot{q} = p \tag{2.63}$$

where the position variable has been represented by the generalized coordinate q (x elsewhere), and for the momentum $p = m\,\mathrm{d}q/\mathrm{d}t$, and here the mass, m, has been set to unity. Likewise, the spring constant has been set to unity. It is generally useful to distill a given problem to its most basic form when attempting to understand the physics. Constants that provide no useful information for trend analysis purposes are conveniently "normalized." Such is common practice, for example, in modeling chaotic systems.

The second-order set can always be reduced mathematically to a first-order pair; however, the pair results naturally from the use of the Hamiltonian as opposed to the Newtonian formulation of mechanics.

2.17.7 Damping and Harmonic Content

Equation 2.52 to Equation 2.54 are the nonlinear, modified Coulomb damping model forms that correspond, respectively, to (i) hysteretic, (ii) amplitude-dependent, and (iii) Coulomb damping. The damping term for each of the three cases can be expressed as follows:

$$\frac{f}{m} = \frac{\pi}{4}\frac{\omega}{Q}[v] \tag{2.64}$$

where f is the friction force, and $[v]$ is the square wave whose fundamental in a Fourier series expansion is equal to the velocity of the oscillator times $4/\pi$; i.e., for a square wave $\pm h$, the amplitude of the fundamental is $\pm(4/\pi)h$. We see that all the damping types that have been considered in this chapter, when expressed in canonical form, correspond to a fundamental friction force $f = m\omega v/Q$. The simplicity of this result is probably why viscous damping has been viewed by so many physicists as "inviolate." One must be careful, however, because (as noted in the previous section) only for the case of hysteretic damping is Q constant. For amplitude-dependent damping $Q_f = Q_{f0}(y_0/y)$ and for Coulomb damping

$Q_c = Q_{c0}(y/y_0)$. The time-dependent Q of nonexponential cases will have significant influence on mode development in many-body systems because of elastic nonlinearity (necessary for mode coupling).

There is another important subtlety of Equation 2.64. When only the fundamental of $[v]$ is retained, equivalent to viscous damping, Q is proportional to frequency. When all odd harmonics are included (full square wave), Q becomes proportional to frequency squared. This means that *harmonics in the friction force are responsible for the primary difference between hysteretic damping and viscous damping*. Something being presently considered is how, in an algorithmic sense, to modify Equation 2.52 to Equation 2.54 to provide for "dispersion," i.e., means for providing Q dependence other than frequency squared. We posit the following: that hysteretic (exponential) damping is the idealized universal form of damping due to secondary creep. When there is an activation process of Zener (Debye) type, such as dislocation relaxation, then additional terms must be added to the hysteretic "background." It may be that this can be accommodated by a suitable removal of harmonics from the square wave of the hysteretic case, and it may happen that Q is constant for systems that vary continuously. It is conjectured that the PLC effect, responsible for discontinuous changes, plays a role in those cases where Q is not constant. Equations of motion based on the modified Coulomb damping model are summarized in Box 2.3.

Box 2.3
Equations of Motion Based on Nonlinear Damping

Equation of motion in terms of energy

$$m\ddot{x} + cm\left[\frac{2E}{k}\right]^2 \operatorname{sgn}(\dot{x}) + kx = 0, \qquad E = \frac{1}{2}m\dot{x}^2 + \frac{1}{2}kx^2$$

Hysteretic-only damping (exponential)

$$\ddot{x} + \frac{\pi\omega}{4Q_k}\sqrt{\omega^2x^2 + \dot{x}^2}\,\operatorname{sgn}(\dot{x}) + \omega^2x = 0$$

Velocity-square (fluid) damping

$$\ddot{x} + \frac{\pi}{4y_0Q_{f0}}(\omega^2x^2 + \dot{x}^2)\operatorname{sgn}(\dot{x}) + \omega^2x = 0$$

Coulomb damping

$$\ddot{x} + \frac{\pi\omega^2y_0}{4Q_{c0}}\operatorname{sgn}(\dot{x}) + \omega^2x = 0$$

All three damping types simultaneously active

$$\ddot{x} + \left[\frac{\pi\omega^2y_0}{4Q_{c0}} + \frac{\pi\omega}{4Q_k}\sqrt{\omega^2x^2 + \dot{x}^2} + \frac{\pi}{4y_0Q_{f0}}(\omega^2x^2 + \dot{x}^2)\right]\operatorname{sgn}(\dot{x}) + \omega^2x = 0$$

Quality factor

$$\frac{1}{Q(t)} = \frac{1}{Q_c} + \frac{1}{Q_k} + \frac{1}{Q_f}$$

2.18 Nonlinearity

2.18.1 General Considerations

Electrical nonlinearity is the type with which most engineers are familiar. It is the very basis for common nondigital forms of communication, such as that of frequency modulation type. A popular form of radio amateur communication is one in which the carrier and one of the two normal sidebands of a signal are suppressed before going to the antenna. At the receiver, the carrier is "regenerated" before going to the demodulator. The demodulator required for ultimate transduction by speaker is also a nonlinear device.

Nonlinearity of mechanical type is encountered throughout nature. The human ear, for example, is not linear, but rather characterized by both quadratic and cubic nonlinearities. If an intense, pure low frequency (inaudible) sound of frequency f is present with a higher frequency audible one of frequency F, then one typically hears (in addition to F) tones at $F \pm f$ due to the quadratic nonlinearity and $F \pm 2f$ due to the cubic nonlinearity.

Very high frequency acoustics (ultrasound) is employed for studies of elasticity. The quasi-linear features of ultrasonic propagation have been the basis for measuring second-order elastic constants (determined by velocity of propagation) and internal friction (by attenuation of the beam, i.e., damping). A commonly employed ultrasonic technique that has been used to study both linear and nonlinear phenomena is the pulse-echo method. By using a thin specimen and extending the pulse width, the overlapped signal can add constructively or destructively and, in the former case, resonance is approached as the width gets very large (Peters, 1973). The pulse-echo method was the basis for this author's Ph.D. dissertation ("Temperature dependence of the nonlinearity parameters of copper single crystals," The University of Tennessee, 1968). The distinguished career of his professor, M.A. Breazeale, has focused on ultrasonic harmonic generation as a means to determine the shape of the interatomic potential of solids (Breazeale and Leroy, 1991). A longitudinal wave distorts because of the anharmonic potential (acoustic equivalence of optical frequency doubling with lasers in a KdP crystal). In like manner, phonon–phonon interactions are possible only because of nonzero elastic constants of order higher than second (second-order constants determining the harmonic potential). Because phonon–phonon interactions are part of damping, there must be consequences, at least for some cases, from nonlinear damping terms.

The unifying theme for this chapter is that damping is fundamentally nonlinear, in spite of the fact that linear approximations have prevailed in modeling and, for many purposes these linear models appear to be acceptable (Richardson and Potter, 1975). In their paper, Richardson and Potter state that "… an equivalent viscous damping component can always be derived, which will account for all of the energy loss from the system. Thus, in measuring the modal vibration parameters for the linear motion of a system, we don't care what the detailed damping mechanism really is."

Although their statement may be true for steady state, it is not expected to be true for the transient processes that lead to steady conditions of oscillation. As demonstrated elsewhere in this chapter, mixtures of different damping types are common among oscillators, and only with viscous or hysteretic damping is the Q independent of amplitude. Other cases may result, for example, from the decay being a combination of hysteretic damping and amplitude-dependent damping. An example used to illustrate this combination was an outgassing pendulum oscillating in vacuum. Similarly, a long, "simple" pendulum, oscillating in air, is found to require a pair of terms — viscous damping and "fluid" damping (Nelson and Olssen, 1986). In the Nelson and Olsson experiment, the drag was found, because of the size of the Reynolds number, to involve both first- and second-power velocity terms. Their case can, incidentally, be treated by the modified Coulomb, generalized damping model of this document.

The presence of either amplitude-dependent damping or Coulomb damping is expected to play a role in determining what modes of a multibody system are actually excited by external forcing. Concerning the latter, Coulomb friction is the basis for exciting chaotic vibrations in mechanical systems (Moon, 1987). Without the nonlinear friction, the excitation would be impossible. In similar manner (although chaotic motion may be present but not in an obvious way), friction from rosin on a violin bow is used to

play the violin. Still another example of similar physics is the "singing rod" that was mentioned elsewhere as exhibiting thermoelastic damping.

Whatever combinations of normal modes are initially excited in a linear system are the only ones that can exist thereafter. Such is not the case, however, for many systems and, since nonlinearity is required for mode coupling, there must be nonlinearity in the equations of motion. There is no question about the existence and importance of elastic nonlinearity. Indeed, thermal expansion would be impossible in the absence of higher order elastic constants. The importance of nonlinear damping remains yet to be quantified, since models to include it have been few in number. For those who have found it advantageous to include the oldest and simplest type of nonlinearity in a damping model — Coulomb damping (sliding friction) — the improvements realized by their choice are unlikely to cause them to revisit the problem and try to solve it in terms of a viscous equivalent linear approximation.

There are many examples of damping of a single type other than viscous. In their efforts to improve the knowledge of the Newtonian gravitational constant $G = 6.67 \times 10^{-11}$ Nm^2/kg^2 (approx.), Bantel and Newman (2000) discovered a pure form of amplitude-dependent damping of internal friction type. They did their experiments at liquid helium temperature (4.2 K) and noted the following: "A striking feature noted in our data is the linearity of the amplitude dependence of Q^{-1} for the three metal fiber materials," and also "Linearity implies that Q may depend on frequency but not on amplitude, while in fact Fig.1 displays a significant amplitude dependence (and hence nonlinearity) of internal friction in all fibers tested." They also considered the temperature dependence of damping and note that there are two independent contributions in Cu–Be. One is linear and temperature-independent and the other amplitude-dependent and independent of temperature. Finally, it is worth noting their statement, "…our results are strongly suggestive of some kind of 'stick–slip' mechanism …," which lends strong support to the modified Coulomb internal friction damping model of the present document.

Repetition is felt to be warranted — such systems cannot always be reasonably described by an equivalent viscous form! For a case of amplitude-dependent Q, the equivalent form has no meaning unless the amplitude is fixed, i.e., it oscillates at steady state. Unfortunately, the evolution of the system to steady state is expected to depend on the damping form(s). Surely a model (not yet realized) that predicts what modes survive is worth much more than one which only characterizes the modes after they have reached steady state. The author and Prof. Dewey Hodges of Georgia Tech's Aerospace School are planning projects to try to develop such predictive capability. The present state of the art applied to structures suggests that a truly predictive model cannot ignore damping nonlinearity.

As demonstrated by Bantel and Newman (2000), the mixture of damping types that can co-exist in a system may change with temperature. Early experiments by Berry and Nowick (1958) also showed, as have many investigators subsequently, that damping generally depends on aging. It is naive to believe that aging would not also change the mix of damping types, when there is more than one type. Thus, an adequate damping model must be able to easily accommodate several damping types that are simultaneously active. A variety of engineering techniques have evolved to treat such problems. The most "successful" ones suffer from the fact that an excessive number of parameters or coupled equations must be adjusted by trial and error to yield decent agreement with experiment. This is reminiscent of the state of high-energy (nuclear) physics before the standard model. The hallmark of physics success has always been *simplification*. As noted by Albert Einstein: "All physics is either impossible or trivial. It is impossible until you understand it. Then it becomes trivial." It is hard to imagine, however, that certain damping physics could ever become trivial. Nevertheless, the simplifying nature of better conceptual understanding is a goal to strive for.

One of the remarkable things about the majority of damping models has been the absence of a direct consideration of energy in describing the dissipation process. After all, the most important quantity transformed by the damping is energy, so its inclusion is natural.

2.18.2 Harmonic Content

When the damping is nonlinear, the waveform of the oscillator in free-decay contains harmonics. The harmonic content is most obvious in the residuals (difference) after fitting a damped sinusoid to the record, as shown in Figure 2.23.

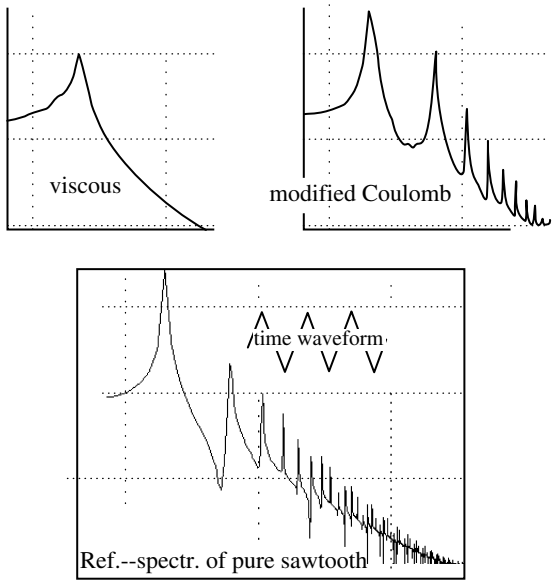

FIGURE 2.23 Harmonic differences between the residuals of the modified Coulomb damping model and the classic viscous damping model. For reference purposes, a pure sawtooth is included in the figure.

Residuals are still present for the viscous case because the equation of motion was integrated numerically and compared against the classic exponentially decaying sinusoid (solution to the equation) that was used for fitting in all cases. There is always some degree of mismatch with the fit because of rounding errors in the computer. In Figure 2.23, the fundamental is smaller for the viscous case because the fit is inherently more perfect by about an order of magnitude in most of the "eye-ball" fits that were performed by Excel after importation of the data.

A test for harmonic content was performed on the seismometer (17-sec period) data displayed in Figure 2.11 illustrating phase noise. The power spectrum of the residuals for that case is shown in Figure 2.24.

The third harmonic is especially noticeable in this case. That the other harmonics are not so "cleanly" displayed may result from the significant phase noise of the record.

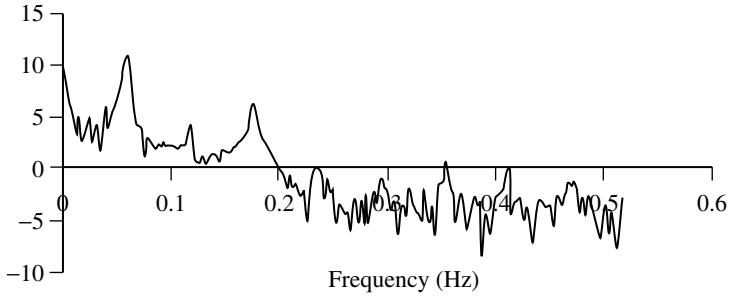

FIGURE 2.24 Power spectrum of residuals, Sprengnether vertical seismometer free-decay, showing harmonic content.

By looking at the FFT of residuals, rather than the experimental record itself, one finds evidence for a combination of both mechanical and electronic noise. At lower frequencies, the noise (largely mechanical) is approximately $1/f$, while at higher frequencies the noise (largely electronic) begins to be more nearly "white" (frequency-independent) because of discretization errors of the resolution-limited 12-bit A to D converter.

In general, more spectral information can be gleaned from a consideration of the residuals than from the experimental data alone, particularly as one looks for harmonic distortion of mechanical type. Spectral "fingerprints" may prove ultimately useful in determining to what extent damping models of engineering type need to be implemented in full nonlinear form as opposed to an "equivalent viscous" form that is more convenient mathematically.

The importance of the harmonics observed in Figure 2.24 in determining system evolution is not completely known. It was noted earlier that they are expected to influence the evolution of a multibody system to steady state. Presently, it appears that they may serve to validate damping models. From one model type to another, there can be significant differences in the spectral character of the residuals, as shown in Figure 2.25. As compared with Figure 2.23, the fit with the modified Coulomb (hysteretic case) model has been tweaked to reduce the fundamental somewhat, but the odd harmonics remain significant. Observe that the spectrum of the residuals is almost the same for this model and the simplified structural model (see de Silva, 2000, p. 354). This is true even though the temporal variation of the friction force is dramatically different for the two, as seen from the lower time traces that were used to obtain the residuals (which are too small to be seen in the graphs).

From this author's perspective, the simplified structural model is unrealistic, since the friction force, given by $f = c|x|\ \mathrm{sgn}(\dot{x})$, vanishes for zero displacement (the absolute value of the displacement being used to get the hysteretic form of frequency dependence). This is seen in Figure 2.26, which compares hysteresis curves for several models. The modified Coulomb case shown is slightly different from Equation 2.52 that was used to generate Figure 2.25; Figure 2.26 was generated with the A_{prev} shown in Equation 2.10.

More studies of this type are obviously called for. The spectrum of residuals is a powerful means for the study of damping physics, and it needs to be more widely employed.

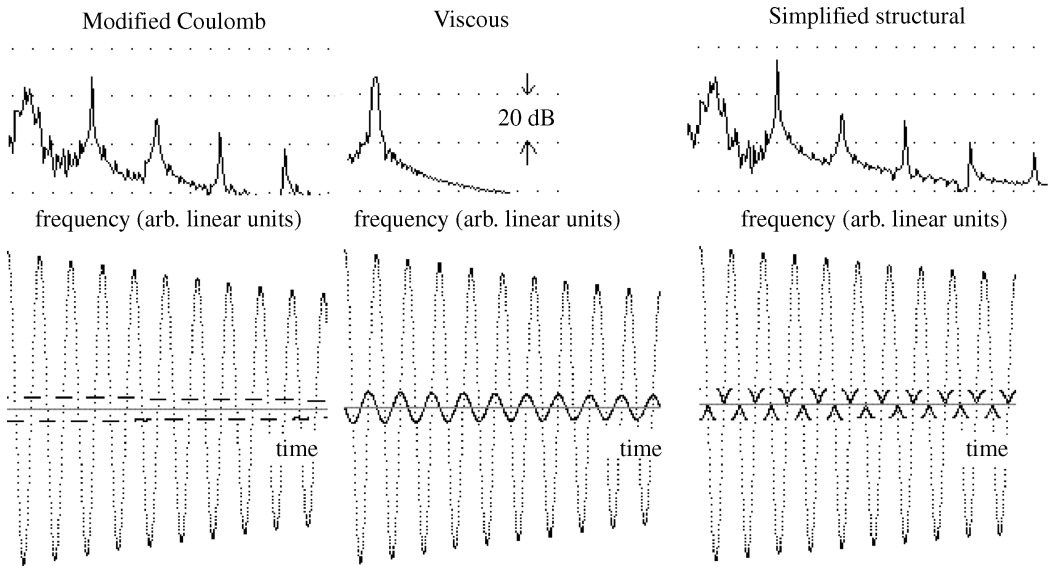

FIGURE 2.25 Illustration of the spectral difference of the residuals for three different damping models. The corresponding temporal records used to generate the spectra are also shown underneath each case.

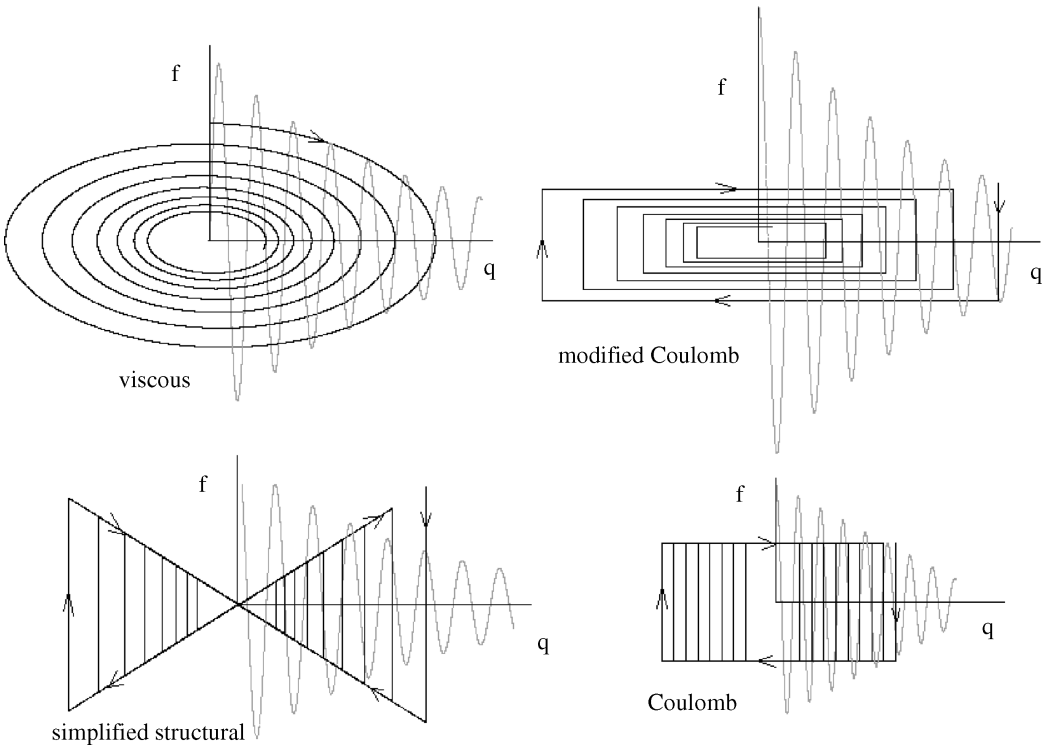

FIGURE 2.26 Comparison of hysteresis curves for some damping models.

2.18.3 Nonlinearity/Complexity and Future Technologies

Nonlinear damping models must improve if we are to overcome various technological barriers. One barrier is in the area of civil engineering. One of the pioneers of finite element modeling (FEM) is Prof. Emeritus Edward L. Wilson, of the University of California Berkeley. In Technical Note 19 (pertaining to "structural analysis programs") — a document published by his company Computers and Structures Inc — Dr. Wilson says the following:

> Linear viscous damping is a property of the computer model and is not a property of a real structure.

Expanding upon the statement, he notes:

> the use of linear modal damping, as a percentage of critical damping, has been used to approximate the nonlinear behavior of structures. The energy dissipation in real structures is far more complicated and tends to be proportional to displacements rather than proportional to the velocity. The use of approximate "equivalent viscous damping" has little theoretical or experimental justification…the standard "state of the art" assumption of modal damping needs to be re-examined and an alternative approach must be developed [in reference to Rayleigh damping].

One of the hi-tech areas where modeling improvements are also sorely needed is that involving miniaturized mechanical systems. For example, MEMS devices have already encountered some of the "strange phenomena" of solid-state physics mentioned by Richard Feynman in his famous 1959 talk. To master or compensate for these phenomena, better understanding of the physics will be necessary.

2.18.4 Microdynamics, Mesomechanics, and Mesodynamics

At least three different broad fields of research have focused on problems associated with the structural defects that cause hysteresis. These are as follows.

2.18.4.1 Microdynamics

In the microdynamics world, the emphasis appears to have been primarily on "contact" friction. The 6th Microdynamics Workshop held at the Jet Propulsion Laboratory in 1999 produced the following statements (quoting Marie Levine's Program Overview): (1) "We have demonstrated that microdynamics exist. The next step is to qualify and quantify microdynamics through rigorous testing and analysis techniques." (2) Microdynamics is "defined as sub-micron nonlinear dynamics of materials, mechanisms (latches, joints, etc.) and other interface discontinuities."

In this workshop, it was noted that frequency-based computational methods *cannot* be used to model quasi-static, transient, and nonstationary disturbances. One of the flight operations they have recommended to minimize adverse effects of microdynamics is dithering.

2.18.4.2 Mesomechanics

Ostermeyer and Popov (1999) have the following to say about mesomechanics: "Real physical objects inherently possess discrete internal structures. Great efforts are needed to formulate continuum models of really granular bodies. The history of the last two centuries in a multitude of ways has been marked by highly successful attempts at formulating and analyzing the continuum models of the discrete world. In spite of great advances of continuum mechanics, a number of physical processes are amenable to simulation within the framework of continuum approaches only to a very limited extent. Among these are primarily all the processes whereby the medium continuity is impaired; i.e., those of nucleation and accumulation of damages and cracks and failure of materials and constructions."

Their paper speaks to one of the difficulties concerning granular materials that was mentioned earlier in this chapter — that the potential energy cannot be defined in the common manner. They introduce a temperature-dependent nonequilibrium interaction potential that is not constant in time due to the relaxation processes occurring in the system.

2.18.4.3 Mesodynamics

The author of this chapter is singlehandedly responsible for the use of the term "mesodynamics" in the context of mechanical oscillators. His research has been conducted independently of those doing mesomechanics; he came only recently to know of the latter. Whereas mesomechanics seems to have been largely concerned with failure, mesodynamics has been concerned with low-level hysteresis. It is probably closely related to the aforementioned microdynamics, except that the latter seems to have focused on surfaces (sliding friction), whereas mesodynamics is concerned with internal friction.

A group of individuals using "mesodynamics" to describe some of their computational physics is part of the Materials Science Division of Argonne National Laboratory. Their description of computational theory includes: (i) atomic-level simulation (using molecular dynamics); (ii) mesoscale simulation, i.e., "mesodynamics" (using FEM); and (iii) macroscale (continuum) simulation (FEM). Like the author of this chapter, they recognize that the mesoscale is not a continuum (meaning, for example, that the foundation of viscoelasticity is, for many cases, on shaky ground). They employ "dynamical simulation methods in which the microstructural elements (grain boundaries and grain junctions) are considered as the fundamental entities whose dynamical behavior determines microstructural evolution in space and time."

At the Theoretical Division of Los Alamos National Laboratory, Brad Lee Holian has been modeling mesodynamics via nonequilibrium molecular-dynamics (NEMD). In his paper, "Mesodynamics from Atomistics: A New Route to Hall-Petch," he notes that (i) the mesoscopic nonlinear elastic behavior must agree with the atomistic in compression; and (ii) the mesoscale cold curve in tension represents surface, rather than bulk cohesion, thereby decreasing inversely with grain size (Holian, 2003).

The complexity of mesodynamics, which this author has labeled "mesoanelastic complexity," is responsible for much of the aforementioned "strange phenomena." To those familiar with the Barkhausen effect and the PLC effect, they are less strange. It is thought that Richard Feynman, if he were still alive, would identify with mesodynamics because of material in his three-volume series (Feynman, 1970). For example, we have already noted his discussion of the Barkhausen effect, and he included in its entirety a reprint of the Bragg–Nye paper on bubbles which show two-dimensional defect structures such as dislocations, "grains," and "recrystallization" boundaries after stirring (Bragg et al., 1947).

Another famous individual, whose work related in an unexpected way to the material of this chapter, was Enrico Fermi. In one of the first dynamics calculations carried out on a computer, he and colleagues treated a chain of harmonic oscillators coupled together by a nonlinear term (Fermi, 1940). The continuum limit of their model is the remarkable nonlinear partial differential equation known as the Korteweg–deVries equation, whose solution is a soliton, used to advantage in optical fibers. Damping of solitons, whether of the KdV type or the Sine Gordon (kink/antikink) type, is not to be described by linear mathematics. Incidentally, the Sine Gordon soliton is used in modeling dislocations (Nabarro, 1987). The earliest theory to describe dislocation damping using kink/anti-kink pairs was that of Seeger (1956).

2.18.5 Example of the Importance of Mesoanelastic Complexity

As noted earlier in this chapter, once hysteretic damping was finally recognized to be important to the Cavendish experiment, better agreement with theory and experiment was possible. Curiously, Henry Cavendish may have been the first person to encounter a "strange" phenomenon (which he did not discuss) (Cavendish, 1798). In his first mass swing to perturb the balance, which used a "fiber" made of copper (silvered), there was an anomalously small period of oscillation that was only 55 sec. The period reported for subsequent trials was about 421 sec.

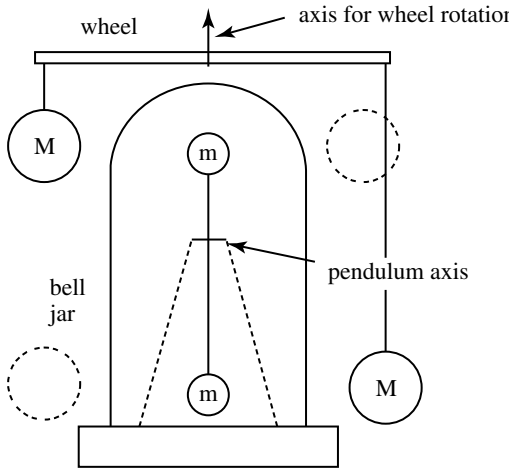

FIGURE 2.27 Physical pendulum used in the late 1980s to try and measure the Newtonian gravitational constant.

Whereas the Michell–Cavendish apparatus was a torsion balance, the instrument of Figure 2.27 is a physical pendulum. The perturbing masses, M, were hung from a bicycle wheel whose axle was suspended from the ceiling. The long-period pendulum was placed under a bell jar so that the instrument would not be driven by air currents. By rotating the wheel at constant angular velocity, the driving force on the pendulum was harmonic. (In the figure, the position of each M one-half period later are shown by the dashed circles.) Knowing the amount of damping, as determined from large amplitude free-decay, it was easy to estimate the number of orbits of the bell jar, at the resonance frequency of the pendulum, required to excite motion to a level above noise in the sensor. Surprisingly, if it were initially at rest, no amount of drive by this means was able to get the pendulum oscillating! The reason involves metastabilities of the defect structures. The potential well is not harmonic (parabolic), but is rather modulated by "fine structure." When located in a deep metastability, the small gravitational force of the drive (in nanoNewtons) is not able to "unlatch" the system. If the pendulum had been dithered (a practice used in engineering) this problem could have been, at least partly, avoided. As it was, the pendulum rested on an isolation table of the type used in optics experiments.

More recently, a Hungarian research team has used a similar apparatus and postulated that the anomalies of their experiment derive from gravity being other than prescribed by Newton (Sarkadi and Badonyi, 2001). Although they claim that there is a "strong dependence of gravitational attraction on the mass ratio of interacting bodies," this author believes that additional experiments must be performed before such a claim has merit. It may be that the anomalous behavior of their pendulum is instead the result of mesoanelastic complexity, i.e., phenomena related to nonlinear damping.

The author's most recent research on damping complexity is based on the premise that the most important scale for the treatment of internal friction is the mesoscale, and not the atomic scale (Peters 2004). Experiments to support this position center around a study of the SMA NiTinol.

2.19 Concluding Remark

Much of the material of this part of the chapter on damping is clearly not appropriate to direct engineering application. It was deemed important to present some of the extensive background information responsible for birthing the practical equations of Section 2.17. In Chapter 3, the reader will find practical aids to the measurement of damping.

Bibliography

Amengual, A., Manosa, L.L., Marco, F., Picornell, C., Segui, C.,, and Torra, V., Systematic study of the martensitic transformation in a Cu–Zn–Al alloy, reversibility versus irreversibility via acoustic emission, *Thermochim. Acta*, 116, 195–308, 1987.

Asa, F., Modal synthesis when modeling damping by use of fractional derivatives, *AIAA J.*, 34(5), 1051–1058, 1996.

Atalay, S. and Squire, P., Torsional pendulum system for measuring the shear modulus and internal friction of magnetoelastic amorphous wires, *Meas. Sci. Technol.*, 3, 735–739, 1992.

Bak, P., Tang, and Wiesenfeld, Self-organized criticality, *Phys. Rev. A*, 38, 364–374, 1988.

Bantel, M.K. and Newman, R.D., High precision measurement of torsion fiber internal friction at cryogenic temperatures, *J. Alloys Compd.*, 310, 233–242, 2000.

Barkhausen, H., *Phys. Z.*, 20, 401, 1919.

Berdichevsky, V., Hazzledine, P., and Shoykhet, B., Micromechanics of diffusional creep, *Int. J. Eng. Sci.*, 35, 10/11, 1003–1032, 1997.

Berry, M.V. and Keating, J.P., The Riemann zeros and eigenvalue asymptotics, *Siam Rev.*, 41, 2, 236–266, 1999.

Berry, B. and Nowick, A., Internal friction study of aluminum alloys containing 4 weight percent copper, *National Advisory Committee for Aeronautics, Technical Note 4225*, online at http://naca.larc.nasa.gov/reports/1958/naca-tn-4225, 1958.

Bert, C.W., Material damping: an introductory review of mathematical models. measures and experimental techniques, *J. Sound Vib.*, 29, 129–153, 1973.

Bethe, H., Lecture at Cornell University online info. at http://www.nd.edu/~bjanko/Copenhagen/Cop3.pdf, 1992.

Bordoni, P., Elastic and anelastic behavior of some metals at very low temperatures, *J. Acoust. Soc. Am.*, 26, 495, 1954.

Bormann P. and Bergmann E., eds. 2002. *New Manual of Observatory Practice*, Institute of Geophysics, University of Stuttgart, online at http://www.seismo.com/msop/nmsop/nmsop.html.

Bragg, Sir Lawrence, F.R.S., and Nye, J.F., A dynamical model of a crystal structure, *Proc. R. Soc. Lond., Ser. A, Math. Phys. Sci.*, 190, 1023, 474–481, 1947.

Braginsky, V.B., Mitrofanov, V.P., and Panov, V.I. 1985. *Systems with Small Dissipation*, The University of Chicago Press, Chicago.

Braginsky, V.B., Mitrofanov, V.P., and Okhrimenko, O.A., Isolation of test masses for gravitational wave antennae, *Phys. Lett. A*, 175, 82–84, 1993.

Breazeale, M.A. and Leroy, O. 1991. *Physical Acoustics: Fundamentals and Applications*, Kluwer Academic/Plenum Publishers, New York.

Brophy, J. 1965. Fluctuations in magnetic and dielectric solids. In *Fluctuation Phenomena in Solids*, R.E. Burgess, Ed., Academic Press, New York.

Bulsara, A.R. and Gammaitoni, L., Tuning in to noise, *Phys. Today*, 49, 39–45, 1996.

Carlson, J.D., Controlling vibration with MR fluid damping, *Sensor Technol. Design*, 19, 2, 2002, online at http://www.sensorsmag.com/articles/0202/30/main.shtml.

Cavendish, H., Experiments to determine the density of the Earth, *Philos. Trans. R. Soc. Lond.*, 469–526, 1798.

Cipra, B., The FFT: making technology fly, *SIAM News*, 26, 3, 1993, online at http://www.siam.org/siamnews/mtc/mtc593.htm.

Cleland, A. and Roukes, M., Noise processes in nanomechanical resonators, *J. Appl. Phys.*, 92, 5, 2758–2770, 2002.

Cooley, J. and Tukey, J., An algorithm for the machine calculation of complex Fourier Series, *Math. Comput.*, 19, 90, 297–301, 1965.

Coy, D. and Molnar, M., Optically driven pendulum, *Proc. NCUR* XI, 1621–1626, 1997.

Cromer, A., Stable solutions using the Euler approximation, *Am. J. Phys.*, 49, 5, 455–459, 1981.

Dean, R., Low-cost, high precision MEMS accelerometer fabricated in laminate online at http://www.eng.auburn.edu/ee/leap/MEMSFabricateTable.htm, 2002.

de Silva, C.W. 2006. *Vibration — Fundamentals and Practice*, 2nd ed., Taylor & Francis, CRC Press, Boca Raton, FL.

Fantozzi, G., Esnouf Benoit, W., and Richie, I., *Prog. Mater. Sci.*, 27, 311, 1982.

Fermi E., Pasta J., and Ulam S., Studies in nonlinear problems I, Los Alamos report (reproduced in R. Feynman, 1970: *Lectures on Physics*, Addison Wesley, Boston, 1940).

Fraden, J. 1996. *Handbook of Modern Sensors, Physics, Designs, & Applications*, 2nd ed., AIP Press (Springer), Secaucus, NJ.

Gammaitoni, L., Stochastic resonance and the dithering effect in threshold physical systems, *Phys. Rev. E*, 52, 469, 1995.

Gere, J., Timoshenko, S. 1996. *Mechanics of Materials*, Chapman & Hall, London.

Granato, A. 2002. High damping and the mechanical response of amorphous materials, Submitted to the Proceedings of the International Symposium on High Damping Materials in Tokyo, August 22, 2002 for publication in the Journal of Alloys and Compounds, private communication preprint.

Granato, A. and Lucke, K., Theory of mechanical damping due to dislocations, *J. Appl. Phys.*, 27, 583, 1956.

Greaney, P., Friedman, L.,, and Chrzan, D., Continuum simulation of dislocation dynamics: predictions for internal friction response, *Comput. Mater. Sci.*, 25, 387–403, 2002.

Grigera, T. and Israeloff, N., Observation of fluctuation–dissipation theorem violations in a structural glass, *Phys. Rev. Lett.*, 83, 24, 5038–5041, 1999.

Gross, B., The flow of solids, *Phys. Today*, 5, 8, 6–10, 1952.

Heyman, J. 1997. *Coulomb's Memoir on Statics: An Essay in the History of Civil Engineering*. Imperial College Press, London, ISBN: 1860940560.

Hilfer, P., ed. 2000. *Applications of Fractional Calculus in Physics*, World Scientific, London.

Hodges, D. 2003. Private communication (Georgia Tech School of Aerospace).

Holian, B. 2003. Mesodynamics from atomistics: a new route to Hall–Petch, private communication preprint.

Horowitz, H. and Hill, W. 1989. *Art of Electronics*, 2nd ed., Cambridge University Press.

Kimball, A. and Lovell, D., Internal friction in solids, *Phys. Rev.*, 30, 948–959, 1927.

Kohlrausch, R., *Ann. Phys.*, 12, 392, 1847, online information at http://www.ill.fr/AR-99/page/74magnetism.htm.

Kuroda, K., Does the time of swing method give a correct value of the Newtonian gravitational constant?, *Phys. Rev. Lett.*, 75, 2796–2798, 1995.
LaCoste, L., A new type long period vertical seismograph, *Physics*, 5, 178–180, 1934.
Lakes, R. 1998. *Viscoelastic Solids*, CRC Press, Boca Raton, FL.
Lakes, R. and Quackenbush, J., Viscoelastic behavior in indium tin alloys over a wide range of frequency and time, *Philos. Mag Lett.*, 74, 227–232, 1996.
Landau, L. and Lifshitz, E. 1965. *Theory of Elasticity*, Nauka, Moscow.
Lorenz, E. 1972. Predictability: Does the flap of a butterfly's wings in Brazil set off a tornado in Texas, presented to AAAS, Washington, DC.
Marder, M. and Fineberg, J., How things break, *Phys. Today*, 49, 24–29, 1996.
Marion, J. and Thornton, S. 1988. *Classical Mechanics of Particles and Systems*, 3rd ed., HBJ, Academic Press, New York, p. 114.
Milonni, P. and Eberly, J. 1988. *Lasers*. Wiley Interscience, Hoboken, NJ, p. 93.
Moon, F. 1987. *Chaotic Vibrations, An Introduction for Applied Scientists and Engineers*, Wiley Interscience, Hoboken, NJ.
Moore, G., Moore's law is described online at http://www.intel.com/research/silicon/mooreslaw.htm, 1965.
Nabarro, F. 1987. *Theory of Crystal Dislocations*, Dover, New York.
Nelson, R. and Olssen, M., The pendulum—rich physics from a simple system, *Am. J. Phys.*, 54, 112–121, 1986.
Ostermeyer, G. and Popov, V., Many-particle non-equilibrium interaction potentials in the mesoparticle method, *Phys. Mesomech.*, 2, 31–36, 1999.
Peters, R., Resonance generation of ultrasonic second harmonic in elastic solids, *J. Acoust. Soc. Am.*, 53, 6, 1673, 1973.
Peters, R., Linear rotary differential capacitance transducer, *Rev. Sci. Instrum.*, 60, 2789, 1989.
Peters, R., Metastable states of a low-frequency mesodynamic pendulum, *Appl. Phys. Lett.*, 57, 1825, 1990.
Peters, R., Fourier transform construction by vector graphics, *Am. J. Phys.*, 60, 439, 1992.
Peters, R., Fluctuations in the length of wires, *Phys. Lett. A*, 174, 3, 216, 1993a.
Peters, R., Full-bridge capacitive extensometer, *Rev. Sci. Instrum.*, 64, 8, 2250–2255, 1993b. This paper describes an SDC sensor with cylindrical geometry. Other geometries, including the more common planar one, are described online at http://physics.mercer.edu/petepag/sens.htm.
Peters, R. 2000. Autocorrelation Analysis of Data from a Novel Tiltmeter, abstract, *Amer. Geo. Union annual mtg.*, San Francisco.
Peters, R. 2001a. The Stirling engine refrigerator — rich pedagogy from applied physics, online at http://xxx.lanl.gov/html/physics/0112061.
Peters, R. 2001b. Creep and Mechanical Oscillator Damping, http://arXiv.org/html/physics/0109067/.
Peters, R. 2002a. The pendulum in the 21st century—relic or trendsetter, *Proc. The Int'l Pendulum Project*, University of New South Wales, Australia, Proceedings, October, 2002.
Peters, R. 2002b. The soup-can pendulum, *Proc. The Int'l Pendulum Project*, University of New South Wales, Australia, Proceedings, October. 2002.
Peters, R. 2002c. Toward a universal model of damping—modified Coulomb friction online at http://arxiv.org/html/physics/0208025.
Peters, R. 2003a. Graphical explanation of the speed of the Fast Fourier Transform, online at http://arxiv.org/html/math.HO/0302212.
Peters, R. 2003b. Nonlinear damping of the 'linear' Pendulum, online at http://arxiv.org/pdf/physics/03006081.
Peters, R. 2003c. Flex-Pendulum—basis for an improved timepiece, online at http://arxiv.org/pdf/physics/0306088.
Peters, 2004. Friction at the Mesoscale. In *Contemporary Physics*, P. Knight, Ed., Vol. 45, no. 6, 475–490, Imperial College, London 2004.

Peters, R. and Kwon, M., Desorption studies using Langmuir recoil force measurements, *J. Appl. Phys.*, 68, 1616, 1990.

Peters, R. and Pritchett, T., The not-so-simple harmonic oscillator, *Am. J. Phys.*, 65, 1067–1073, 1997.

Peters, R., Breazeale, M., and Pare, V., Temperature dependence of the nonlinearity parameters of Copper, *Phys. Rev.*, B1, 3245, 1970.

Peters, R., Cardenas-Garcia, J., and Parten, M., Capacitive servo-device for microrobotic applications, *J. Micromech. Microeng.*, 1, 103, 1991.

Portevin, A. and Le Chatelier, M., Tensile tests of alloys undergoing transformation, *C. R. Acad. Sci.*, 176, 507, 1923.

Present, R. 1958. *The Kinetic Theory of Gases*. McGraw-Hill, New York.

Press, W., Flannery, B., Teukolsky, S., and Vetterling, W. 1986. *Numerical Recipes—the Art of Scientific Computing*. Cambridge University Press.

Purcell, E., Life at low Reynolds number, *Am. J. Phys.*, 45, 3–11, 1977.

Richardson, M., and Potter, R. 1975. Viscous vs structural damping in modal analysis, *46th Shock and Vibration Symposium*.

Roukes, M., Plenty of room indeed, *Scientific American*, 285, 48–57, 2001.

Sarkadi, D. and Badonyi, L., A gravity experiment between commensurable masses, *J. Theor.*, 3–6, 2001.

Saulson, P., Stebbins, R., Dumont, F., and Mock, S., The inverted pendulum as a probe of anelasticity, *Rev. Sci. Instrum.*, 65, 182–191, 1994.

Seeger, A., On the theory of the low-temperature internal friction peak observed in metals, *Philos. Mag.*, 1, 1956.

Singh, A., Mohapatra, Y., and Kumar, S., Electromagnetic induction and damping, quantitative experiments using a PC interface, *Am. J. Phys.*, 70, 424–427, 2002.

Speake, C., Quinn, T., Davis, R., and Richman, S., Experiment and theory in anelasticity, *Meas. Sci. Technol.*, 10, 430–434, 1999. See also Quinn, Speake and Brown, 1992: Materials problems in the construction of long-period pendulums, *Philos. Mag.* A 65, 261–276, 1999.

Steinmetz, C.P., *Complex Number Technique*, *paper given at the International Electrical Congress*, Chicago, 1893.

Stokes, G., On the effect of the internal friction of fluids on the motion of pendulums, *Trans. Cambridge Philos. Soc.*, IX, 8, 1850, read December 9, 1850.

Strang, G., Wavelet transforms versus Fourier Transforms, *Bull. Am. Math. Soc.*, 28, 288–305, 1993.

Streckeisen, G. 1974. *Untersuchungen zur Messgenauigkeit langperiodischer Seismometer*, Diplomarbeit, Institut für Geophysik der ETH Zürich (communicated privately by E. Wielandt).

Tabor, M. 1989. The FUP Experiment. In *Chaos and Integrability in Nonlinear Dynamics: Introduction*. Wiley, New York.

Thomson, W., Tait, G. 1873. *Elements of Natural Philosophy, Part I*. The Clarendon Press, Oxford, (Thomson was later known as Lord Kelvin).

Urbach, J., Madison, R., and Markert, J., Reproducibility of magnetic avalanches in an Fe–Ni–Co alloy, *Phys. Rev. Lett.*, 75, 4694, 1995a.

Urbach, J., Madison, R., and Markert, J., Interface depinning, self-organized criticality, and the Barkhausen effect, *Phys. Rev. Lett.*, 75, 276, 1995b.

Venkataraman, G. 1982. Fluctuations and mechanical relaxation. In *Mechanical and Thermal Behavior of Metallic Materials*, Caglioti, G. and Milone, A., eds., pp. 278–414. North-Holland, Amsterdam.

Visintin, A. 1996. *Differential Models of Hysteresis*. Springer, Berlin.

Westfall, R. 1990. Making a world of precision: Newton and the construction of a quantitative physics. In *Some Truer Method. Reflections on the Heritage of Newton*, F. Durham and R.D. Purrington, eds., pp. 59–87. Columbia University Press, New York.

Wielandt, E. 2001. *Seismometry*, section Electronic Displacement Sensing, online at http://www.geophys.uni-stuttgart.de/seismometry/hbk_html/node1.html.

Zemansky, M.W. 1957. *Heat and Thermodynamics*, 4th ed., McGraw-Hill, New York, p. 127.

Zener, C. 1948. *Elasticity and Anelasticity of Metals*, Chicago Press, Chicago.